Bioactive Materials 19 (2023) 717–757

Contents lists available at ScienceDirect

Bioactive Materials

journal homepage: www.keaipublishing.com/en/journals/bioactive-materials

Review article

Progress in bioactive surface coatings on biodegradable Mg alloys: A critical review towards clinical translation

Navdeep Singh [a], Uma Batra [a], Kamal Kumar [b,*], Neeraj Ahuja [a], Anil Mahapatro [c]

[a] Department of Metallurgical and Materials Engineering, Punjab Engineering College, Chandigarh, 160012, India
[b] Department of Mechanical Engineering, Punjab Engineering College, Chandigarh, 160012, India
[c] Department of Biomedical Engineering, Wichita State University, Wichita, KS, 67260, United States

ARTICLE INFO

Keywords:
Mg alloys
Corrosion resistance
Bio-functionality
Conversion coating
Multilayered hybrid coating
Coating failures

ABSTRACT

Mg and its alloys evince strong candidature for biodegradable bone implants, cardiovascular stents, and wound closing devices. However, their rapid degradation rate causes premature implant failure, constraining clinical applications. Bio-functional surface coatings have emerged as the most competent strategy to fulfill the diverse clinical requirements, besides yielding effective corrosion resistance. This article reviews the progress of biodegradable and advanced surface coatings on Mg alloys investigated in recent years, aiming to build up a comprehensive knowledge framework of coating techniques, processing parameters, performance measures in terms of corrosion resistance, adhesion strength, and biocompatibility. Recently developed conversion and deposition type surface coatings are thoroughly discussed by reporting their essential therapeutic responses like osteogenesis, angiogenesis, cytocompatibility, hemocompatibility, anti-bacterial, and controlled drug release towards in-vitro and in-vivo study models. The challenges associated with metallic, ceramic and polymeric coatings along with merits and demerits of various coatings have been illustrated. The use of multilayered hybrid coating comprising a unique combination of organic and inorganic components has been emphasized with future perspectives to obtain diverse bio-functionalities in a facile single coating system for orthopedic implant applications.

1. Introduction

Magnesium and its alloys are becoming research frontier in the field of biodegradable materials due to their adequate strength, lightweight, and natural biodegradability. For orthopedic implant application, Mg alloys possess similar mechanical characteristics with identical young's modulus (20–45 GPa) comparable to cortical bone (20–27 GPa) [1]. Additionally, Mg alloys mimic the mechanical anisotropic characteristic of cortical bone, which endows superior load-bearing capacity [2]. The combination of such unique properties renders Mg alloys as a promising candidate for orthopedic implant applications. An ideal biodegradable implant is supposed to stimulate the healing response of injured tissue/bone, promote osteointegration, and provide necessary mechanical support at the early stages of implantation [3]. With prolonged immersion in physiological media, implant degradation rate must be synchronized with bone healing rate. During degradation, the supply of released ions must be adequate for the healthy growth metabolism of osteoblast and neovascularization [4]. After providing necessary mechanical fixation upto bone healing time, the implant should be degraded completely and replaced by new bone tissue, eliminating unnecessary follow-up and secondary surgery [5]. However, in the last few decades, researchers have put continuous efforts into synchronizing the degradation rate of Mg-based biodegradable implants. Unfortunately, investigated studies show compromised bio-functionalities during clinical testing, which need to be addressed for full-scale orthopedic implant applications [6–10].

There are multiple outstanding concerns with Mg and its alloys, limiting their application potential for a biodegradable orthopedic implant. The primary issue about Mg-based implants is rapid degradation in a complex physiological environment, which deteriorates mechanical integrity and causes implant failure (within 4–6 weeks), even before the complete healing of natural bone, which usually takes 8–12 weeks [11]. Moreover, if the fracture type is transverse, bones like femur, tibia, and fibula may take longer time (up to 24 weeks) to regain

Peer review under responsibility of KeAi Communications Co., Ltd.
* Corresponding author.
E-mail address: kamaljangra@pec.edu.in (K. Kumar).

https://doi.org/10.1016/j.bioactmat.2022.05.009
Received 15 March 2022; Received in revised form 6 May 2022; Accepted 6 May 2022

native mechanical strength [12]. Mg alloys are prone to micro-galvanic corrosion due to the highly electronegative electrode potential of −2.37 V, which further accelerates the degradation phenomena in the presence of physiological media [13]. Secondly, Mg suffers from an abnormal phenomenon of negative difference effect (NDE) where corrosion rate and hydrogen evolution increase rapidly with an increase in corrosion potential, which may lead to blockage of blood paths and cause tissue necrosis by H_2 accumulation [14]. Thus, wound healing after prosthetic surgery becomes a major challenge. Additionally, the formation of highly alkalized micro-environment at the tissue/implant interface cause cell-apoptosis [15]. Other issues, like difference in in-vivo and in-vitro corrosion resistance, limit the clinical translation of Mg-based implants because the corrosion performance in in-vitro conditions ignores the role of proteins and enzymes present in actual physiological media [16,17]. Nevertheless, it is still debatable to determine whether the proteins assist or hinder the corrosion phenomena of Mg alloys [18]. Another possible reason for such differences may be the presence of dynamic physiological conditions inside human body. However, some studies reported creating semi-dynamic and quasi-static conditions during the in-vitro investigation, but a significant difference exist between the in-vitro and in-vivo degradation response of Mg alloys [19–23].

The degradation rate must be controlled up to the bone healing period to adopt Mg alloys for safe clinical applications. Extensive efforts have been devoted to resolve the degradation issue, mainly dominated by microstructural and surface modification strategies [24]. Micro-alloying considered as a promising method to tailor the degradation rate [25,26] by alloying the Mg with relatively noble elements like Calcium (Ca), Zinc (Zn), Aluminium (Al), Manganese (Mn), Lithium (Li), Scandium (Sc), Strontium (Sr), and rare earth (RE) elements [27]. Some of the Mg alloys such as Mg-Zn-Ca [28], Mg-Ca-La [29], Mg-Sr [30], Mg-Mn-Ca-Zn [31] demonstrated bio-safe degradation rates in the range of 0.2–0.5 mm/year in physiological media due to their tendency to form noble composite oxide layers which act as effective shields against aggressive ions of physiological media [32]. Nowadays, various ceramic reinforcements including β-TCP [33], HA [34], and calcium polyphosphate (CPP) [35] have also been reported to enhance corrosion resistance, bioactivity and mechanical strength of Mg alloys. However, the versatility of their bio-functionalities for clinical qualification is yet to be established. Moreover, alloying of Mg is always challenging due to the low solubility and non-uniform distribution of most alloying elements, resulting in heterogenous and coarse secondary phases [36]. These phases act as potential sites for micro-galvanic cell set-up and thus accelerate the degradation of Mg alloy [37].

Alternatively, surface modification techniques are more convenient and straightforward approach to control the degradation rate of Mg alloys [38,39]. Surface modification techniques can be categorized based upon the requirement of different energy sources like mechanical, thermal, electrical, biological, and chemical energy, as described in Fig. 1. Coating processes with electric energy as source are widely used for Mg alloys. This category includes Electrodeposition, Micro arc oxidation, Electrospinning, Anodic oxidation, Physical Vapor Deposition, Ion implantation and Chemical Vapor Deposition [40]. These processes can be performed at room temperature or at relatively low temperatures, which is a notable advantage of this category. These coatings are characterized by their highly uniform crystalline structure, improved bonding strength, wear resistance, reproducibility, and facile thickness control [41]. In addition, they can be easily applied to Mg substrates with complex geometries. The surface modification techniques like friction stir processing (FSP), shot peening (SP), and surface mechanical attrition treatment (SMAT) employ mechanical working to physically alter the surface properties of Mg alloys by grain refinement [42,43]. In comparison, thermal surface modification techniques like laser surface melting (LSM) and laser shock peening (LSP) utilize the application of high temperature and pressure to obtain grain refinement [44]. In the case of biodegradable Mg alloys, such surface modifications are extensively reported to enhance the mechanical properties. However, they are not adequate to improve the corrosion resistance of Mg alloys in physiological media [45–47]. Additionally, the unwanted residual stresses generated after thermal or mechanical working affects the corrosion and mechanical properties of Mg alloys [48].

In contrast, surface coatings play an efficient role to act as a physical barrier between the substrate and physiological media to improve the corrosion resistance without disturbing the grain morphology of Mg alloys. However, the surface coating does not improve mechanical properties but plays a vital role in minimizing the mechanical integrity

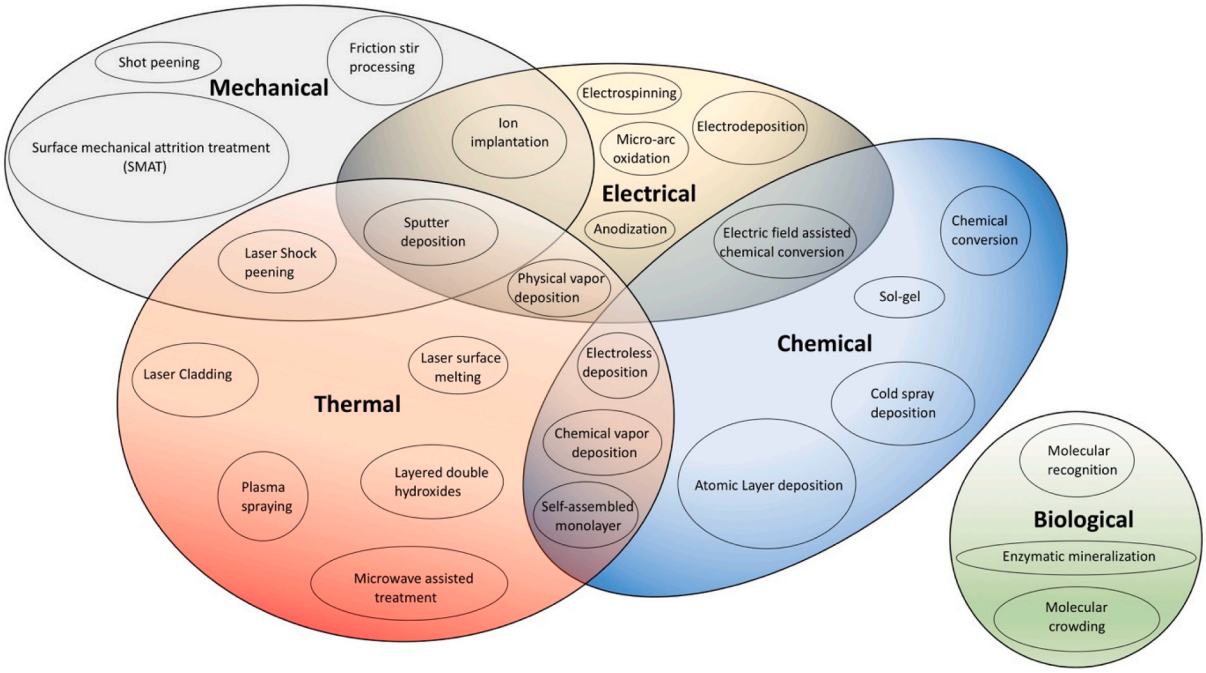

Fig. 1. Classification of surface modification processes based on various energy sources.

loss of Mg alloys with prolonged immersion in physiological media [49,50]. Surface coatings on Mg alloys are metallic, ceramic, and polymeric. Nowadays, bioactive ceramics, including Ca–P compounds and biodegradable polymers like Polylactic acid (PLA), Poly (lactic-co-glycolic) acid (PLGA), Polydopamine (PDA), and Polycaprolactone (PCL) are gaining interest in orthopedic applications due to superior biocompatibility and biosafe degradability in physiological media.

Among numerous surface coating techniques, the selection of appropriate coating architecture is challenging to meet the diverse clinical requirements. In the last few decades, umpteen research has been conducted to explore the various surface coatings on Mg alloys to fulfill clinical bio-functionalities. With a focus on corrosion resistance, adhesion strength, biocompatibility, and other bio-functionalities of surface coatings, this review paper summarizes the progress of various conversion and deposition types of coatings on Mg-based alloys for biodegradable implant application. Hence, the latest developments for a wide range of coating techniques from methodological, structural, and functional perspectives are discussed. A comprehensive analysis between bio-functionalities and simultaneous corrosion performance of the latest coating strategies has been performed to establish the fulfillment of clinical goals.

2. Coatings on Mg alloys: clinical requirements

Generally, Mg-based implants do not have bioactive surfaces, which promote good osseointegration and ward off infection from the implantation site. Accordingly, attention has been focused on developing coating systems that complement essential clinically features [51]. Coatings must be biocompatible and do not trigger any immune or foreign body response to endow such requirements. In any case, the coating must produce an efficient anti-inflammatory response, necessary for the first 3–7 days of implantation [52]. Apart from providing necessary corrosion resistance, Nowadays, specially designed coating serves as a potential stock-house for performing various bio-functionalities to meet the essential clinical requirement. Coatings on Mg implant must be osteoconductive to promote significant osteoblasts' adherence, proliferation, and growth. Additionally, coatings with angiogenesis differentiation are highly recommended for the formation of new blood vessels from pre-existing vessels of host tissue at the early stages of implantation, which accelerates surgical wound-healing and osteoinduction response of implant [53,54].

Coatings must have adequate cohesion and adhesion strength to withstand dynamic stresses associated with locomotive events in the human body. The lack of cohesion or adhesion strength will result in mechanical damage or delamination of coating from the implant surface. Apart from the loading aspect, polymeric coatings are highly prone to damage partially (i.e., scratching, debonding) even during the implant fixation process [55]. Thus, a coating system with self-healing/sealing characteristics is desirable to counter such failures. Finally, coatings must possess anti-microbial properties to deter the risk of surgical site bacterial infections (SSBI), which may lead to surgery failure or death of a patient under severe circumstances [56]. Following traumatic fracture, the inorganic and organic phases of natural bone must rapidly biomineralize. The coating is required to direct the alignment of mineralized phases so that maximum penetration occurs within the bone. Otherwise, randomly aligned mineralized phases can cause a larger space between the bone and implant, which could result in implant loosening. During implant fixation surgery or after implant fixation, dynamic loading conditions within the human body, coatings are prone to damage. Thus, coatings with intelligent self-healing features are essential. The fulfillment of these bio-functionalities by an ideal coating architecture/design will lead the idea of Mg-based biodegradable implant towards the product development phase.

3. Coatings and their current status

Surface coatings on Mg alloys can be obtained by mechanical, thermal, biological, and chemical methods. The surface modifications achieved independently or combined by mechanical or thermal energy are categorized under physical coatings. Surface coatings involving biological methods like biomimetic, bio-inspired, or molecular recognition are called biochemical coatings. Among various surface modification techniques, chemical coatings are the most widespread and investigated technique for the biomedical application of Mg alloys. According to the formation mechanism, the chemical coatings on Mg alloys are generically categorized as conversion and deposition coatings. Conversion coatings are in-situ grown coatings by utilizing the base metal for specific chemical reactions to form a protective layer. In contrast, deposited coatings are produced ex-situ by numerous techniques to be discussed in this review. The detailed classification scheme of conversion and deposited coatings are shown in Fig. 2.

3.1. Conversion coatings –

Conversion coatings are in-situ fabricated coatings produced by a chemical reaction between the substrate and the coating media. Generally, the surface of metallic substrate undergoes complex reactions in aqueous media by chemical or electrochemical method [57]. Such treatment resulted in oxide/hydroxide formation on the surface of base metallic substrate. The in-situ growth environment provides excellent adhesion strength as compared to deposited coating. Thus, many studies highlighted the application of conversion coatings as an adhesive layer sandwiched between Mg substrate and deposited organic coating [58–60]. The chemical conversion, micro arc oxidation (MAO), layered double hydroxides (LDHs), ion-implantation and alkaline treatment are important conversion coatings on Mg-based alloys for bioimplant applications thoroughly discussed in the present study.

3.1.1. Chemical conversion coatings (CCCs)

CCCs are achieved by the formation of oxide/hydroxide of native or other desirable elements on Mg substrate, which can enhance corrosion resistance, biocompatibility, and osteoconductivity of coated samples. Typically, a chemical conversion process involves a sequence of steps: cleaning in an alkaline environment, etching in an acidic environment, immersion in conversion bath, drying, and water rinsing [61]. In general, a conversion coating works by stimulating the interfacial reactions with the subsequent precipitation/coating formation. The process is triggered by a decrease of the pH and an increase of the Mg^{2+} concentration at the metal/solution interface [62]. Mg's low standard electrode potential allows protons (H^{+}) and water to be reduced simultaneously upon dissolution. After immersion in aqueous bath solutions, magnesium hydroxide was rapidly formed on the Mg substrate. In neutral (pH 7) or alkaline bath solutions (pH 10) magnesium hydroxide is chemically stable, which results in passivation and inhibits conversion reactions [63]. However, in acidic bath conditions, magnesium hydroxide may be easily attacked by the plentiful protons that are continually supplied to the coating/metal interface by the acidic solution [62]. As a result, localized dissolution occurs on the hydroxide layer, causing the breakdown of passivity and ensuring continued conversion reactions. In an acidic conditions, Mg specimen dissolves aggressively and releases abundant amount of Mg^{2+} cations. Therefore, in the vicinity of the Mg surface, localized accumulation of OH^{-} ions abruptly increase pH at coating/metal interface (The bulk pH will also rise with prolonged immersion, but that is not relevant during the timescale of coating) [64]. As a result of this local pH increase, a conversion layer over the Mg substrate rapidly forms and precipitates. With prolonged immersion in bath media, the oxide/hydroxide formed on Mg substrate dissolved in a localized manner, facilitating penetration of conversion media. Once bath media reaches the surface of Mg substrate, conversion phenomena again initiated, which facilitates the enrichment of coating density [65].

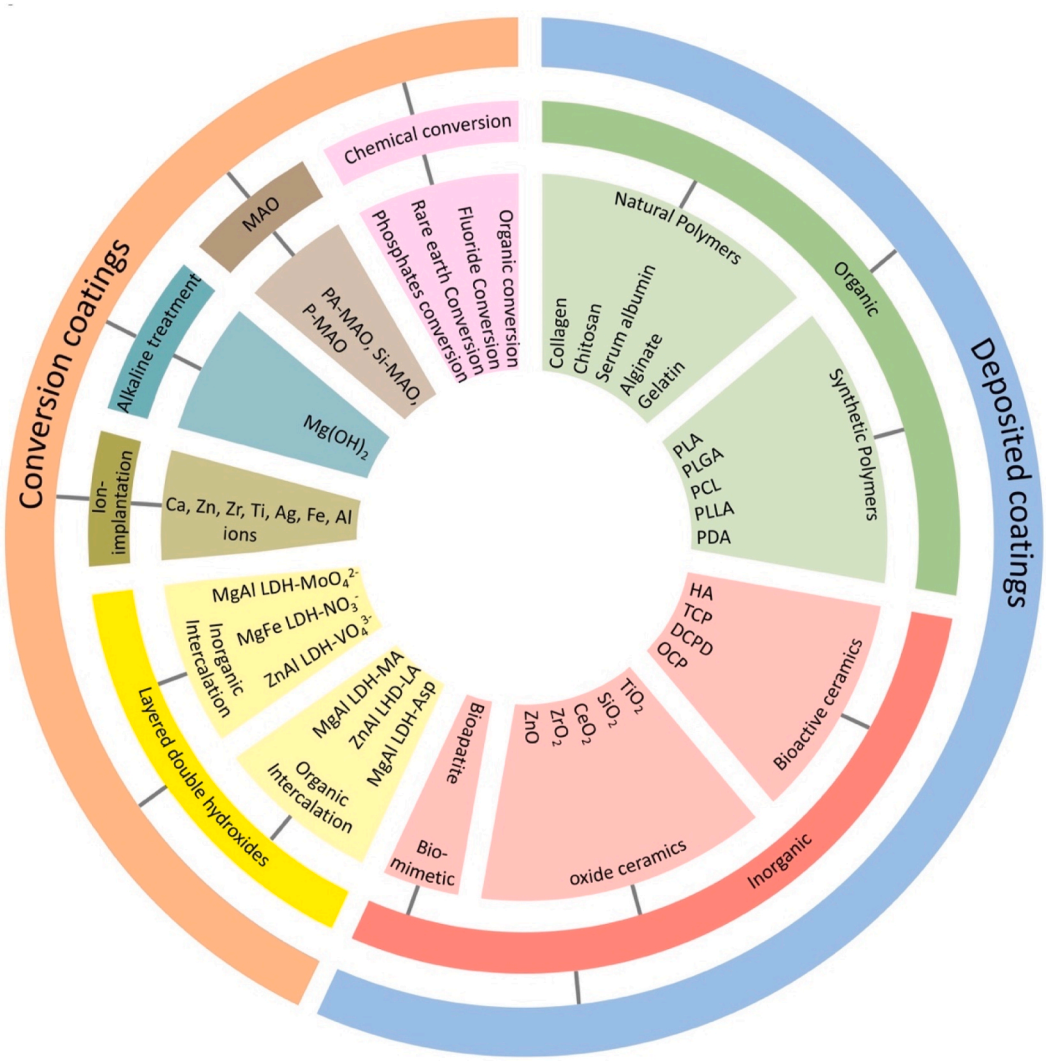

Fig. 2. Generic classification of coatings for biodegradable Mg alloys.

Hence, the density of deposited coating is increased by prolonged immersion in bath media. Additionally, process parameters like concentration, pH, and temperature of bath media play essential roles in coating quality [66]. Majorly reported chemical conversion coatings on Mg alloys are based on chromates, fluorides, phosphates, and rare earth (RE) elements [67]. Despite excellent corrosion resistance possessed by chromate coatings, its usage has been banned under EU regulations for biosafety purposes [68]. Fluoride conversion coatings have limited bioactivity and poor stability with prolonged immersion in physiological media [69]. Thus, in recent years, various metal-phosphate and rare earth (RE) element based conversion coatings have been extensively researched for effective corrosion resistance and biocompatibility of Mg alloys, as discussed below:

- *Phosphate conversion coatings (PCCs):* Various PCCs containing trace metallic complexes are shown in Fig. 3. Studies reported the doping of additional trace elements to improve the biocompatibility and osteoinduction response of phosphate conversion coatings. Due to the hydroxyapatite (HA) layer formation, Ca–P conversion coatings are of particular interest. HA most closely mimics the mineral phase of natural bone among various Ca–P phases and is highly recognized as an osteoconductive mineral [70]. Additionally, the lowest solubility offers effective corrosion resistance in physiological media. Although HA coatings can be achieved by various techniques like sol-gel and electrochemical deposition, coating's adhesion strength reported for such techniques is relatively low [71,72].

However, due to in-situ coating formation, the average adhesion strength of chemical conversion coatings is exceptionally superior up to 19–28 MPa [73]. The osteointegration response of HA coatings is dependent on surface morphology. Nano-plate and nano-sphere like structures greatly enhance the cell attachment compared to whisker or flake-like HA crystal structures [74]. The chemical conversion method can quickly obtain such desired coating morphologies by varying the process parameters like pH, bath temperature, and treatment time, which is difficult to control by other coating techniques [75]. Despite controlled morphology and uniform coating thickness, the fabrication of HA coating free from the fragile surface and spatial defects is still a challenge.

Rahman et al. [73] developed a double-layered Ca–P coating comprised of dicalcium phosphate dihydrate (*DCPD*) and HA on WE43 and pure Mg alloy. The author reported that after alkaline treatment, *DCPD*'s non-homogeneous flake-like structure got transformed into a uniform plate-like HA structure completely devoid of defects as shown in Fig. 4. The chemically driven HA formation on Mg substrate resulted in significantly high adhesion strength of 28.5 MPa. However, the study lacks a long-term immersion test in physiological media to assess the loss of adhesion strength that may occur during prolonged immersion.

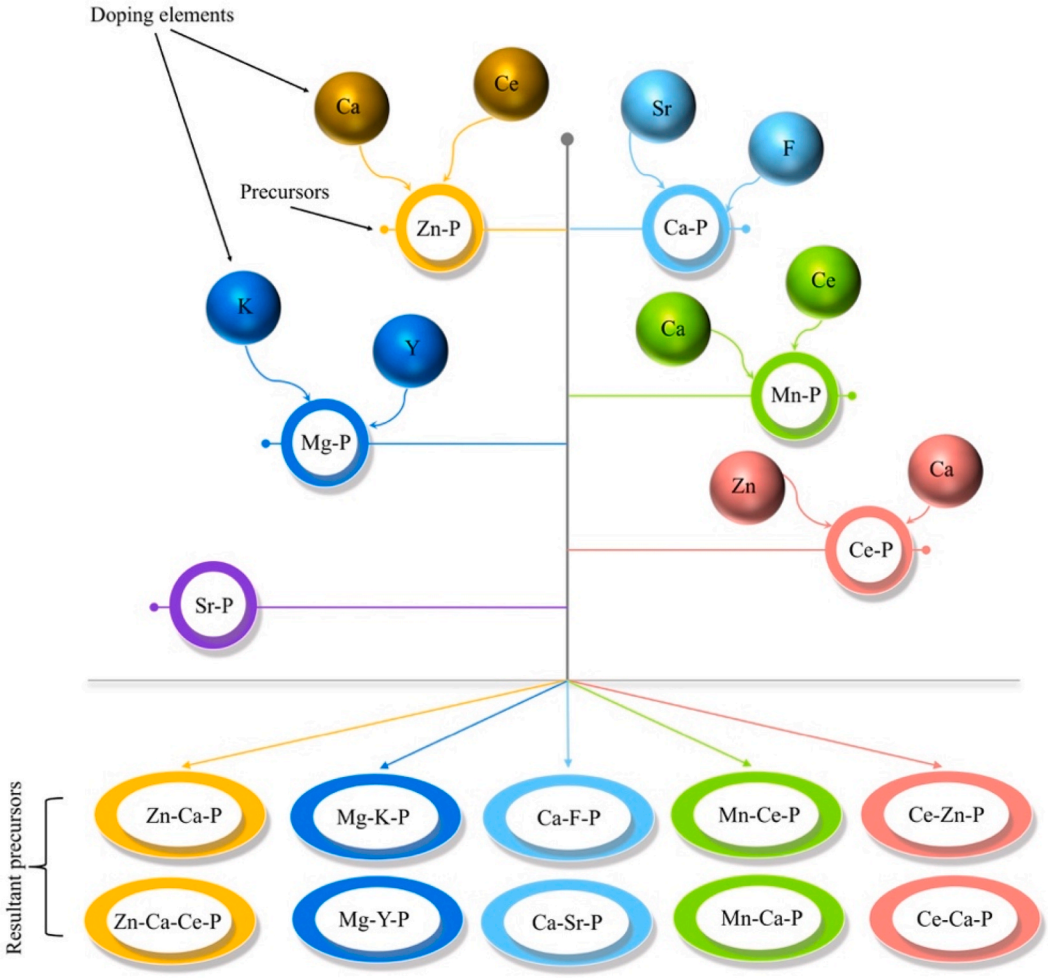

Fig. 3. Elemental doping and resultant conversion baths used for various phosphate conversion coatings on Mg alloys for orthopedic applications.

Table 1 reports the fabrication parameters, pre/post treatments and performance details of various PCCs achieved on Mg alloys. Maurya et al. [83] deposited bioactive HA coating on Mg–Li alloy by a two-step conversion coating technique to observe in vitro biomineralization response and corrosion resistance. The author reported that the biomineralization tendency of HA-coated substrate became twice when compared to the uncoated sample. However, considerable residual stress value (~200 MPa) in the coatings result in fatigue cracking and loss in adhesion strength under dynamic loading conditions [84].

Since Ca–P coatings possess no biocidal response toward bacterial activity, phosphate conversion coatings must be evaluated for osteomyelitis risk. Hu et al. [85] fabricated Ag/HA composite conversion coating on Mg–2Zn–1Mn-0.5Ca alloy. The Ag/Ha coated sample displayed significant zone of inhibition (ZOI) against *S. aureus,* compared to uncoated samples. By uniform dispersion of Ag particles, the adhesion strength of Ag/HA coatings was enhanced by 3.5 times compared to HA coatings. However, the electrochemical response of composite coating was not attractive due to spatial defects originating from Ag addition. Study has not addressed biocompatibility of Ag/HA composite coating. Ideally, HA (stochiometric Ca/p ratio, 1.67) having lowest solubility index (K_{sp} 3.7 × 10^{-58}) is considered the most stable form of apatite [86]. However, the leaching of Mg^{2+} ions occurred via coating defects, causing the substitution of Ca ions in HA. Such a substitution creates structural disorder in HA lattice, which results in high solubility and poor crystallinity with prolonged immersion in physiological media [87]. Being inert to such substitutions, other alternatives like RE-based conversion coatings have gained interest in recent years.

- *RE-based conversion coating (REEs)*: RE elements are well known for their chemical stability and long-term insolubility in physiological media. Rudd et al. [88] firstly introduced RE conversion coatings for Mg alloys for bioimplant application. It was reported that RE conversion coatings provide uniform Mg degradation in aqueous chloride media over large pH fluctuations, usually occurring during Mg corrosion [89]. Generally, famous RE elements applied for conversion coatings on Mg alloys, like cerium (Ce), Yttrium (Y), Lanthanum (La), have no antagonistic effect on living cells at lower concentrations. They play a vital roles in the bio-functioning of the kidney, liver, skeletal muscles, and glands, indeed regulating the immune system by triggering anti-inflammatory reactions [90]. Recently, Han et al. [91] fabricated a Y-based conversion coating on AZ91 D Mg alloy. The coating morphology is composed of dry river-bed type micro-cracks. A post coating treatment by dipping the coated substrate into 30% silica sol sealed the micro-pores. The E_{corr} of coated substrate is positively shifted with respective drop in I_{corr} by 10^2 folds. A 72-h immersion study conducted in a NaCl environment showed coating stability without any signs of delamination.

Saranya et al. [92] investigated the role of selenium (Se) conversion coating on AZ31 Mg alloy for bio-mineralization and anti-bacterial response. A Bath with 0.2% selenous acid solution was prepared by mixing propanol and water. The substrate was immersed for 3 h to obtain conversion coating. A hydrophobic coating surface with 98.5° ± 1.4 was obtained, which significantly shifted the E_{corr} to −0.39 V compared to −1.61 V of uncoated substrate. After seven days of

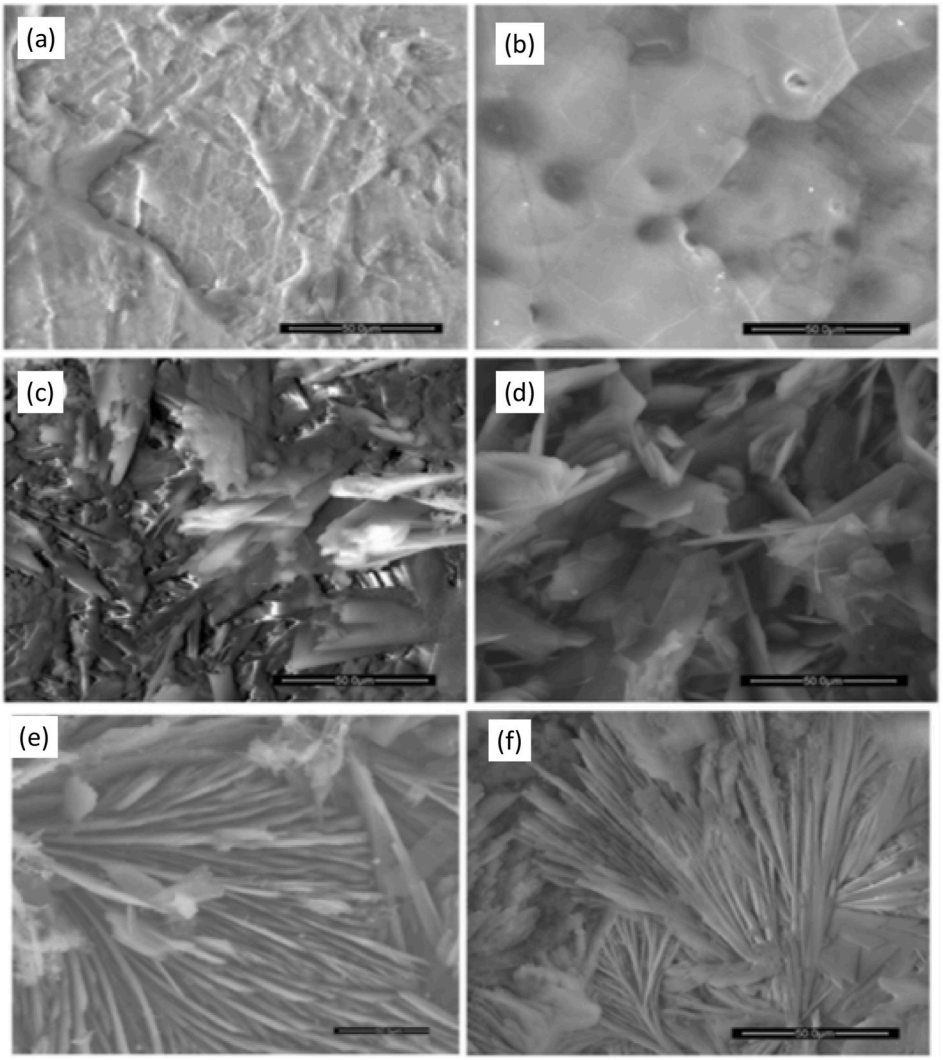

Fig. 4. **(a)** Surface morphology of WE43 Mg alloy, **(b)** pure Mg, **(c)** non-homogenous flake-like structure of *DCPD* coating on WE43 Mg alloy, **(d)** non-homogenous flake-like structure of *DCPD* coating on pure Mg, **(e)** homogenous plate-like structure of HA coating obtained after alkalization on WE43 Mg alloy, **(f)** homogenous plate-like structure of HA coating obtained after alkalization on Pure Mg. Reproduced with permission [73]. Copyright 2020, Elsevier.

immersion in Earle's solution, a dense apatite growth significantly improved the coating's protective efficiency. However, a higher release of Se ions (29 μg/cm^2/day) was observed during initial immersion hours, but with apatite growth, it slowed down to 12 μg/cm^2/day, which was below the daily requirement of the human body. The anti-bacterial response of coated sample against *P. aeruginosa* and *S. epidermis* was found 52 and 61%, respectively, which is nearly 4–6 times higher than uncoated substrate. Additionally, coated sample exhibits an inhibition zone of 18 mm diameter against *S. aureus*. The author reported the selenium's capability of producing superoxide radical ions, which destroy the cell metabolism of both gram-positive and gram-negative bacteria. Extending the similar antagonistic properties of RE elements, Kannan et al. [93] reported anti-cancer activity of electrophoretically obtained samarium (Sm) conversion coating on AZ31 Mg alloy. The Sm^{3+} ions enhanced the affinity of Sm-tetraaza macromolecules towards *CXCR4* receptors, which exceptionally boosted the anticancer activity to 87 and 96% after 48 and 72 h, respectively. The biocompatibility of coated samples for mesenchymal stem cell (*MSC*) line was found 72%, considered to be bio-safe as per ISO standards. Recently, Jian et al. [94] proposed a novel Ce/Mn composite conversion coating for Elektron (EV) 31 Mg alloy with efficient corrosion resistance and self-healing features. Composite bath comprised of 0.1 M $KMnO_4$, 0.02 M $Ce(NO_3)_3$ was adjusted at pH 1.5 in room conditions. Thus Mg substrate is treated in the bath for various intervals (i.e., 15, 30, and 60 s). The coating morphology for 30 s treated sample was reported more uniform and compact with a thickness of 680 nm. After seven days of immersion in a 3.5% NaCl environment, the coating shows an adhesion strength of 5B grade. It was observed that the presence of Mn^{2+} ions facilitates the conversion of $Ce(OH)_3$ (K_{sp} 1.6 × 10^{-20}) to a highly insoluble $Ce(OH)_4$ compound with a much lower solubility index (K_{sp} 2.0 × 10^{-48}) [95]. Thus formed stable cerium species deposited at the scratched sites and limited expansion of scratch. In contrast, continued scratch growth was observed for conventionally coated samples by phosphate conversion method due to active corrosion. Nevertheless, Ce compounds are known for suppression of oxidative stress and free radical production, which otherwise, could promote several neurodegenerative diseases, such as Parkinson's disease, trauma, ischemic stroke, Alzheimer's disease (AD), and aging [96]. Recently, Ce based compounds are reported for promoting angiogenesis induction [97] and peroxidase mimicking activity [98] for breast cancer cell detection. However, being a rare-earth element, several studies reported the systemic toxicity and genotoxicity associated with Ce compounds. Pulido et al. [99] investigated that higher surface content of Ce^{3+} (40–58%) exhibited a toxic effect, due to superoxide dismutase (SOD) mimetic activity and H_2O_2 production, which is toxic to the cells. However, at lower percentage (between 26% and 36%) it displayed catalase mimetic activity, which broke down

Table 1
Various PCCs with subsequent pre/post coating treatment details for biodegradable Mg alloys.

Coating	Bath Composition	pH	Temp, °C	Duration, mins	Adhesion strength (MPa)	E_{corr} (V/SCE)		I_{corr} (A/cm^2)		Corrosion rate (mm/year)	Pre/post treatment	Ref.
						Uncoated	Coated	Uncoated	Coated			
Ca–P	0.7 M calcium nitrate and 1.5 M phosphate acid (85% V/V)	2.8–3.0	40	5	–	−1.43	−1.35	67 × 10^{-6}	6 × 10^{-6}	0.22 ± 0.03	–	[76]
Mn–P	0.1–0.5 M $H_2PO_4^-$, 0.1–0.5 M Mn^{2+}, 0.01–0.05 M NO^{3-}, 0.01–0.05 M $EDTA^{4-}$	3.0–4.0	60	10	–	−1.65	−1.62	31.5 × 10^{-6}	13.2 × 10^{-6}	–	Pre-treatment of uncoated AZ91-T4 Mg substrate in bath containing $EDTA^{4-}$ and NO^{3-} complexing agents to remove the unwanted $Al_x(Mn,Fe)_y$ phase	[77]
Ca–Mn–Ba–P	10 ml/L Mn $(NO_3)_2$, 10 g/L $Ba(NO_3)_2$, 6 g/L $Ca(NO_3)_2{\cdot}4H_2O$, and 20 g/L $NH_4H_2PO_4$	3	30	30	–	−1.58	−1.51	45.2 × 10^{-6}	24.1 × 10^{-6}	–	–	[78]
La–P	$(MgNH_4PO_4){\cdot}6H_2O$, $(MgHPO_4){\cdot}3H_2O$, 20 g/L La $(NO_3)_3$	3.75–4.25	55	20	–	−1.54	−1.59	40.7 × 10^{-6}	7.07 × 10^{-6}	0.046	–	[79]
Mn–Ce–P	0.1 M $KMNO_4$, 0.02 M Ce $(NO_3)_3$, 0.02 M $K_4P_2O_7$	1.5	25	1	5B	−1.62	−1.52	15.6 × 10^{-6}	2.2 × 10^{-6}	–	Pre-treatment of LZ91 Mg substrate in alkali environment to achieve thin layer of Mg $(OH)_2$/LiOH and MgO/Li_2O	[80]
Sr–P	0.5–1.0 M Sr $(NO_3)_2$, 0.03–0.6 M $NH_4H_2PO_4$	1.0–3.8	80	15	–	–	–	–	–	–	–	[81]
Mg–P	0.4 m/L Mg $(NO_3)_2$, 0.2 m/L H_3PO_4	2.7	60	20	9.4	−1.51	−1.54	18.8 × 10^{-6}	0.20 × 10^{-6}	–	–	[82]
Zn–P	0.1 m/L Zn $(NO_3)_2$, 0.2 m/L H_3PO_4				1.8		−1.50		1.79 × 10^{-6}			
Zn–Mg–P	0.4 m/L Mg $(NO_3)_2$, 0.1 m/L Zn $(NO_3)_2$, 0.2 m/L H_3PO_4				5.6		−1.43		2.57 × 10^{-6}			
Ca–Mg–P	0.4 m/L Mg $(NO_3)_2$, 0.2 m/L Ca $(NO_3)_2$, 0.2 m/L H_3PO_4				5.2		−1.68		0.31 × 10^{-6}			
Zn–Ca–P	0.1 m/L Zn $(NO_3)_2$, 0.2 m/L $Ca(NO_3)_2$, 0.2 m/L H_3PO_4				2.5		−1.47		3.54 × 10^{-6}			
Zn–Ca–Mg–P	0.4 m/L Mg $(NO_3)_2$, 0.1 m/L $Zn(NO_3)_2$, 0.2 m/L $Ca(NO_3)_2$, 0.2 m/L H_3PO_4				6.3		−1.39		2.19 × 10^{-6}			

H_2O_2 to molecular oxygen, protecting the cells against oxidative damage. There is still a lack of adequate knowledge regarding the environmental and health risks associated with RE elements. Studies reported that exposure to RE elements might cause neural damage, which declines the locomotor frequency of body bending, head thrashing, and pharyngeal pumping. Under chronic exposure, significant loss of dendrite and soma of neurons induced down-expressions and other behavioural deficits [6,100].

- *Fluoride Conversion Coatings (FCCs):* Several authors [101–104] reported the development of FCCs on Mg alloys for biomedical implant applications. The coating procedure is typically performed by immersing Mg or Mg alloy substrates in 40%–48% hydrofluoric (HF) acid solution [69,105]. The Mg alloys passivate spontaneously by the formation of $Mg(OH)_2$. In a highly acidic solution like 40–48% HF, the stability of $Mg(OH)_2$ is very poor, and hence it would involve an exchange reaction with HF. Thus, The FCCs are composed a mixture of MgF_2 and $Mg(OH)_{2-x}F_x$. However, the spontaneous passivation as well as slow rate of conversion of $Mg(OH)_{2-x}F_x$ to MgF_2 limit the FCCs thickness [106]. The low-solubility characteristics of FCCs in aqueous physiological solutions possess significant corrosion resistance potential for magnesium alloys. The FCCs often reduces hemolysis to as low as 5%, promotes cell adhesion and proliferation, and does not cause any cytotoxicity. Nevertheless, hydrogen evolution during coating formation leads to the generation of pores in the FCCs, while internal stress promotes cracking of the coated layer. Additionally, the lower thickness, presence of pores and cracks, and a lower F/O ratio determined by the volume fraction of the hydroxyl to fluoride fraction of $Mg(OH)_{2-x}F_x$ limit the ability of FCCs to offer long-term corrosion protection in NaCl as well as in physiological solutions. Dziková et al. [107] developed fluoride conversion coating on AZ31 Mg alloy at two coating temperatures, 430 °C, and 450 °C, and three coating times, 0.5, 2, and 8 h in $Na(BF_4)$ molten salt. Increased coating temperatures and coating times led to higher coating thicknesses with reduced defects that were uniformly distributed on the coating surface, thereby enhancing corrosion resistance. The defect-producing intermetallic compounds in coatings were stabilized by an increase in temperature and time.

In physiological media, a single FCC is unable to provide meaningful shielding from aggressive ions. Recently, Sathyaraj et al. [108] fabricated a fluoride conversion coating on pure Mg. Following deposition of magnesium phosphate coating in the first stage, magnesium fluoride-magnesium phosphate duplex coating was developed in the second stage. The author reported that the structural homogeneity of the duplex coating was increased with an increase in treatment time from 0.5 to 2.0 h. The positive shift in E_{corr} and decrease in I_{corr} reduced the corrosion rate of duplex coated Mg to 0.023 mm/year, whereas the corrosion rate of MgF_2 coated Mg was 0.32 mm/year. The bonding strength of the duplex coating was 13.46 MPa, almost similar to the recommended value of 15 MPa for biomedical applications as per ISO 13779–2 standard. Zhang et al. [109] prepared a stearic acid (SA) modified composite fluoride conversion film (CaF_2/MgF_2) on AZ31 Mg alloy. The results indicated superhydrophobic response of composite fluoride conversion coating with an average water contact angle of 152°. Therefore offered better corrosion resistance than the fluoride conversion film and fluoride-treated AZ31 alloy. Despite a non-toxic response towards bone marrow mesenchymal stem cells (BMSCs), the coating was not conducive to BMSCs adhesion.

- *Organic Conversion Coatings (OCCs):* The currently investigated inorganic coatings show excellent adhesion strength, yet there are several issues like poor osteointegration, non-biodegradability, metal contamination that need to be addressed for its clinical usage [110]. Organic conversion coatings based on biodegradable organic polymers are a promising alternative approach. Organic polymers with chelating functional groups can be quickly bonded with the Mg surface [111]. Such chelating groups on the top coating layer provide anchoring sites for deposition of additional coating layers of the same or different composition. Moreover, they act as inherent hosts for inhibitors-loaded nanoreservoirs to impart self-healing characteristics at mechanically damaged coating sites. Most OCCs are carried out using weak organic acids like tannic acid (TA), vanillic acid (VA), stannic acid (SA), gallic acid (GA), and phytic acid (PA) [112]. They form insoluble complexes by chelation with metallic ions released from the substrate at damaged site, which imparts self-healing coating characteristics [113]. Additionally, the OCCs are widely explored for producing super-hydrophobic anion surfaces, which show significant corrosion resistance [114,115]. Saji et al. [112] investigated that the presence of β-phases in Mg alloys affects the reaction kinetics of conversion phenomena by galvanic coupling, resulting in non-uniform coating thickness. Therefore, pre-treatments are primarily required before the deposition of OCCs. Similarly, Post-treatments play an essential role in sealing spatial defects of OCCs. Several attempts have been made to improve the corrosion resistance of organic conversion coatings. The conversion coating is dependent on bath composition, conversion parameters, and pre/post coating treatments, and Table 2 summarizes the fabrication parameters, pre/post treatments, and performance details of various OCCs developed on Mg alloys.

Liu et al. [130] obtained PA/Ca^{2+} conversion coating on Mg–Sr alloy by layer by layer self-assembly method to deter spatial defects. The introduction of Ca^{2+} significantly enhanced PA's inter-molecular chelation ability, which resulted in spatial defect-free coating morphology with self-healing characteristics. The PA/Ca^{2+} coated substrate demonstrated improved electrochemical corrosion resistance compared to uncoated substrate. The PA/Ca^{2+} coated sample showed an increase in expression for alkaline phosphatase activity (ALP) by 60% compared to the uncoated sample, signifying osteoblast and osteogenic differentiation response of coated substrate. To enhance the corrosion resistance of OCCs, Lin et al. [131] fabricated a noble coating architecture with an organic gallic acid layer sandwich between synthetic PLGA polymer layers on ZK60 Mg substrate for bioresorbable coronary artery stents. The coated sample shows a positive shift in E_{corr} to −0.24 V_{SCE} from −1.59 V_{SCE} for bare substrate with a decrease in I_{corr} nearly 10^4 times. Apart from highly corrosion resistance behaviour, coated samples show a hemolysis rate of 2.1%, which was less than the clinical bio-safety limit of 5%. Interestingly, GA acts selectively against smooth muscle cells (*SMCs*) and endothelial cells (*ECs*). In a 48-h long wound closure study, coated samples show 14% more proliferation towards *ECs* and inhibit *SMCs* growth by 4%. Additionally, the uniform release of GA via sandwich PLGA layers enhanced the free radical scavenging by 35% compared to bare substrate in diphenyl-2-picrylhydrazyl (*DPPH*) media. Thus, anti-oxidative ability eliminates the oxidant stress for vascular tissues and promotes endothelialization. The investigations on OCCs are limited to weak organic acids only. A comprehensive research gap is available to investigate composite/hybrid forms of phenolic molecules like TA, SA, PA, ECGC with synthetic polymers like PCL, PLA, PDA, and PLGA for enhanced corrosion resistance and bio functionalities.

Furthermore, many polyelectrolytes and nanoparticles are known to induce Ca–P conversion coatings on Mg alloy. Cui et al. [132] have developed a novel SnO_2-doped Ca–P coating on AZ31 Mg alloy. The embedded SnO_2 nanoparticle enhanced the structural integrity and crystallization of the coating. Additionally, they acted as heterogeneous nucleation sites where Mg^{2+} and Ca^{2+} combined with PO_4^{3-} ions [133]. Unfortunately, the porous structure of the coating results in poor bonding strength, not sufficient to be used for clinical applications. Polyelectrolytes have recently attracted attention by inciting Ca–P conversion coatings on Mg alloys as they facilitate heterogeneous nucleation of Ca–P precipitates with uniform coating deposition. Shanaghi et al. [134] reported that the Ca–P layer deposited on PAA-coated AZ91 Mg alloy significantly improves the osseointegration response. Using a special heat treatment, yang et al. [135] developed a defect-free SiO_2/PAA coating that acts as a template for mineralizing Ca–P layers on AZ31 Mg alloy. The dense precipitation of Ca–P on SiO_2/PAA enhances the corrosion resistance and cytocompatibility response.

3.1.2. Micro arc oxidation (MAO) coatings

MAO, also known as plasma electrolytic oxidation (PEO) or anodic spark deposition (ASD), is an electrochemical technique to grow oxide

Table 2
Various OCCs with subsequent pre/post coating treatment details for biodegradable Mg alloys.

Coating	Bath Composition	pH	Temp, °C	Duration, mins	Adhesion strength (MPa)	E_{corr} (V/SCE)		I_{corr} (A/cm^2)		Corrosion rate (mm/year)	Pre/post treatment	Ref.
						Uncoated	Coated	Uncoated	Coated			
PA-HA composite	0.70 wt % PA Soln, 35–50% (wt/wt) HA	4.5	40	20	–	−1.60	−1.41	40.20×10^{-6}	2.28×10^{-6}	–	–	[116]
PA-Ce(III) nanocomposite	5 mM PA, 20 mM $CeCl_3$	–	–	3	5B	−1.46	−1.37	3.47×10^{-3}	4.71×10^{-8}	–	Coated sample treated in ethanol/HDMS (10μl/10 ml) solution for 6 h to obtain superhydrophobicity with contact angle (167.3°).	[117]
Vanillic acid	1.0 mmol/L Vanillic acid soln.	–	20	1440	–	−1.53	−1.40	56.9×10^{-6}	0.58×10^{-6}	–	Pre-treatment of uncoated substrate in 1 M NaOH for 24 h.	[110]
Vanillic acid	1.0 mmol/L Vanillic acid soln.	–	20	1440	–	−1.41	−1.25	–	–	–	Pre-treatment of uncoated substrate in NaOH for 1.5 h	[118]
PA-Stannic acid multilayer	2 g/L $Ce(NO_3)_3$, 10 ml/L H_2O_2) (Step-1)	6	40	20	–	−1.42	−1.28	1.81×10^{-4}	2.12×10^{-7}	–	MAO Pre-treatment in 10 g/L Na_2SiO_3, 3 g/L NaOH, and 10 ml/L triethanolamine.	[119]
	20 g/L Na_2SnO_3, 4 g/L NaF, 3 g/L NaOH (Step-2)	12.5	60	60						–		
PA/Silane hybrid	PA and γ-APS Soln. with molar ratios (1:1, 1:2, 2:1), mixed with 40 ml EtOH/H_2O soln.	8	20	30	–	−1.70	−1.61	49.41×10^{-6}	3.95×10^{-6}	–	Pre-treatment of uncoated substrate in 3 M NaOH at 80 °C for 24 h	[120]
CaP/Collagen	23.6 g/L $Ca(NO_3)_2{\cdot}4H_2O$, 34.2 ml/L H_3PO_4, 7 mg/ml Col-I Soln prepared in 0.005 acetic acid.	2.8	37	10	–	−1.47	−1.23	27×10^{-6}	87×10^{-8}	–	Post treatment of Ca–P converted sample by dipping in Col soln. for 15 min.	[121]
HA/Tannic acid	0.05 g Na_3PO_4, 0.25 g $Na_2B_7O_4$, 0.04 g $C_{76}H_{52}O_{46}$, 0.05 g NH_4VO_3, 0.055 g K_2ZrF_6, and 0.02 g HNO_3 in 50 ml DI H_2O (Step-1)	4	37	540	–	−1.46	−1.30	4.89×10^{-6}	5.64×10^{-8}	–	Pre-treatment of uncoated substrate in 1 M NaOH for 24 h followed by heating at 150 °C for 24 h.	[122]
	14 mmol/L $Ca(NO_3)_2$, 8.4 mmol/L NaH_2PO_4, 4 mmol/L $NaHCO_3$ (Step-2)	–	37	2880						–		
MgF-Tannic acid	40% HF (v/v) soln., TA was dissolved in 2 mg/mL Tris–HCl soln to obtain 2 mg/mL final conc.	10	25	1440 (HF) 180 (Ta)	–	–	–	–	0.24×10^{-6}	–	Pre-treatment of uncoated substrate in 5 M in boiled NaOH for 3 h	[123]
Chitosan-Tannic acid	Chitosan (Mw 1.8×10^6) and tannic acid (Mw 1701.2 g/mol) were dissolved (50:50, 50:80) in 0.1 M acetic acid with 2% conc.	–	–	–	σ_{max} (UTS) of coating after 0, 24 and 48 h of immersion in PBS was 3.5, 7.5 and 5.5 MPa	–	–	–	–	–	To analyse tannic acid release profile coated sample immersed in SBF (pH 7.4), SGF (pH 1.2), SIF (pH 6.8) and found suitable for pH around 7.	[124]
Chitosan (CHI)/Bioactive glass(BG)	1.5–6.0 g/L CHI soln. in 1% vol acetic acid, 6 g/L BG	3.31–3.62	75	15–120	–	–	–	–	–	–	–	[125]

(*continued on next page*)

Table 2 (*continued*)

Coating	Bath Composition	pH	Temp, °C	Duration, mins	Adhesion strength (MPa)	E_{corr} (V/SCE)		I_{corr} (A/cm^2)		Corrosion rate (mm/year)	Pre/post treatment	Ref.
						Uncoated	Coated	Uncoated	Coated			
Gallic acid (GA)-hexamethylenediamine (HD)	GA and HD were mixed (wt % 1:3, 1:1 and 2:1)	–	37	360	–	−1.59	−1.61	54.0 × 10^{-5}	8.0 × 10^{-7}	–	An in-situ MgO/$Mg(OH)_2$ layer chelated beneath coating layers, obtained from 1:1 and 2:1 bath soln.	[126]
Catechol (CA)/ polyethyleneimine (PEI)	2 mg/ml CA, 4 mg/ml PEI	8.5	22	720	5B	−1.59	−1.37	Log (−4.19)	Log (−7.34)	0.01	Heparinization treatment was given to coated samples by immersion in 4 mg/ml Heparin dissolved in water-soluble carbodiimide and a mixed solution of 1 mg/ml 1-ethyl-3-(3-(dimethylamino)propyl) carbodiimide hydrochloride (EDC) and 9.8 mg/ml 2- morpholino ethanesulfonic acid (MES).	[127]
Epigallocatechin gallate (EGCG)/ polyethyleneimine (PEI) multilayer	1 mg/ml EGCG and 1 mg/ml PEI Soln in Tris-buffer.	7.4	37	30	5B	−1.33	−1.25	Log (−4.46)	Log (−6.65)	0.05	–	[128]
CaF_2- Stearic acid (SA)	Saturated $Ca(OH)_2$ and 0.05 M/L SA ethanol soln.	–	70	240	5B	−1.57	−1.10	4.25 × 10^{-6}	4.13 × 10^{-8}	0.94	Pre-treatment in 40 wt% HF soln. for 5 days	[109]
MnO_2 – Stearic acid (SA)	0.1 M $MnSO_4$, 0.02 M SA in ethanol soln.	–	22	240 (MnO_2) 300 (SA)	5B	−1.61*	−1.32*	*6.84 × 10^{-7}	2.70 × 10^{-8}	–	Pre-treatment in 0.01 M $MnSO_4$ soln. for 1 h.	[129]

layers on metallic substrates. MAO produces stable coatings with higher bonding strength and wear resistance, when compared to other anodization techniques like electrophoretic or electrochemical deposition [136]. The set-up consists of an anode (i.e., the substrate), an electrolytic media, and a cathode, usually stainless steel. The coating composition and morphology are dependent on process parameters; applied voltage, bath chemistry, pulse frequency, and reaction time [137]. Typically, MAOed Mg substrates have micro-sized pores [138]. Porous coatings are not recommended for long-term implant applications, because ions can penetrate the pores and damage the Mg substrate with prolonged immersion in physiological media. Thus, alone MAO coatings are not enough for significant shielding of Mg-based implants.

Several studies [138–141] indicated that the addition of trace elements like Ca, P, and Zn to the electrolytic media significantly reduced the pore sizes in MAO coatings. This may be attributed to their deposition at pore openings. Bakhsheshi-rad et al. [112] deposited Zn-HA incorporated MAOed coating on Mg–Ca alloy. The corrosion rate of the Mg–Ca sample (4.5 mm/year) was reduced to 0.2 mm/year, further reduced to 0.02 mm/year by adding TiO_2. Additionally, author claimed enhanced anti-bacterial response and cellular adhesion of TiO_2-ZnHA MAOed sample towards gram-negative bacteria and *MG-63* cell line, respectively. Tang et al. [142] added ZrO_2 nanoparticles in an electrolytic solution to produce Zr doped MAO coating on AZ91 Mg alloy. The author claimed that under the high temperature of discharge spark, a stable Mg_2ZrO_5 compound is formed and deposited in the micro-pores of coating. Compared to MAOed AZ91, the average pore size reduced from 40 mm to 10 mm, which increased corrosion resistance by six orders of magnitude. Wen et al. [143] reinforced the HA matrix with graphene oxide (GO). The GO-HA MAOed coating substantially reduced the pore-density as shown in Fig. 5 (a) and (b), which resulted in a 58-fold drop in I_{corr}, from 2.12 mA/cm^2 for an uncoated sample to 36.43 μA/cm^2, respectively. Additionally, GO contains abundant carboxy and carbonyl functional groups, which created strong interfacial bonding via Vander-wall forces with HA molecule and promoted HA attachment resulting in adhesion strength of 40.7 MPa. An alkaline electrolytic solution using Ethylenediaminetetraacetic acid (*EDTA)* was prepared by Gu et al. [144] After the MAO coating of AZ31 Mg alloy, the sol-gel dip-coating technique deposited the HA layer. The chelating ability of *EDTA* resulted in strong and uniform HA deposition with effective sealing of spatial defects, as shown in Fig. 5(c). Consequently, The E_{corr} from −1.24 V for MAOed AZ31 shifted to −0.309 V for the HA-MAOed AZ31 sample. The HA-MAOed AZ31 sample maintained E_{corr} values of −0.59 V after immersion in physiological media for seven days, indicating effective corrosion inhibition.

To obtain a novel self-sealing approach, Daavari et al. [145] proposed in situ formations of biocompatible and high strength multi-walled carbon nanotubes (MWCNTs) on MAO coating. Besides promoting tissue response and lubricity, MWCNTs have a unique ability to bridge crack-tips caused by high electric discharges, resulting in a smooth and uniform coating surface. The I_{corr} was significantly decreased by nearly 10^3 times when compared to the MAOed AZ31 sample. Authors also claimed the introduction of MWCNTs to improve the dry wear performance of MAO coating by reducing the coefficient of friction (μ) by 15% and wear depth by 60% compared to MWCNT free coating.

A polymeric top-coat is widely reported to seal pores, and many studies on polymer-MAO composites/multilayer coatings have also been reported [146–149]. However, the permeable matrix of polymer coating offer pathways for the diffusion of aggressive ions. With prolonged immersion, such ions successfully reached the base Mg substrate. Once corrosion phenomena are initiated, the abundant release of H_2 causes blisters formation. The accumulation of H_2 under polymeric layer makes them grow and ultimately burst with prolonged immersion [150]. Additionally, polymeric layers are prone to swelling and subsequent delamination in the presence of physiological media [151]. Therefore, recent studies are oriented to address the challenges related to polymeric

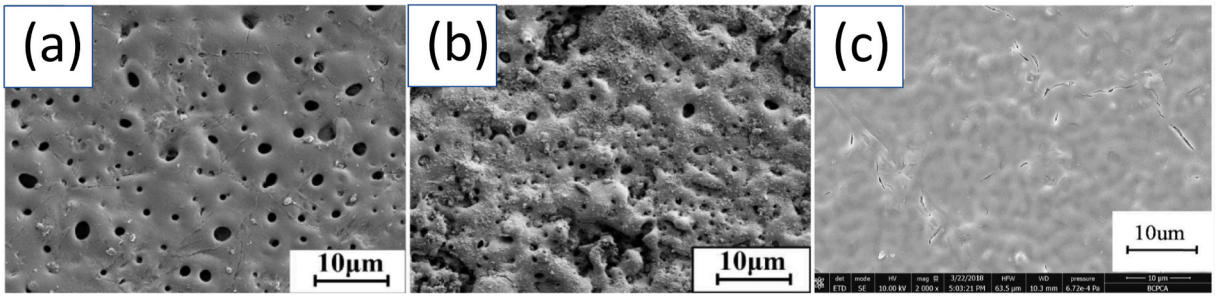

Fig. 5. SEM morphologies of (a) MAOed AZ31 (b) HA/GO coated MAOed AZ31 Mg alloy, reproduced with permission [143]. Copyright 2017, Elsevier and (c) *EDTA* functionalized HA coating on MAOed AZ31 alloy. Reproduced with permission [144]. Copyright 2018, Springer.

top-coats for MAO pore sealing. Kannan et al. [152] fabricated an inorganic Ca–P layer sandwiched between the MAOed and PLLA layers on pure Mg substrate using a spin coating technique. The triple-layer barrage positively shifted the E_{corr} with significant drop in I_{corr} from 28.79 μA/cm^2 to 0.24 μA/cm^2. However, the evaporation of organic residue from the Ca–P layer and chloroform from the PLLA matrix creates spatial defects in the polymeric top layer. Butt et al. [153] cladded a 5–10 μm thick PLA layer on MAOed AZ31 Mg alloy by injection moulding. The author reported that micro-anchoring sites on MAOed surfaces resulted in mechanical locking of the PLA layer. The electrostatic interaction between PLA and MAOed layers resulted in a highly compact two-layered coating with effective sealing. Only 0.14% weight loss was observed after immersion in Hank's solution for 30 days. After immersion, the drop in ultimate tensile strength (UTS) for the PLA-cladded MAO sample was 15% lower than alone MAOed sample. Currently, Polyacrylamide (PAM) hydrogels are gaining interest in enhancing MAO coatings' shielding efficiency. PAM hydrogels have a unique combination of hydrophilic and hydrophobic functional groups that promote in-situ binding in aqueous media and expand the 3D polymeric network for effective covering of underlying substrate. Guo et al. [154] coated Ce-loaded PAM hydrogel on MAOed AZ31 Mg alloy. The Ce^{2+} ions encapsulated in the polymer matrix oxidized to the more stable Ce^{4+} ionic state during exposure to physiological media. The packing of Ce^{4+} ions compacts as the PAM is swallowed by an aqueous solution, which effectively sealed MAO defects. When the coating is mechanically scratched, the release of Ce ions from the PAM matrix forms a compact layer of CeO_2 on the scratched area, imbuing it with self-healing properties. Similarly, Zhang et al. [155] deposited a highly stable and biosafe compound Ce-IV between the MAO micro-pores. The pore size of MAOed Mg ranging between (1–5 μm) were entirely closed by the cerium compound, which enhanced the corrosion rate from 10.25×10^{-3} to 4.27×10^{-3} mm/year. Recently, Zhang et al. [156] reported the achievement of self-healing characteristics for pore sealing on MAOed AZ31 alloy by incorporation of bovine serum albumin (BSA) in PBS media. BSA adsorption was caused by electrostatic attraction due to the difference in isoelectric point of BSA (pI_{BSA} 4.7 < pH 7.4) and MAOed AZ31 (pI_{MAO} 12.4 > pH 7.4). During active corrosion of MAOed AZ31 sample in PBS media, the $RCH(NH_2)COO^-$ group of BSA molecule combined with Mg^{2+} ions formed an $(RCH(NH_2)COO)_2Mg$ complex on the surface that effectively sealed the MAO pores and acted. Thus effective shielding against aggressive ions significantly drops the I_{corr} by 10^4 times compared to alone MAOed coated sample. Typically, MAO is an anodic coating deposited on secondary phase particles in Mg alloy. Ly et al. [157] observed that coarse size and randomly distributed secondary particles in Mg alloy increase the coating porosity. The author carried out Equal angular channel pressing (ECAP) Mg–Zn–Ca alloy before deposition of MAO layer. The secondary phase particles $Ca_2Mg_6Zn_3$ were fragmented and uniformly redistributed. The smaller grain size resulted in small-sized micro-arc discharge channels, which resulted in the reduction of avg. pore size from 0.77 μm for MAOed sample to 0.43 μm ECAP/MAOed sample. The corrosion rate of the ECAP/MAOed (0.087 mm/year) sample was nearly ten times lower than the MAOed sample. Xiong et al. [158] pre-treated AZ80 Mg alloy with LSP to obtain grain refinement. The fine-grained surface attributed limited pore channels and reduced average porosity. According to the stress corrosion cracking (*SCC*) results, AZ80 Mg LSP/MAOed samples fail after 22 h at ultimate tensile stress (*UTS*) of 267.3 MPa, while the MAOed samples fail after 13 h at 225.5 MPa. The size and distribution of micro-porosities strategically influence the corrosion resistance, adhesion, and biocompatibility response of MAO coatings. More chemically and mechanically driven pre-treatments and post-treatments techniques must be explored deliberately to tailor the micro-porosities in MAO coatings.

Electrophoretic deposition (EPD) is another widely used electrochemical technique for the preparation of bioactive coatings on MAOed Mg alloys. Combining their approaches can significantly reduce degradation rates and improve the biocompatibility, or other desirable properties of Mg alloys. Typically, a thick oxide layer was fabricated using MAO to enhance the corrosion resistance of the underlying Mg substrate; EPD was used to seal the porosity associated with MAO layer and provide desired functionalities. Wu et al. [159] developed MAO and MAO/EPD coatings on AZ31 Mg alloy. MAO coatings exhibit improved corrosion resistance with increasing coating thickness. By increasing the thickness of the EPD coating, the corrosion resistance was marginally enhanced. However, the EPD coating effectively reduces micro porosity and micro cracks in MAO coating, MAO and EPD together yielded corrosion resistance in the range of 10^8 Ω cm^2 in corrosive media. Several studies have reported the fabrication of various Ca–P coatings including HA [160–163] and FHA [164,165] by combination of MAO and EPD techniques. Yu et al. [140] fabricated EPD processed FHAp coating on MAOed AZ31 Mg alloy. Compared to FHAp and MAO alone, FHAp/MAO coating significantly improved cell adhesion, proliferation, and alkaline phosphatase expression. Bakhsheshi-Rad et al. [166] prepared a TiO_2 incorporated micro-arc oxidation coating (TMAO) followed by electrophoretically deposited zinc doped HA (ZnHA) coating on Mg-0.7Ca alloy. In comparison to TMAO and ZnHA alone, TMAO/ZnHA coatings demonstrated a greatly enhanced inhibition zone against Escherichia coli (*E. coli*) without compromising the cell-viability of MG63 osteoblast cells.

3.1.3. Anodic oxidation

The anodic oxidation coating technique uses the principle of classical electrochemical conversion to create a film of varying thickness (5–200 μm) on a substrate. During anodization, Mg (i.e. substrate) serves as an anode and an oxide film is grown on the Mg substrate in presence of aqueous or non-aqueous electrolyte [167]. Being simplest surface modification technique, anodic oxidation coatings are widely reported for efficient corrosion resistance and bioactive response on Mg alloys [168–171]. However, it is difficult to grow protective anodic layers on Mg and Mg alloys due to the unfavorable Pilling-Bedworth ratio (PBR) for MgO [172]. PBR is defined as the ratio of the volume of metal oxide to the volume of the corresponding metal oxidized to produce the oxide.

The Oxide layer would not protect a metal surface if PBR is less than unity, because the oxide film formed in that case would be porous or cracked, as usually happened in magnesium's case. Therefore, it is necessary to promote the incorporation of species other than O^{2-} in the electrolytic media to improve the Mg and Mg alloy corrosion resistance through anodic oxide layers. Recently, Zaffora et al. [172] carried out anodic oxidation of AZ31 Mg alloy in K_2HPO_4 and K_3PO_4 containing hot glycerol electrolyte to facilitate the formation of $Mg_3(PO_4)_2$, which exhibits superior PBR and corrosion resistance than MgO layer. Additionally, $Mg_3(PO_4)_2$ containing oxide layer show better cellular response for MC3T3-E1 cells compared to MgO layer. According to Geng et al. [173] the composition of Mg alloys effects the corrosion resistance offered by oxide layers. Using the same anodization parameters, Mg-1Gd and Mg–1Zn-1Gd yielded MgO, and $Mg_3(PO_4)_2$ containing oxide layers with more crystalline and defect-free structures, while MgO and Al_2O_3 containing oxide layers on AZ31 Mg alloy showed higher porosity and larger pores. Consequently, Mg–Gd alloys shows better long-term degradation performance compared to anodized AZ31 Mg alloy. Since, anodic oxidation coatings singularly cannot full fill diverse clinical demands several studies reported their combination with chemical conversion [174,175], electrodeposition [176], LDHs [177], sol-gel [178] coating techniques. These coatings exhibit promising improvement in corrosion resistance and bioactivity of Mg alloys.

3.1.4. *Ion implantation-*

Ion implantation/Ion beam processing is a technique for introducing highly energetic ions (10–200 KeV) on substrate surface via bombardment. Ion implementation set-up consists of three main components: an ion source, ion accelerator, and target material. This surface coating method modifies the surface tribological characteristics, resulting in improved adhesion between the coating layer and substrate [179]. Two methods can achieve ion implantation: conventional beam-line ion implantation and Plasma Immersion ion Implantation (*PIII*). The primary advantages like selective surface modification, low temperature, and reproducibility are significant for coating Mg alloys [180,181]. However, amorphization caused during ion implantation causes surface devoid of grain boundaries, resulting in enhanced corrosion [182]. As ion implantation is a non-thermodynamic process, studies have reported the generation of compressive residual stresses and increased surface roughness of the ion-implanted surface. A wide range of ion implantations on biodegradable Mg alloys is reported in the literature, as shown in Table 3. Implantation of Al, Zr, Ce, Sn, Ca, and N ions revealed that the gradient structure of ions in the metal matrix provided a passive oxide layer of the metal substrate and implanted ion [183–185]. The compactness of the composite oxide layer formed at the ion-implanted surface plays a crucial role to enhance the in vitro corrosion resistance. Liu et al. [186] conducted Ag, Fe, and Y ion implantation on Mg -1Ca alloy. The non-uniform aggregation of second phase particles at grain boundaries resulted in an oxide layer with uneven thickness. Additionally, the increase in surface roughness enhanced the corrosion activity for Ag and Fe ion-implanted samples. However, Y ion implantation resulted in a compact Y_2O_3 layer with minimal MgO presence, decreased the corrosion rate to 0.69 mm/year. Jamesh et al. [187] fabricated Zr ions using the *PIII* method on ZK60 Mg alloy. Authors reported that Zr exists as Zr^{4+} ions due to the high energy imparted by *PIII* (i.e., 182.2 KeV). Zr^{4+} possesses a very high tendency to form zirconium phosphates instead of calcium phosphates in psychological media, resulting in unstable and soluble apatite [188].

Dual ion implantation has been reported to overcome the limitations associated with single ion implantation. Jamesh et al. [189] investigated the effects of dual ion Zr/N *PIII* coating on corrosion resistance of WE43 Mg alloy. The formation of ZrN, ZrO_2 oxides efficiently passivates the Mg substrate and promotes the mineralization of calcium phosphate instead of Zr–P after immersion in *DMEM* solution. Similarly, Cheng et al. [190] conducted Zr/N dual ion implantation on AZ91 Mg alloy in female Sprague-Dawley rats. In vitro cytocompatibility test on *MG-63* cell line enhanced cell viability and ALP activity. Consequently, in-vivo bone formation improved significantly, as shown in Fig. 6. Despite the anti-inflammatory response, mature and intact bone tissues were found on Zr–N coated AZ91 implant compared to the uncoated implant. The compact oxide layer consisting of metal nitrides/oxides features neutral pH and limited release of Mg ions in the *DMEM* media. Limited work has been reported for the complex corrosion behaviour of dual ion implemented Mg alloys in physiological media.

Recently, Istrate et al. [196] employed a unique atmospheric plasma jet (APS) method in order to deposit ZrO_2–Y_2O_3 and ZrO_2–CaO coatings on Mg–Ca and Mg–Ca–Zr substrates. Both coating types show similar Young moduli and a hardness within the range of 0.2–0.4 GPa. For ZrO_2–Y_2O_3 and ZrO_2–CaO, the elastic modulus values were measured between 11-27 GPa and 16–31 GPa, respectively. Compared to ZrO_2–Y_2O_3, ZrO_2–CaO provides a superior corrosion rate and better adhesion. In the MTT colorimetric tests, moderate cell viability was observed between both coating types, indicating no significant differences in cytocompatibility.

3.1.5. *Alkali heat-treatment coatings-*

In alkali heat-treatment coatings, Mg alloys are exposed to a supersaturated aqueous solution of $NaHCO_3$, Na_2HPO_4, and Na_2CO_3 alkaline

Table 3
In-vitro corrosion performance of Mg and Mg alloys after implantation of various ions.

Substrate	Ion implanted	ionic oxide layer (nm)	Ionic Penetration (nm)	In Vitro corrosion conditions	I_{corr} uncoated (A/cm^2)	I_{corr} Coated (A/cm^2)	Corrosion rate (mm/year)	Ref.
AZ31	Al	–	13	*SBF*, 37.5 °C	2.82×10^{-5}	3.36×10^{-5}	–	[184]
AZ91					1.50×10^{-4}	5.82×10^{-5}	–	
ZK60	Zr, O	23	80	*SBF*, 37 °C	4.09×10^{-4}	1.1×10^{-7}	–	[187]
WE43	Ti, O	32	64	*SBF*	3.27×10^{-4}	1.44×10^{-5}	–	[191]
Mg–1Ca	Ag	50	70	Hank's solution, 37 °C	–	–	–	[186]
	Fe	70	110–120			–	–	
	Y	95	105			–	0.69 ± 0.18	
Pure Mg	Ce	26	70	Artificial Hand sweat	1.06×10^{-4}	3.99×10^{-5}	–	[183]
				Ringer's solution	4.18×10^{-5}	2.68×10^{-5}	–	
				DMEM	2.04×10^{-5}	5.20×10^{-6}	–	
Mg-Gd-Zn-Zr	Sn	–	90	*SBF*	1.17×10^{-5}	5.74×10^{-6}	–	[192]
AZ91	Zr, N	16	80	NaCl	4.26×10^{-6}	1.16×10^{-6}	–	[190]
				DMEM	1.08×10^{-5}	3.92×10^{-7}	–	
Mg–1Ca	Zn	–	150	*SBF*, 37 °C	2.48×10^{-4}	3.21×10^{-4}	–	[193]
Pure Mg	Ca	45	30	*SBF*, 37.5 °C	1.61×10^{-4}	1.00×10^{-4}	–	[182]
	Zn					1.40×10^{-4}	–	
AZ31	N	–	200	Hank's solution, 37 °C	–	–	–	[194]
Pure Mg	Zr	30	60	*SBF*	5.26×10^{-5}	1.99×10^{-5}	–	[195]

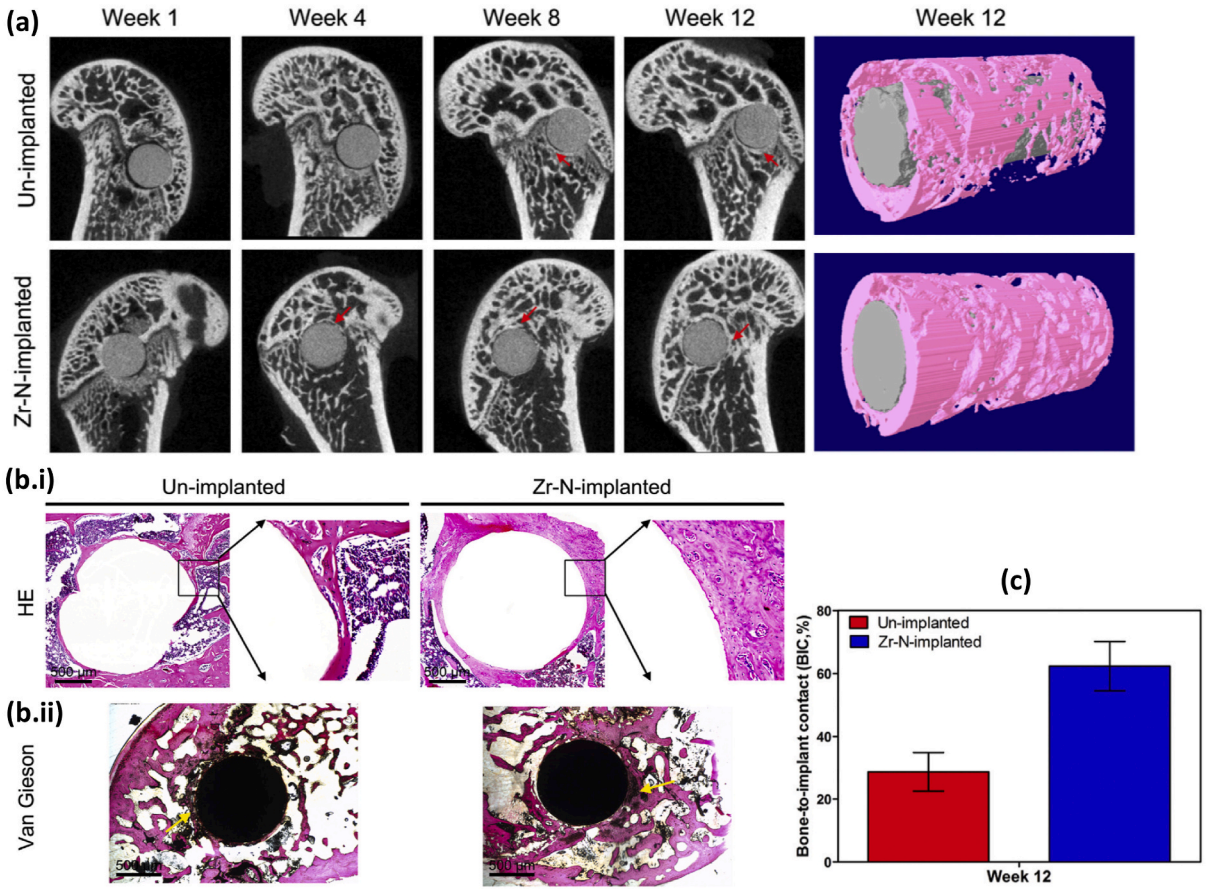

Fig. 6. **(a)** Micro-CT 2D characterization of uncoated and Zr–N coated AZ91 Mg alloy after 4, 8, and 12 weeks of implantation at predrilled bone tunnels of lateral femur epicondyles in female Sprague-Dawley rats (The red arrows depict the formation of new bone, the yellow arrows show formation of gas cavities) and 3D reconstruction of bone (pink color) and implant (white color) after 12 weeks of surgery, **(b.i)** Hematoxylin and eosin (*H&E*) stained images, **(b.ii)** Van Gieson's picrofuchsin stained images showing bone formation (yellow arrows) at uncoated and Zr–N coated AZ91 implant, **(c)** Bone-to-implant contact percentage of uncoated and Zr–N coated AZ91 after 12 weeks of implantation. Reproduced with permission [190]. Copyright 2016, Elsevier.

compounds in an autoclave maintained at high temperature (i.e. ~ 500 °C). The pH value of solution decides the density, thickness, and morphology of the coated layer [197]. Usually, alkali heat treatment produces thick coatings consisting of crystalline $Mg(OH)_2$ flakes and a stable hydroxide with good adhesion and corrosion resistance. Tang et al. [198] reported adhesion strength of 60 MPa between $Mg(OH)_2$ layer obtained by alkali heat-treatment. However, numerous spatial defects like pores and cracks limit its tendency as an efficient physical barrier to isolate underlying Mg substrate in corrosive media for longer immersion times. Additionally, chlorine ions in the SBF transform Mg $(OH)_2$ into a highly soluble MgCl2 compound, as shown in Equation (1):

$$Mg(OH)_2 + Cl^- \rightarrow MgCl_2 + OH^- \quad (1)$$

The excess of OH^- ions increases H_2 evolution, which enhances the degradation rate of Mg substrate with prolonged immersion [199]. Therefore, these coatings are not preferable as a top layer. However, as a primer layer, they are well established for better corrosion resistance and the middle layer for strengthening the adhesion between the substrate and the outer layer [200]. In contrast, some studies utilized it as a post-treatment technique to convert amorphous dicalcium phosphate dehydrate (*DCPD)* coatings to highly crystalline HA coatings, which efficiently shielded the Mg substrate in physiological media [3,141,201,202].

Recently, Pan et al. [203] employed alkali heat-treatment as a pre-treatment on AZ31 B Mg alloy before the deposition of a multilayered self-assembled 3-aminopropyltrimethoxysilane (*APTMS*), poly (ethylene glycol) (PEG), and fibronectin/heparin complex coating. The significant hydrophilicity exhibited by alkali heat treatment promoted the immobilization of coating layers and resulted in stable multilayered coating architecture. The alkali heating treatment significantly improved the corrosion resistance, resulting in favourable cellular growth conditions. Hence, the cytocompatibility towards endothelial cells was significantly augmented. Additionally, Author reported a notable enhancement in hemocompatibility due to significantly lower hemolysis rate and higher platelet adhesion.

3.1.6. *Layered double hydroxide (LDHs) coatings*

LDHs coatings possess a unique class of coatings on Mg alloys, which can be achieved by in-situ and ex-situ deposition techniques. LDHs are hydrotalcite-like (HT) compounds composed of noble anionic clays with layered brucite structures [204]. The General formula for LDHs is $[M^{2+}_{1-X} M^{3+}_X (OH)_2]^{X+} (A^{m-})_{x/m}. nH_2O$, here M^{2+}, M^{3+} symbolizes layer of divalent metallic cations (e.g. Mg^{2+}, Co^{2+} Zn^{2+}, Mn^{2+}, Cu^{2+}, Ni^{2+}) and trivalent metallic cations (e.g. Al^{3+}, Cr^{3+}, V^{3+}, Fe^{3+}, Mn^{3+}, Y^{3+}) respectively [205]. A^{m-} is the layer of intercalated anions between two subsequent cationic layers. The nature of intercalated anion may be either organic (e.g. Asp, PA, LA) or inorganic (e.g. NO_3^-, Cl^-, PO_4^{3-}, CO_3^{2-}). M is the charge of intercalated anion; whereas x represents the molar ratio of $M^{3+}/(M^{3+} + M^{2+})$ typically ranging between 0.20 and 0.33 [206]. The LDHs synthesis involved the controlled dissolution of the Mg substrate. Generally, Al-rich Mg alloys like AZ31 are the most favourable and investigated alloy for LDH coatings. The release of Mg^{2+} and Al^{3+} ions from the substrate during dissolution provides a necessary supply of cations for the formation of the cationic layer [207]. These

cations occupy the octahedral holes in the brucite $Mg(OH)_2$ layer, and interlayer anions intercalate such cationic layers to balance the charge [208]. In the presence of corrosive media, the anions in the double layer structure are replaced by the aggressive anions (such as Cl^-), and anion exchangeability is decided by anion exchange equilibrium constants of various LDH anions in the order: $CO_3^{2-} > SO_4^{2-} > OH^- > F^- > Cl^- > Br^- > NO_3^- > I^-$ [208]. The significant capturing of Cl^- ions reduces aggressive ions in corrosive media. Furthermore, the replaced ions from double-layer structures bind with metal ions to form physio-chemically stable precipitates on the coating surface. The corrosion effectiveness of coating depends on the ion-exchange rate of intercalated ions. Thus, the anions equipped with corrosion inhibition, self-healing, self-cleaning, biocompatible, anti-bacteria features provide great potential for a multifunctional approach of LDHs coating on Mg alloy for implant application. It can be seen that the majority of intercalated ions are inorganic and participation of organic anions is minor, although organic compounds are considered more bio-functional than inorganic compounds [209]. One major reason behind such observation is high temperature and pressure conditions. However, ex-situ LDH techniques like co-precipitation (CPT), electrochemical deposition (ED), and Spin coating are suggested as substitutes, but they have limitations of poor adhesion and time consumption [210].

Recently, various inorganic/organic composite and hybrid LDH coatings have been developed to enhance corrosion inhibition, as summarized in Table 4. Cao et al. [208] fabricated Superhydrophobic MgAl-LDH coating by intercalating F^- anion. An additional layer of stearate acid was created on MgAl–F-LDH by immersion method. The superhydrophobic behavior (CA = 152.6°) given by stearic acid significantly reduces the adsorption of Cl^- ions. The superior ion exchangeability of F^- stockpile a large amount of Cl^- ions and make a stable MgF_2 compound on the coating surface, which further suppress the attacking of aggressive ions. Coating remains intact after 30 days of immersion in a 3.5% NaCl atmosphere with only 3% water uptake compared to 18% shown by alone LDH coating. Recent attempts have been made to achieve self-healing LDH coating by depositing an additional layer of healing agents on LDH coating or introducing healing molecules as an active cation in the double-layered structure. Li et al. [211] proposed a bio-friendly thiophene derivate corrosion inhibitor (CI) for self-healing of Mg–Al-LDH coating by fabricating a noble *N*-alkyl-N, *N*-dimethyl-*N*-(3-thienylmethylene) ammonium bromide (*NTA*) molecule and deposited on MgAl-LDH by immersion method. Along with a highly positive shift in E_{corr}, the stable physiochemical adsorption of NTA provides significant self-healing character on damaged Mg site as systematically shown in Fig. 7. It is worth noting that the biocompatibility of the *NTA* molecule was not reported. In a unique approach for self-healing, Asl. et al. [212] replaced Al^{3+} cation in the conventional MgAl–CO_3^{2-} structure with Ce^{3+} cation by co-precipitation (CPT) method. On mechanical scratching of the coated substrate, the oxidation of trivalent Ce^{3+} ion resulted in the formation of tetravalent Ce^{4+} ion, which formed a highly stable metallic complex with a low solubility index (K_{sp}, 2×10^{-48}), giving super self-healing characteristic. However, due to the size mismatch between Mg^{2+} and Ce^{3+} ions, the long-term stability of coating architecture with prolonged immersion in physiological media is yet to be established.

The latest LDH coatings are still struggling to impart in-situ biofunctional behavior, although they have tremendous encapsulation ability to deliver drugs, corrosion inhibitors, and other biomolecules. However, the unfavorable processing parameters (i.e., high temperature, pressure) and the use of carbonated anions (i.e., CO_3^{2-}), which suffer from poor ion-exchangeability, limit the ability for in-situ loading and release of bioactive molecules in LDH coatings. To address this issue, Petrova et al. [226] demonstrated the formation of Mg–Al-LDH coating on AZ91 alloy by application of organic chelating agents sodium-diethylenetriamine-pentaacetate (*DTPA)* and Salicylic acid (SA) at a low temperature of 95 °C. The Mg substrate was treated in a solution maintained at pH value 10 ± 0.1, consisting of chelating agents and AZ91 flakes as a source of Mg and Al ions. *DTPA* enhances the dissolution of Mg, while SA promotes adsorption and accelerates the growth of LDH coating on the Mg surface. Both chelating agents' synergistic functioning successfully resulted in the formation of LDH coating without the use of high temperature and pressure conditions, which shows its potential to enhance bio-functionalization for clinical applications. However, Al, considered to be neurotoxic, may impede bone calcification and result in osteomalacia when present in excessive levels [210].

Meanwhile, manganese (Mn) happens not to be toxic and activates a variety of enzymes in a physiological environment. Thus, the in-situ synthesis of Mg–Mn hydrotalcite-like films on magnesium alloys appears suitable for clinical applications. Kuang et al. [227] developed Mg–Mn LDHs coatings on pure Mg by an in-situ growth method, which were chemically modified by adsorption of myristic acid (MA). After modification with myristic acid, the solid-liquid contact angle of the Mg–Mn LDHs film (6.8°) was increased to 152.2°, qualifying as a superhydrophobic coating (i.e. Contact angle >150°). The Superhydrophobic coatings exhibited a polarization resistance of approximately 20,000 Ω cm^2. This was more than twice as of Mg–Mn LDHs film, and ten times more than pure Mg substrate. However, the drop in contact angle to 60° after 48 h of immersion indicated gradual deterioration of LDH film with prolonged immersion. Recently, Zhang et al. [228] fabricated a black Mg–Mn(II)-Mn(III) LDH coating on AZ31 Mg alloy to evaluate the biodegradation, osteosarcoma destruction, anti-bacteria, and bone defect regeneration abilities. Due to the unique properties of the constructed black LDH film, including near-infrared optical absorption and reactive oxygen species (ROS) generation in the tumor-specific microenvironment, tumor cells and tissue were significantly eliminated. Furthermore, concomitant bacteria were killed by localized hyperthermia. As a result of the improved corrosion resistance and synergistic bio functions of Mn and Mg ions of the constructed black LDH film, cells were able to adhere, spread and proliferate. This resulted in the promotion of osteogenic differentiation in vitro, and the acceleration of bone regeneration in vivo. Thus, MgMn-LDHs offered an interesting coating architecture for use on orthopedic implants for the treatment of bone tumors and related tissue defects.

3.2. Deposited coatings

3.2.1. Physical vapor deposition (PVD) –

PVD is a standard coating process for Mg and Mg alloys effectively used for four decades for clinical applications. PVD is widely reported for producing high-density coatings with excellent adhesion strength [229,230]. In vacuum conditions, a negatively charged solid target is energized by the bombardment of inert gas atoms. The excited atoms are then transported and condensed at the positively charged Mg substrate. PVD can be achieved by e-beam evaporation and Magnetron sputtering [231]. Magnetron sputtering is preferred over e-beam as it is directional, covers fewer steps, and forms shadow effect [232]. In magnetron sputtering, a magnetic field is configured parallel to the target surface for constraining the electron motion; thus, highly uniform coatings are yielded [233]. The fabrication of Ca–P and various ion substituted Ca–P coatings by PVD magnetron sputtering is widely reported for Mg alloys, as shown in Fig. 8.

The Ca–P coatings produced by magnetron sputtering are highly crystalline, contributing to better bone cell attachment, growth, proliferation, and anti-bacterial properties. Additionally, the Ca/P ratio can be controlled explicitly to form desired Ca–P compound. Yadav et al. [234] achieved hydroxyapatite coating on AZ31 by RF magnetron sputtering with a Ca/P ratio of 1.65, close to the stoichiometric Ca/P ratio of 1.67. The author reported the exponential increase in coating thickness with exposure time. The roughness, R_a of the bare substrate (101 ± 3 nm) increased with coating time up to 6 h and then further decreased to a constant value (115 ± 5 nm) up to 10 h. Contact angle results revealed that uncoated samples with CA (78 ± 1°) were

Table 4
Inorganic and organic intercalated anionic LDH coatings for Mg alloys.

Substrate	Coating	Coating Method	Thickness (μm)	Intercalated anion (inorganic)	E_{corr} (V/SCE)		I_{corr} (A/cm^2)		Corrosion rate (mm/year)	Additional Bio functionality	Ref.
					Uncoated	Coated	Uncoated	Coated			
AZ31	ZnAl-LDH	Hydrothermal treatment	9.49 9.46 10.27 12.71 15.95	NO_3^- Cl^- PO_4^{3-} MoO_4^{2-} VO_4^{3-}	−1.51 −1.51 −1.51 −1.51 −1.51	−1.33 −1.20 −1.09 −0.98 −0.88	7.48×10^{-5} 7.48×10^{-5} 7.48×10^{-5} 7.48×10^{-5} 7.48×10^{-5}	2.13×10^{-5} 7.18×10^{-6} 3.68×10^{-6} 3.42×10^{-6} 3.02×10^{-7}	–	–	[213]
AZ31	MgAl-LDH	Hydrothermal treatment	–	GO	−1.56	−0.65	–	–	–	–	[214]
Mg–Ca	MgFe-LDH	Two-step in-situ growth	–	CO_3^{2-}	−1.67	−1.51	4.31×10^{-5}	3.78×10^{-6}	–		[215]
Mg–3Zn-0.5Zr-0.5Sr	Ag–MgAl-LDH	Hydrothermal treatment	–	–	−1.58	−1.42	2.56×10^{-5}	2.09×10^{-6}	–	Enhanced Cytocompatibility for MC3T3 cell line. Significant Anti-bacterial response against *E.coli* and *S. aureus.*	[216]
AZ31	MgFe-LDH/MAO	Hydrothermal treatment	17	NO_3^-	–	–	–	–	–	–	[217]
AZ31	MgAl-LDH/PGA	Co-precipitation and hydrothermal treatment	44	NO_3^-	−1.40	−1.34	2.39×10^{-6}	8.95×10^{-8}	–	Biocompatibility towards *NIH-3T3* mouse embryonic fibroblast cells was enhanced	[218]
AZ31	MgAl-LDH/PLLA	Steam coating/Dip coating	–	CO_3^{2-}	−1.46	−1.29	1.18×10^{-5}	3.69×10^{-8}	–	Cytocompatibility for *NIH3T3* cell line was improved significantly.	[219]
AZ31	MgAl-LDH/Zn-PDA	Hydrothermal treatment/immersion	20–50 nm	NO_3^-	−1.50	−1.52	1.22×10^{-5}	1.60×10^{-6}	–	Anti-inflammatory response by polarizing *RAW 264.7*, Anti-bacteria response against *S. aureus* and enhanced osteogenic differentiation was shown for *MC3T3-E1* cell line.	[220]
AZ31	MgAl-LDH/Bg	Hydrothermal treatment/Dip coating	5	NO_3^- F^-	−1.51 −1.51	−0.255 −0.324	6.65×10^{-5} 6.65×10^{-5}	3.13×10^{-6} 1.40×10^{-7}	–	Self-repair of coating assisted by ion exchange process, the erosion pits were filled by deposition of fluorapatite/MgF_2	[221]
				Intercalated anion (Organic)							
AZ31	ZnAl-LDH MgAl-LDH	Hydrothermal treatment	9.49 17.01	Asp Asp	−1.44 −1.44	−1.50 −0.8	6.98×10^{-5} 6.98×10^{-5}	3.93×10^{-7} 2.76×10^{-8}	–	–	[222]
AZ31	ZnAl-LDH	Hydrothermal treatment	15.65 17.39	Asp LA	−1.51 −1.51	−1.50 −1.07	7.48×10^{-5} 7.48×10^{-5}	3.93×10^{-7} 2.77×10^{-7}	–		[223]
AZ31	MgAl-LDH	In-situ growth	–	8-HQ	−1.55	−0.766	8.36×10^{-6}	1.70×10^{-7}	–	–	[224]
AZ31	MgAl-LDH	Steam coating	–	MA	−1.45	−1.29	1.29×10^{-5}	1.04×10^{-5}	–	–	[225]

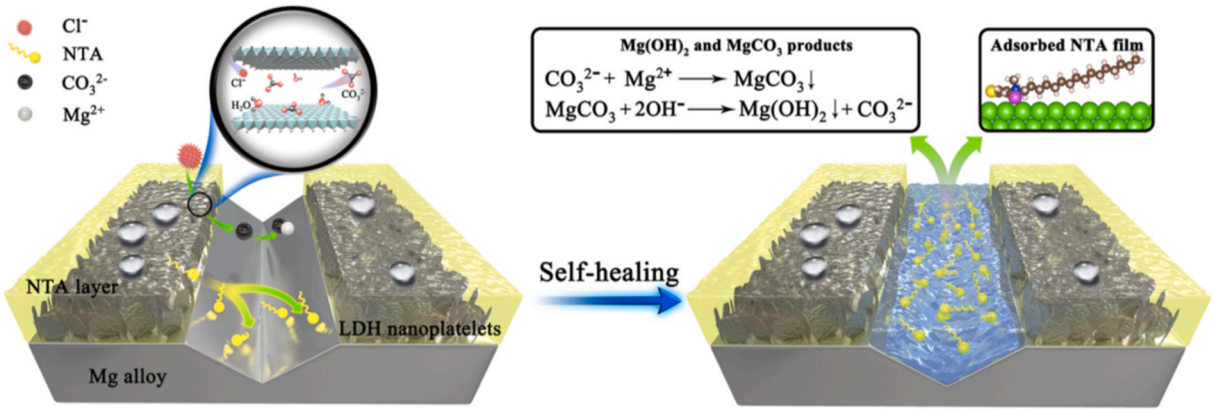

Fig. 7. Schematic illustration of self-healing mechanism by *NTA* adsorption on mechanically damaged MgAl-LDH coating. Reproduced with permission [211]. Copyright 2020, Elsevier.

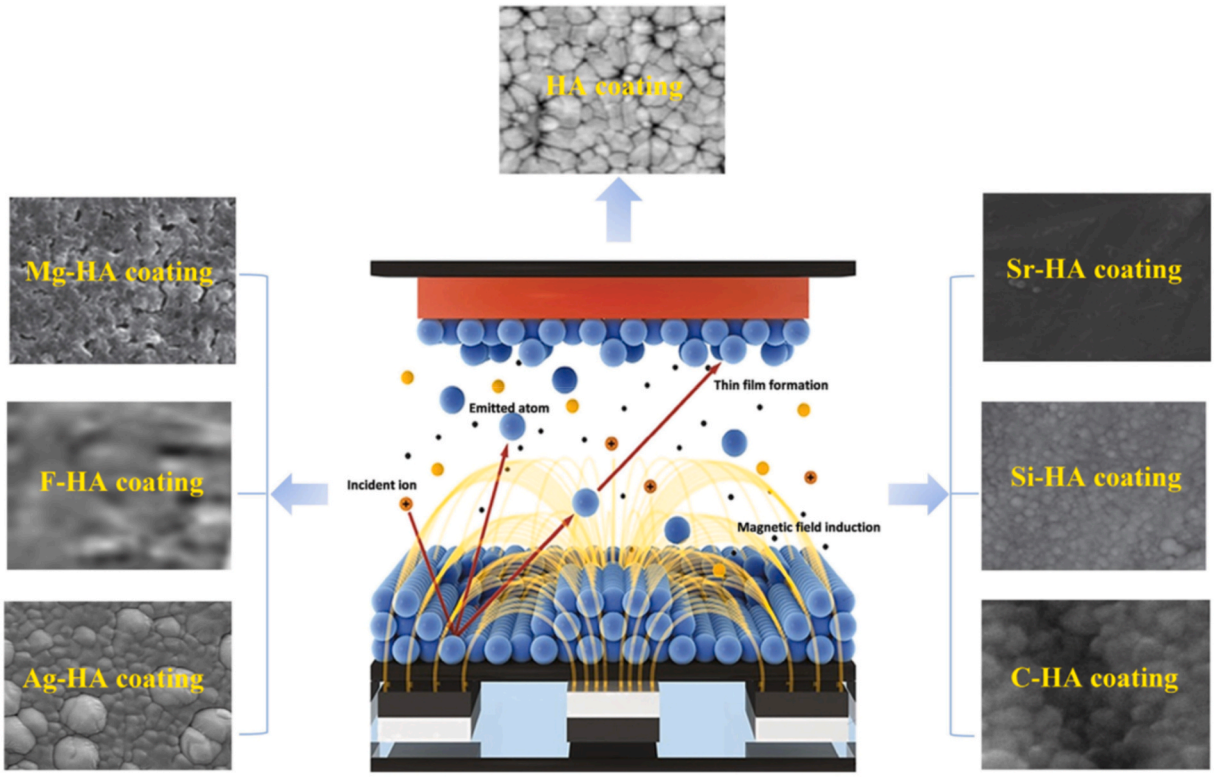

Fig. 8. Schematic illustration of physical vapor deposition via magnetron sputtering for various ion-substituted Ca–P coatings. Reproduced with permission [233]. Copyright 2019, Elsevier.

hydrophilic, whereas, after *RFMS* deposited coating of HA, the sample became hydrophobic (109 ± 2°) due to micro-scale finished coating surface. The immersion study up to 48 days in SBF revealed that the degradation rate constant (K_d) of coated sample (0.015 h^{-1}) lower than the uncoated AZ31 sample (0.020 h^{-1}).

Dinu et al. [235] investigated the tribological behaviour of RF-magnetron sputter-deposited hydroxyapatite coatings in physiological solution on AZ31 Mg alloy. The Ca/p ratio obtained (ranging between 1.83 and 1.97) similar to trabecular bone is due to the re-sputtering of phosphorus ions by negatively charged oxygen ions. Texture weakening of the (002) plane of HA is observed under the target erosion zone due to the atomic peening effect; as a result, the final coating surface is uniform and smooth. The low friction coefficient μ (0.184 ± 0.025) was found for the coated AZ31 substrate as compared to an uncoated substrate (0.306 ± 0.004). Similarly, a low wear rate was determined for coated (4.83 × 10^{-5} mm^3 N^{-1} m^{-1}) than uncoated AZ31 substrate (0.00518 mm^3 N^{-1} m^{-1}). Due to the same phenomena of texture weakening, Surmeneva et al. [236] reported the elastic strain to failure (H/E) and the plastic deformation resistance (H^3/E^2) for an RF Magnetron sputtering HA-coated AZ31 Mg alloy increased by nearly 30 and 74%, respectively.

Zhang et al. [237] fabricated Hafnium (Hf) coating on AZ91D by Magnetron sputtering. The porosity of coated structure was improved from 0.98 to 1.27%. Thus, generated denser structure significantly decreased the I_{corr} with increase in polarization resistance by nearly 100 folds. However, the micro-galvanic sites were evidenced due to the droplet effect and columnar grain size in Hf coatings. Zin et al. [238] achieved a 4.8 μm thick Ta_2O_5 layer on ZK60 Mg alloy. The coated sample yields an I_{corr} of 1.334 ± 0.066 μA/cm^2, comparatively 543 times smaller than the I_{corr} of an uncoated sample. EIS results depicted

that the film resistance and charge transfer resistance of the coated sample in SBF increased by 10^4 folds compared to uncoated sample. Defect-free and uniform formation of Ta_2O_5 promotes corrosion resistance. Hence fewer Mg^{2+} ions leached from the coated surface, and the Ta layer provides a favourable surface for cell attachment and proliferation. Other ceramic oxide coatings like TiO_2, Al_2O_3, AlO_xN_y, SiO_2, GO, Ce_2O_3 [239–242] achieved by Magnetron sputtering improve corrosion and tribological behavior.

3.2.2. Atomic layer deposition (ALD) –

ALD is based on the chemical vapor deposition (CVD) method. In contrast to conventional CVD, which requires high deposition temperature, ALD is a low-temperature technique carried out in two half-cycles. In the first half cycle, a primary precursor, usually an inorganic coordination compound, i.e., a metal center with ligands (TiO_2, HfO_2, ZrO_2,) is pumped into the reactor chamber until it reacts with available surface groups at substrate for the formation of atomic monolayer [243]. Next, the precursor is removed from the chamber using an inert gas (N_2, Ar). In the second cycle, a co-reactant is applied, which reacts with the surface molecules of the primary precursor. This process is repeatedly carried out to increase coating thickness [244]. Thus, obtained ALD coatings are self-limiting due to the occupation of all surface groups [245]. They possess excellent conformality, facile thickness control, and pin-hole free structure [246–248].

Yang et al. [249] deposited a 40 nm thick atomic layer of ZrO_2 Nanofilm on Mg–Sr Alloy. The substrate was treated under different ALD cycles (i.e., 100,200, 300, 400) and found that the deposition becomes denser with the increase in no. of cycles. Thus, better corrosion resistance is observed with an increase in coating thickness. The E_{corr} of ZrO_2 (400 cycles) shifted positively from -1.928 V_{SCE} to -1.75 V_{SCE}, and I_{corr} (4.8×10^{-6} A/cm^2) reduced by two-folds of magnitude as compared to an untreated substrate (3.06×10^{-4} A/cm^2). EIS study revealed that the impedance of coated layer (R_1) and charge transfer resistance (R_2) were enhanced by 10^3 times compared to the untreated surface**.** In vitro study depicted that ALD deposited ZrO_2 nanofilm composed of sufficient binding sites for cell growth and adhesion. Efficient shielding provided by densely packed coated layers mitigates the high alkalization conditions and hydrogen evolution, enhancing biocompatibility. Considering corrosion-assisted cracking phenomena, such as stress corrosion cracking (SCC) and corrosion fatigue, Peron et al. [250] studied the effect of a 100-nm-thick ALD zirconia coating on the SCC susceptibility of AZ31 alloy in SBF. The susceptibility index for ultimate tensile strength (I_{UTS}) and elongation to failure (I_ε) is remarkable dropped from 8.97 (bare) to 2.68 (Zr coated) and 75.1 (bare) to 18.3 (Zr coated) Mg alloy. A decrease in susceptibility from Zr-coated sampled coincided with less hydrogen evolution during immersion, resulting in decreased hydrogen embrittlement. Thus, ALD-coatings show potential to protect Mg alloys in SCC conditions.

Due to its pore sealing tendency, ALD is widely employed in composite form with other coating architectures [251,252]. Recently, Chang-yang li et al. [253] fabricated Ta_2O_5 nanofilm on MAO-coated AZ31 Mg alloy. ALD coating effectively seals the micropores and microcracks presented in MAO coating. Linear polarization results showed that three orders of magnitude decrease the I_{corr} of MAO/Ta_2O_5 coating compared to the substrate and alone MAO coating. Hydrogen evolution experiment conducted by immersion test for 294 h in Hank's solution revealed that MAO/Ta_2O_5 had lesser *HER* (0.005 ml cm^{-2} h^{-1}) than MAO coated (0.012 ml cm^{-2} h^{-1}) and uncoated substrate (0.023 ml cm^{-2} h^{-1}). However, pitting corrosion was observed at random sites due to nano-gapes in the Ta_2O_5 surface layer, resulting in localized substrate damage. Similarly, li et al. [247] prepared Al-doped ZnO (AZO) film by ALD on plasma electrolytic oxidation (PEO) coated AZ31 Mg alloy, which positively shifted the E_{corr} from -1.561 V to -1.343 V in 3.5% NaCl solution. After ALD, the E_{corr} was further shifted to -0.550 V with a decrease in I_{corr} by two orders of magnitude compared to bare Mg alloy. The water contact angle was significantly improved to 130° for composite AZO coating compared to PEO coating (~40°). The high surface finish and nano morphology of the AZO coating contributed to enhanced hydrophobicity, resulting in superior corrosion resistance.

3.2.3. Cathodic electrodeposition -

Cathodic electrodeposition can be achieved by two ways: Electrophoretic deposition (EPD) or Electrolytic (ELD) deposition process. EPD is widely associated with the coating of bio-ceramics, mainly Ca–P, due to its versatility, short deposition time, room temperature conditions, and slight limitation on substrate shape compared to the ELD process [254,255]. Recently, coatings of bio-ceramics like merwinite, diopside, and graphene oxide have also been reported [256–258]. EPD is an electric field-assisted process where the suspended charged particles in a dielectric fluid are deposited on the oppositely charged substrate [259]. The coating morphology is influenced by the suspension parameters like particle size, liquid dielectric constant, conductivity, viscosity, and Zeta protentional of medium [260]. Additionally, the process parameters like deposition time, applied voltage, the concentration of solid suspension, and substrate conductivity significantly affect the process [260].

Kumar et al. [162] developed an EPDed HA coating at 20 V (10 min) on Mg–3Zn alloy for orthopedic application. Firstly, as-casted samples were grounded by 1200 and 2000 grit-sized silicon carbide paper and heat-treated at 300 °C and 400 °C were referred to as HA-12- 300, HA-12-400, HA-20-300, and HA-20-400. Through fine polishing, surface roughness decreases from 130 to 150 (1200 grit) nm to 15–20 nm (2000 grit), which significantly influences the mechanical characteristics of the deposited coating. The critical load-bearing capacity, hardness, elastic modulus, and fracture toughness of the HA-20-400 sample was improved by 50%, 30%, 26%, and 73%, respectively, compared to the HA-12-400 sample. In terms of temperature conditions, the HA-20-400 sample exhibited increased hardness, elastic modulus, and fracture toughness by 37%, 47%, and 48%, respectively, compared to the HA-20-300 sample. The crystalline needle-like structure of HA achieved by increased annealing temp improves the cohesive and adhesive strength of the coating. The E_{corr} of HA-20-400 coated Mg sample was shifted positively compared to the casted substrate from -1.67 $V_{Ag/AgCl}$ to -0.21 $V_{Ag/AgCl}$ with marginal change in I_{corr} from 135 μA/cm^2 to 5μA/in SBF due to the presence of microcracks and pores in the coating.

In contrast, Song et al. [261] focused on obtaining uniform flake-like morphology of HA coating using lower voltage (i.e., 4 V for 2 h) for Orthopaedic application. The flaked HA coating was helpful for the bone tissue to infiltrate into the implants to heal the damaged bone at an accelerated rate. The study reported a two-step ED process; Firstly dicalcium phosphate dihydrate (*DCPD)* and tricalcium phosphate (β-TCP) was formed on AZ91 Mg alloy; secondly, the as-deposited *DCPD* and β-TCP on samples were transformed into HA, which further reduced the I_{corr}. Current density is also a deciding factor for the morphology of Ca–P coatings obtained by ED. Li et al. [262] evaluated the influence of variation in the current densities (i.e., 2.5, 5.0, and 7.5 mA/cm^2) on the properties of HA coating. Increasing current density from 2.5 mA/cm^2 to 7.5 mA/cm^2 decreases the grain size from 413.65 ± 63.12 nm to 264.56 ± 65.33 nm by facilitating the nucleus formation of new crystals and inhibition of growth phenomena. Additionally, the highest crystallinity of 73.52% was yielded at a current density of 7.5 mA/cm^2. Importantly, HA morphology was changed to spherical particles, plate-like, flake-like, and needle-like crystals when electro-deposited for 15, 30, 45, and 60 min, respectively, as shown in Fig. 9. Therefore, increasing current density promotes nucleation, and increasing time promotes growth phenomena.

Although ED is a promising candidate for Ca–P coatings with firm control over morphology and crystallinity, literature reported poor adhesion strength of coatings, resulting in debonding and delamination in physiological media. During the electrochemical deposition, the OH^- ions produced at the cathode due to water reduction, accumulate H_2 bubbles on the cathode (i.e., substrate). It severely affects the nucleation and adhesion of coatings [263]. Pulsed-electrodeposition is investigated

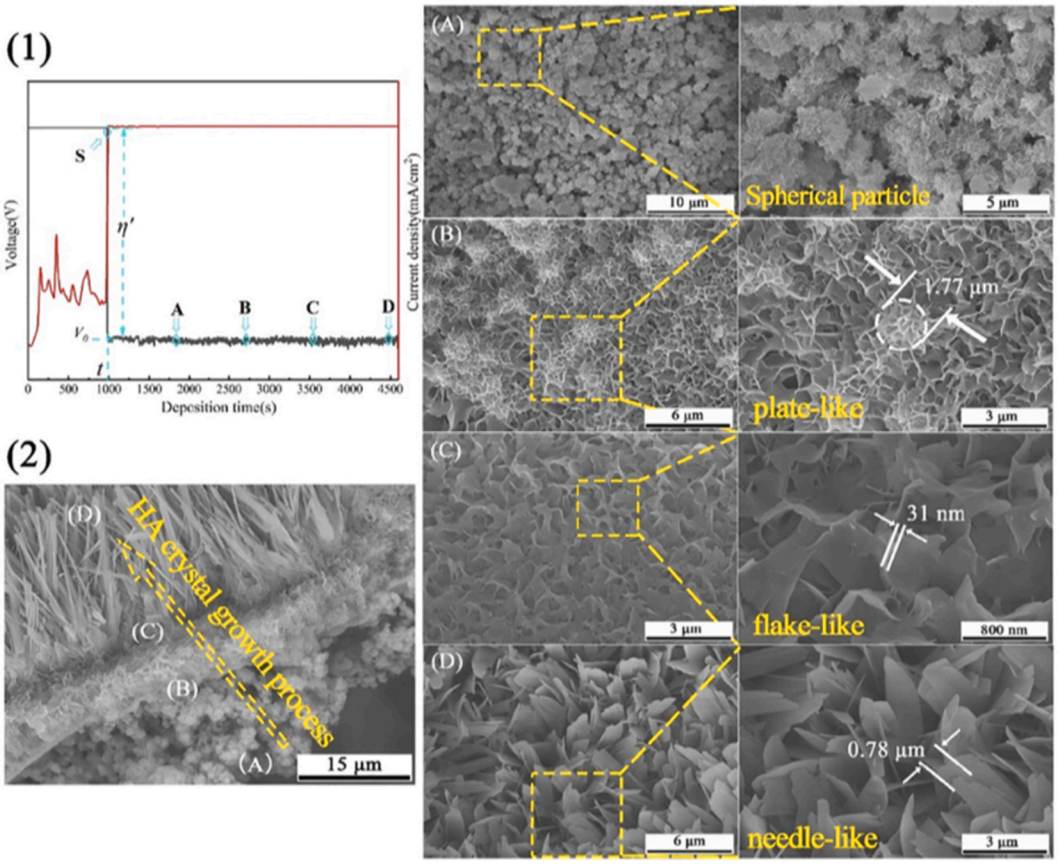

Fig. 9. **(1)** Voltage-current time curve, **(2)** A, B, C, and D represent deposition after 15, 30, 45, and 60 min since reaching the balanced voltage (V_o). Reproduced with permission [262]. Copyright 2019, Elsevier.

to address this issue; recently, Mohajernia et al. [264] compared the HA coating fabricated by conventional and Pulsed ED on AZ31 Mg alloy at −3000mV with a duty cycle of 0.2 s. Pulsed-ED HA coatings had a higher adhesion strength of 16.5 MPa than 11.5 MPa for conventional ED HA coatings. A pulsed-ED HA coating with a uniform and defect-free coating structure reduced the hydrogen evolution rate from 0.01 to 0.001 ml cm^{-2} h^{-1}. The minimum adhesion strength of HA coatings reported for clinical applications is 35 MPa [265]. Researchers follow the MAO-ED composite coating approach to increase the adhesion strength [266]. Chen et al. [267] fabricated HA coating by ED on MAO treated Mg–Zn–Ca alloy. The rod-like nanohydroxyapatite (RNHA) effectively sealed the MAO pores. The pinning force generated by RNHA deposition in the MAO pores increased the adhesion strength of HA coating up to 40 MPa. The coated samples planted in rabbit femora for 50 weeks degraded at a slower rate of 1.24 mm/year when compared to 2.15 mm/year of uncoated substrate. The HA-coated substrate retained structural integrity, whereas the uncoated substrate was suffered from localized corrosion cavities and pits. The histological images of the bone/implant interface in Fig. 10 indicated lymphocytic and plasmablastic inflammations around the uncoated implant, alternatively absent in coated implant. After 50 weeks of implantation, coated implant successfully transformed newly formed osteoclasts and bone trabecular into mature bone.

3.2.4. *Biomimetic and bioinspired coatings* –

Biomimetic coatings impart bioactivity by enhancing the osseointegration response of coated surface [268]. These coatings are employed to biomineralize the bone like inorganic (apatite) and organic (collagen I) phases of natural bone on the surface of an orthopedic implant. Conventionally Ca–P coatings are achieved by chemical conversion, sol-gel techniques facilitate rapid HA mineralization. However, they do not ensure the alignment of mineralized HA with collagen fibrils to determine resemblance with the fundamental nanostructure of natural bone. The mineralized HA must have its c-axis [001] parallel to longitudinal fibrils of cortical bone to deeply penetrate inside collagen fibrils for better adhesion [269]. Biomimetic coatings have a unique mechanism to mineralize apatite with the desired orientation that conventional Ca–P coatings lack. Several organic compounds like dopamine, *EDTA*, arginine-glycine-aspartic acid-cysteine (RGDC) peptides are widely recognized for their unique molecular recognition feature, which accelerated HA formation on implant surface [270].

Currently, research interests are associated with the chelation of bioapatite (BAP), which mimics elements of natural bone [271–273]. BAP is an idealized HA consisting of minor groups of CO_3^{2-}, HPO_4^{2-}, Na^+, Mg^{2+} and trace elements like Sr^{2+}, K^+, F^- up to bio-safe ppm levels [274]. Bio-macromolecules, gelatine, polysaccharides, silk-fibroin, Dihydroxyphenylalamine (DOPA), and lysine can chelate BAP elements via non-covalent bonding like metal coordination, van-der Waals forces, hydrogen bonding, and π- π interactions together with electrostatic effects [275]. Apart from molecular recognition, enzymatic mineralization and molecular crowding techniques are effectively reported for rapid mimicking of natural bone [276,277]. Enzymatic mineralization is carried out by adding an organic phosphate source like alkaline phosphatase (ALP), which catalyses the hydrolysis of water-soluble phosphate esters and Ca^{2+} ions, thus promoting rapid precipitation of Ca–P particles. Colaco et al. [278] investigated enzyme-induced Ca–P biomineralization using ALP extracted from the bovine intestinal mucosa. The author reported that with an increase in ALP concentration from 0.7 mM to 7 mM, the % crystallinity of HA was increased by 22%. However, a further increase in concentration to 70 mM resulted in an amorphous phase. The electron morphology and diffraction patterns are shown in Fig. 11 (b), confirming [002] planer

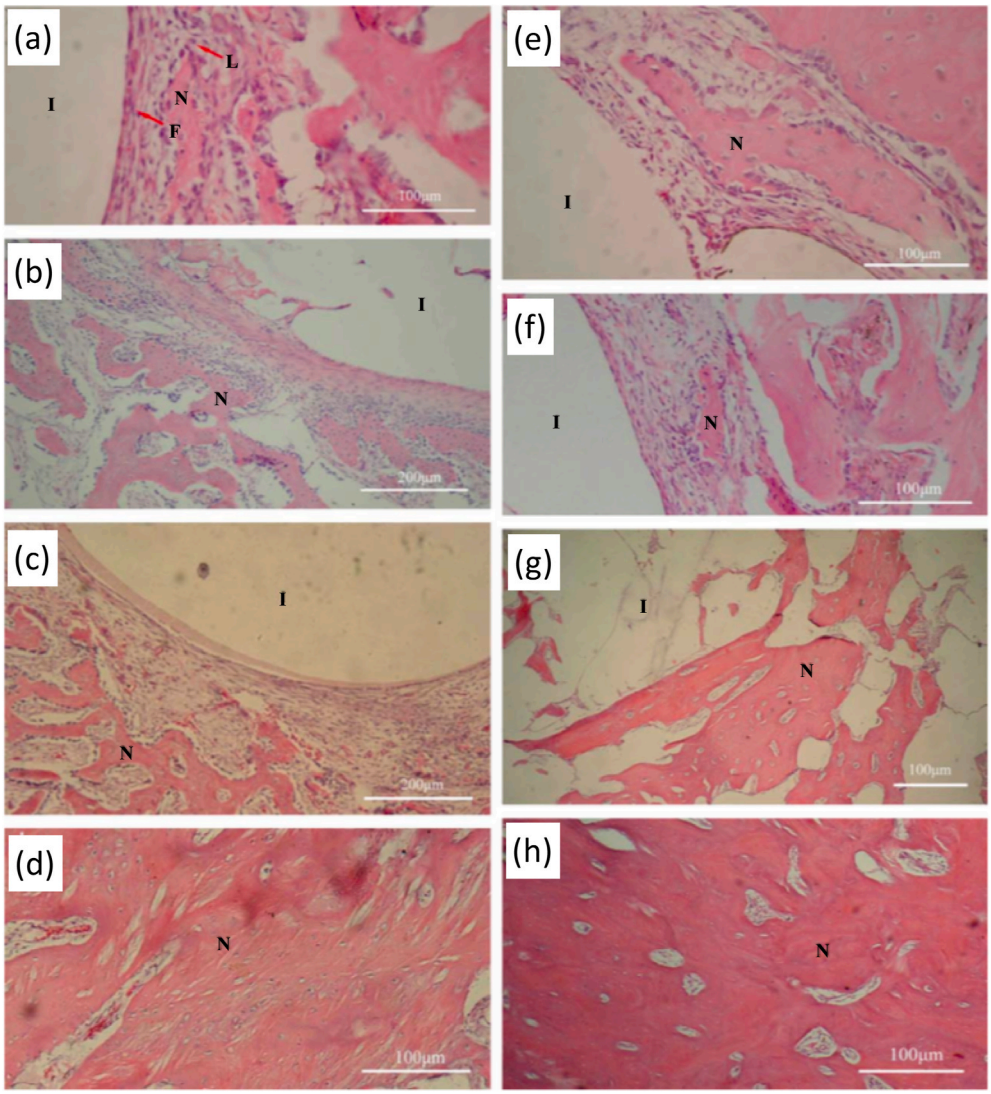

Fig. 10. Histological images of the implant/bone interface around the uncoated substrates **(a–d)** and coated **(e–h)** samples at 8, 12, 18, and 50 weeks. I, L, F, and N represent implant, lymphocytic infiltration, fibroblast band, and new bone tissue, respectively. Reproduced with permission [267]. Copyright 2011, John Wiley and Sons.

orientation of HA crystals. However, the size of HA platelets (length - 61.3 nm, width - 43.9 nm) was greater than gap-zones (i.e., 40 nm) of collagen fibrils, which may inhibit the intrafibrillar growth of HA crystals. Polymer induced liquid precursor (PILP) is an important bio-inspired technique to promote such orientation of biological apatite by using various negative charged polypeptide acids which can act as PILP directing agents such as poly-L-aspartic acid (PASP), poly-allylamine hydrochloride (PAH), and poly-acrylic acid (PAA) [275]. A synergistic effect of electrostatic interaction and capillary action enabled intra-fibrillar mineralization of biological apatite [272]. Additionally, poly-peptides stimulate *N*- and C- terminal domains of non-collagen proteins (*NCP*), which act as potential binding sites for Ca and P ions along with essential trace elements [269,279]. These techniques are widely accepted for bone regeneration scaffolds, but no significant work has been reported to achieve such orientated Ca–P mineralization through the coating.

Recently, Sun et al. [280] took a bio-inspired idea of micro-nano structured natural bone particles for conducive growth of apatite. The author reported the formation of a micro-nano structural HA coating on AZ31 Mg alloy. After 14 days of immersion in SBF, the coating cracks are covered by a thick uniform layer of deposited Ca–P. As a result, the corrosion rate was decreased to 0.3 mm/year from 0.44 mm/year. Even after 147 days of immersion, the corrosion rate was less than 0.5 mm/year, which signified that dense Ca–P precipitation provides efficient shielding against aggressive ions in physiological media. Few studies reported doping bone-seeking trace elements like Zn, Sr as an efficient stimulator for Ca–P mineralization. Zhou et al. [281] modelled a Zn-doped nano-whisker HA coating on ZK 60 Mg alloy. The study reported that up to a particular concentration HA-Zn (5%), with the addition of Zn, the lamellar HA crystal degenerated into a nano-whisker, which has noble osteogenic potential to mimic Ca–P mineralization. The resulting Ca/P ratio of apatite formed on such whiskers was 1.67, identical to natural bone.

Yu et al. [282] examined microwave-assisted Sr doped HA coatings' effect on biomineralization tendency. The addition of Sr significantly enhanced the osteoblast differentiation and induced the osteoclast apoptosis, resulting in apatite formation on the second day of immersion and complete coverage of coated substrate after the fourth day of immersion in SBF with a Ca/P ratio of 1.64. The effective shielding provided by apatite deposition limits the degradation rate from 0.29 mg/cm^2/day to 0.16 mg/cm^2/day with prolonged immersion of 30 days. Currently, organic molecules like chitosan, stearic acid, and bio-metal-organic framework coatings are recognized for exhibiting excellent biochemical signalling for in-vitro mineralization of biological

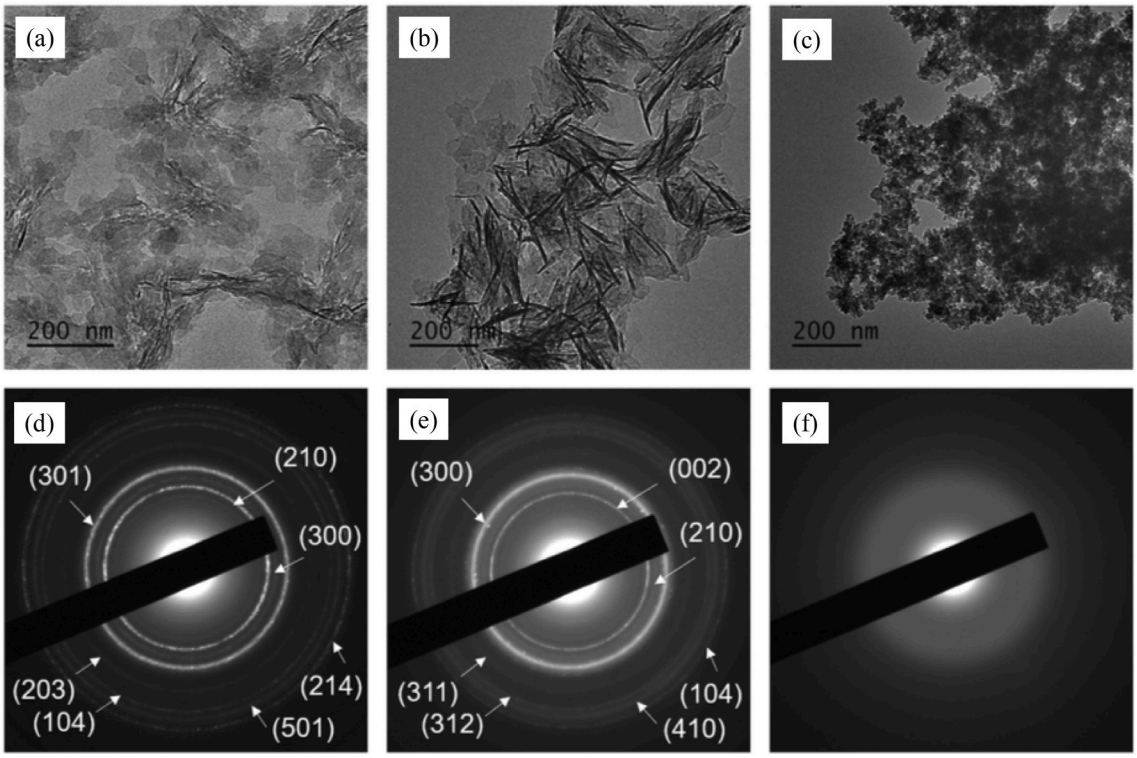

Fig. 11. **(a–c)** TEM images and **(d–f)** SAED patterns of enzyme induced Ca–P mineralized after 24 h at ALP concentration equal to **(a,d)** 0.7 mM, **(b,e)** 7 mM, and **(c, f)** 70 mM, respectively. Reproduced with permission [278]. Copyright 2020, Elsevier.

apatite. Rahimi et al. [283] developed electrospun chitosan/mineralized bone allograft (*MBA)* nanocoating on AZ31 Mg alloy for enhanced bone regeneration ability. Li et al. [284] investigated bio-mineralization by fabricating HA/Stearic acid composite coating on AZ31 B alloy. Apatite with a Ca–P ratio of 1.48 mineralized uniformly after three days of immersion in physiological media. The Ca/P ratio was further improved to 1.54 after 21 days of immersion. Bio-metal-organic framework (Bio-MOF) coatings are known for high specific area, pore-volume, and multifunctional hydroxyl groups that act as nucleation sites for BAP crystals. Liu et al. [274] prepared a Bio-MOF-1 model with zinc and adenine primary elements interconnected with biphenyl dicarboxylate linker, and this phosphorous-rich anionic skeleton provides excellent adsorbing of Ca^{2+} cations. The astronomical mineralization rate resulted in a thick flower-shaped apatite layer with a Ca/P ratio of 1.84 after seven days of immersion in SBF.

3.2.5. *Organic coatings* –

In recent years, organic coatings have received extensive attention for their superior corrosion resistance and multiple bio-functionalities [131,285,286]. Sol-gel is the highly reported coating technique for Mg and its alloys due to its capability to coat organic and inorganic materials on Mg alloys [287]. This coating technique comprises a colloidal suspension of a molecular precursor in a solvent, resulting in subsequent oxide network formation at low temperature and pressure [288]. The process occurs in two phases; the first phase deals with the suspension's hydrolysis and condensation. In the second phase, the polycondensation responsible for the 3-d oxide network is achieved by either dip, spin, immersion, or spray coating methods [289,290]. Mild chemical conditions, low temperature, and pressure enable Sol-gel to be a suitable technique for inciting inorganic phases in the organic matrix and vice versa [291]. Organic coatings can be classified into synthetic and natural polymer coatings. The FDA-approved bio-degradable synthetic and natural polymers coatings are discussed in this section.

3.2.5.1. *Synthetic Polymer coatings* –.

- *Polylactic acid (PLA),* a biodegradable lactic acid polymer (2-hydroxypropionic), is a chiral molecule containing two enantiomers, L-lactide and D-lactide. It is extensively explored for surgical devices, tissue engineering, bone fixation, and drug delivery applications due to its biocompatibility, hydrophobicity, and thermoplastic processability [292]. Fig. 12 (a) shows that the coating is free of spatial defects and has a uniform structure. Studies reported excellent pore sealing capability of PLA when applied as a topcoat on MAOed/inorganic coated Mg substrates to provide an efficient barrier between Mg substrate and electrolyte. However, some issues limit its applications: (i) high tendency towards hydrolysis in aqueous media, (ii) poor load wearing tendency, and (iii) weak adhesion strength with Mg substrates. Few researchers attempted to counter limitations by increasing the coating thickness, but adhesion became poorer [293,294]. Dusselier et al. [295] proposed manipulating the physical properties and hydrolytic degradation of PLA by the racemization of D - and L -isomers or utilizing a hydroxyl acid co-monomer component but still thorough investigation is needed to tailor the physicochemical properties of PLA for long-term implant applications.

- *Poly(lactic-co-glycolic) acid (PLGA)* comprises monomer units as lactic acid (LA) and glycolic acid (GA) [296]. The physical, chemical, and mechanical properties of PLGA can be tailored by altering LA/GA ratio [297]. PLGA coatings are widely recognized for corrosion resistance and drug delivery applications [298,299]. The coating structure shown in Fig. 12 (b, c) is characterized by its clear spatial defect-free appearance. Despite efficient corrosion inhibition, a few generic limitations like high susceptibility towards hydrolysis, entrapment of H_2 during in-vitro immersion, and poor adhesion towards Mg substrate hampers its usage for orthopedic implant application [300]. Recent attempts have overcome these problems,

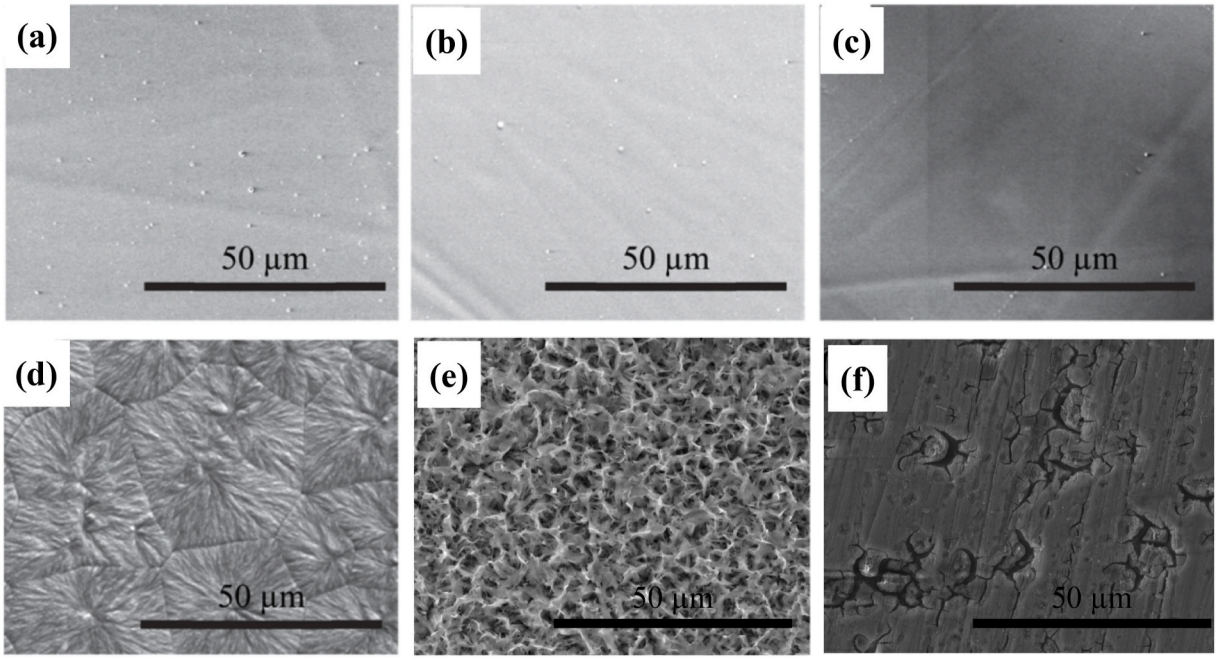

Fig. 12. SEM images of (a) PLLA, (b) PLGA (90:10), (c) PLGA (50:50), (d) PCL, reprinted with permission [303], Copyright 2017, American Chemical Society., (e) PDA/Col (f) PDA coated Mg alloys. Reprinted with permission [121]. Copyright 2020, Elsevier.

but the outcomes still do not fulfill the clinical requirements [301, 302].

- *Polycaprolactone (PCL)* is the highly investigated biodegradable polyester. Fig. 12 (d) shows the crystalline morphology of PCL coating on pure Mg. It has a relatively much lower degradation rate when compared to PLA and PLGA [303]. Moreover, the hydrolysis in PCL can be further retarded by co-polymerizing with polymers like DL-lactide valerolactones, which significantly enhance its degradation time in physiological media [304]. Due to low glass transition temperature (i.e., 60 °C), PCL promotes fabrication of unique microporous networks, which can be achieved by Non-solvent - Solvent induced phase separation (*NIPS*) techniques. Specially designed pores assist the escape of H_2, which otherwise may cause delaminating or debonding coatings. Such micro-pores acted as cell-anchoring sites, promoting osseointegration and cell viability [305]. Alone, PCL coatings suffered from poor adhesion with Mg substrates due to a limited number of oxygen sites in PCL structure, resulting in weak electrostatic interaction with Mg substrate. Recent studies suggest adding inorganic components like HA to enhance the adhesion strength; however, such inorganic particle-matrix increases PCL's water uptake ability and enhances hydrolytic degradation [306]. Thus, more research needs to be done to intensify the usefulness of PCL on Mg-based alloys for implant applications.

- *Polydopamine (PDA)* has been synthesized from an organic compound of catecholamine and phenethylamine families known as dopamine (DA). DA is exposed to air in a basic aqueous solution to achieve PDA [307]. It possesses unique features like excellent adhesion strength, protein adsorption, and hydrophobicity in physiological media. Fig. 12 (e, f) is a typical SEM image showing a variety of micro-cavities. Combining PDA with inorganic coatings like TiO_2 and HA significantly enhances Mg alloy biocompatibility and corrosion resistance [308,309]. Additional application features biosensing and target drug delivery make it a suitable candidate for the coating of biodegradable Mg implants [310].

3.2.5.2. *Natural Polymer coatings* –.

- *Chitosan (CS)* consists of glucosamine and *N*-acetylglucosamine units linked together by glucoside bonds [311]. Unlike synthetic polymers, the degradation of natural polymers does not alter physiological pH values; hence, considered more biocompatible [297]. Besides corrosion resistance, chitosan is applied in artificial skin and drug release applications. It is widely reported as a versatile carrier for healing agents in self-healing coatings. Jia et al. [312] reported that CS in polysaccharide form is loaded with trivalent cerium. After mechanical scratching, a controlled release of cerium ions from the CS nano-reservoirs validates the self-healing characteristic. Other chitosan/HA duplex coatings reported enhanced biocompatibility and corrosion resistance [313–315].

- *Collagen (Col)* is one of the most abundant polymers present inside the organic matrix of dentin, bone, tendons, and ligaments in the human body [316]. A primary reason for its application as a coating agent is its ability to promote an identical tissue structure on coated implants similar to natural bone [317]. Thus, generated assemblies provide adequate mechanical resilience and toughness to tissue functioning [318]. Studies reported that the collagen coating on Mg alloys improves the hydrophobicity in physiological media. However, Zhao et al. [319] reported that fibrils on the Col-coated AZ31 Mg alloy were initiated only when the Col-1 monomer reached a particular concentration. The electrostatic interactions originating from pH change of physiological media regulated the shape and density of mineralized fibrils. Wang et al. [320] reported faster degradation of Col coated Mg substrate in SBF when compared to Mg alloy coated with synthetic polymers. The application of collagen for Mg alloys is not thoroughly investigated yet, and detailed studies regarding corrosion resistance, drug delivery, and other functionalities can open new gateways for implant applications.

3.2.5.3. *Other organic coatings* –.

- *Phytic acid (PA)* is a naturally occurring polymer, mainly extracted from plant seeds, roots, and stems [321]. The unique presence of six phosphate groups and twelve hydroxyl groups facilitates its chelating ability towards metal ions (Mg^{2+}, Ca^{2+}, Zn^{2+}, etc.), as

shown in Fig. 13. During in-vitro degradation of Mg alloys, the leached Mg^{2+} ions are chelated by phosphate groups present in PA, resulting in the formation of stable compounds like $Mg_3(PO_4)_2$, which has a shallow solubility index (K_{sp}) of 1.04×10^{-24} [322]. Additionally, the chelating of Ca^{2+} ions from physiological media promotes osteoinductivity by mineralizing various Ca–Mg–P and Ca–P compounds like Whitlockite, Magnesium-phytate, and HA [112]. Puvada et al. [323] investigated the antimicrobial efficacy of PA by the addition of *NaOCl* and *EDTA* ingredients. Along with promising biocompatibility, PA showed an efficient anti-bacterial response against *E. Faecalis*. PA coating developed using chemical conversion, and microwave-assisted treatment is suffered from spatial defects, which adversely affect the corrosion resistance [119, 324]. Several attempts have been made to address the issue by pre-treatment and compounding with other elements, but it further alleviates the problem [116]. The noble presence of negatively charged OH^- ions on PA provides sufficient potential for deposition by layer by layer (LbL) self-assembly and Sol-gel coating techniques, which are not investigated yet. The implementation of such coating techniques may address challenges associated with the deposition of PA coating on Mg alloys.

- *Serum-albumin (SA)* is a major component of the circulatory system responsible for drug deposition and maintaining blood pressure [325]. Earlier investigations reported enhanced corrosion resistance and biocompatibility of SA towards Mg alloy [326,327]. Recently, Harandi et al. [328] reported the short-term corrosion protection ability of SA in phycological media. However, *SA* starts making chelates with the corrosion product and destabilizes the coating with prolonged immersion. Hence, the corrosion phenomena accelerated, which increased the susceptibility towards SCC for SA coated AZ91D compared to the uncoated substrate. El-Taib et al. [329] investigated corrosion behavior of AZ80 Mg alloy in SA modified SBF with different concentrations ranging between 0 and 40 g/L. The positive shift of OCP is observed for only the 10–20 g/L range. Lower SA dose causes the formation of soluble metal complex due to chelating effect, and higher SA dose results in protein aggregation. Both the conditions imply a negative shift towards OCP. Only a few literature studies have reported the BSA for orthopedic application, yet there is significant potential for SA, which can be achieved by manipulating its chelation ability. Thus, SA needed to be investigated comprehensively for its complete scale applications on biodegradable Mg alloy.

3.3. Multilayered hybrid coatings –

The multilayer coating architectures are gaining interest to tailor the corrosion rate of Mg alloys. A multilayer coating system including a combination of organic and inorganic phases is a promising alternative to fulfill the diverse functionalities such as improved corrosion resistance, cell viability, osteogenesis, angiogenesis, anti-bacterial and anti-inflammatory response with the additional benefit of target drug delivery at the implantation site. To better understand the synergy between Mg-organic-inorganic interfaces, six combinations of organic-inorganic multilayer assemblies on Mg substrates are categorized, as shown in Fig. 14.

Class A, B, C, and D represent the inner layer-outer layer on Mg substrate as inorganic-organic, organic-inorganic, organic-organic, inorganic-inorganic, respectively. The composite organic/inorganic layer on Mg substrate is represented by class E. Class F represents the organic/inorganic composite layer as an inner layer, and the outer layer can be either composite, organic or inorganic alone. Accordingly, the multilayered coatings on Mg alloys matched with these classes are investigated. The detailed corrosion performance and reported bio-functionalities of such coatings are discussed in Table 5. It is observed that Class A coatings exhibit higher corrosion resistance and adhesion strength than other classes. The spatial defects present in the inner inorganic layer (L1) are sealed by the top organic layer (L2), resulting in effective shielding towards aggressive ions. Apart from cytocompatibility and anti-bacterial features, Class A lacks necessary bio-functionality components such as self-healing, super-hydrophobicity, drug delivery, etc. Comparatively, Class B shows lower corrosion resistance due to the inorganic layer at the top. The spatial defects provide significant anchoring sites to aggressive ions, resulting in rapid degradation. However, studies reported that Class B provides additional hydrophobicity and drug release features compared to Class A. Class C is generically distinguished for its drug release feature. Usually, the inner polymer layer performs corrosion resistance, while the outer layer of amorphous polymers acts as a drug reservoir. However, corrosion resistance offered is comparatively inferior to Class A, and B. Class D has inorganic-inorganic multilayers showing characteristic mapping with class A, i.e., significant corrosion resistance but lacking in performing bio-functionalities. Typically, the top inorganic layer is added, focusing on the pore-sealing of the inorganic bottom layer (L1). Limited studies have reported the self-sealing and anti-bacterial features for this class.

Class E represents the inorganic/organic composite layer over Mg substrate. The filler effect may be attributed to such coating structures demonstrating improved corrosion resistance [366]. The path for electrolyte diffusion in the organic matrix becomes more complex and

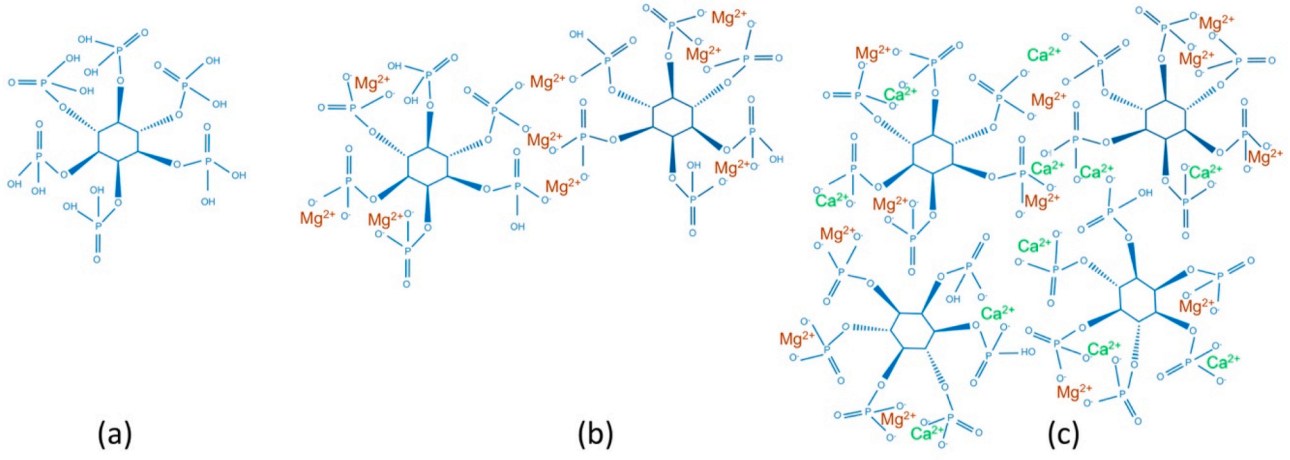

Fig. 13. **(a)** PA molecule containing six phosphate and twelve hydroxyl groups, **(b)** chelation of Mg^{2+} ions to form Mg–P compounds, **(c)** Mg^{2+}/Ca^{2+} chelation to form various Ca–P, Mg substituted Ca–P (whitlockite) compounds.

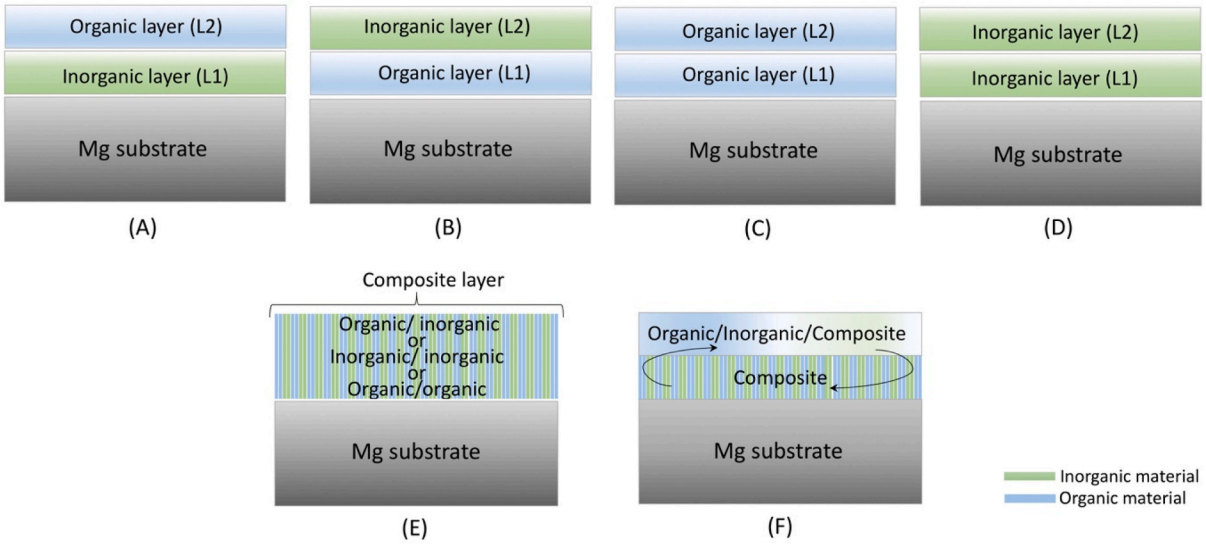

Fig. 14. Classification of multilayered hybrid coatings based on (a) organic – inorganic layers, (b) inorganic – organic layers, (c) organic – organic layers, (d) inorganic – inorganic layers, (e) organic/inorganic or inorganic/inorganic or organic/organic composite layers, (f) organic/inorganic/composite – composite or composite – organic/inorganic/composite layer assemblies on Mg alloys.

protracted due to inorganic particles. The reinforcement provided by inorganic particles results in improved mechanical properties. Bakhsheshi-Rad et al. [367] dip coated a noble PCL/Chitosan composite coating on Mg. An additional ZnO layer was applied to seal the micro-defects, which significantly improved the corrosion resistance and anti-bacterial properties of the coating. However, at higher concentrations, ZnO exhibited cytotoxicity towards osteoblast cells. Li et al. [368] developed hydroxyapatite/graphene/graphene oxide composite coating on ZK60 Mg alloy. As a result of the GO addition, highly dense flower-shaped HA crystals are formed, which result in superior corrosion resistance and osteogenic differentiation. Combining biomimetic and spin-coating methods, Dong et al. [369] developed a PDA/Ca–P/GO composite coating to stimulate cell growth and adhesion for improved biocompatibility of Mg alloys. To address poor adhesion strength and mechanical strength of organic coatings, Fang et al. [370] incorporated sodium alginate in silk-fibroin, the composite coating demonstrated enhanced critical load (L_c) and H^3/E^2 values (H and E denote the coating's hardness and modulus, respectively), indicating that composite coating will resist failure due to strain for a longer time. Besides providing a variety of bio-functionalities, as discussed, composite coatings can produce a range of results within the confines of a single function. A superhydrophobic HA/stearic acid composite coating [284] with a contact angle of 152° and a superhydrophilic HA/hydroxypropyltrimethyl chloride chitosan (HACC) composite coating [371] with a contact angle of 4° have been reported for their outstanding anti-bacterial properties. The quaternary ammonium groups in the latter provide bacterial resistance and kill bacteria without compromising the viability of MC3T3-E1 cells. Class F reported the complex multifunctional coating, the unique assembly of layers widely covers the biocompatibility components. This coating class is widely reported for Self-healing, self-repairable, target drug delivery, super-hydrophobicity, and biocompatibility. One of the limitations of this class is corrosion performance. The corrosion studies reported are not promising to fulfill the clinical requirement.

To address the challenges of Class F coatings, Singh et al. [372,373] fabricated a TiO_2-HA-PCL hybrid coating on ZM21 Mg alloy, where TiO_2-HA composite coating was applied as an inner layer. The *NIPS* technique was utilized to fabricate the outer layer of PCL with homogeneously distributed and interconnected micro-pores. The process parameters include dipping cycle, drying cycle, and sintering temp., depicted in Fig. 15. The sandwiched TiO_2-HA layer enhanced the adhesion strength of PCL by 76% due to electrostatic interaction and H_2 bonding. The E_{corr} value of Mg substrate (−1.444 V) was significantly suppressed to −0.407 V. After 28 days of SBF immersion, the corrosion inhibition efficiency shown by hybrid coating was 99.2%, which successfully managed the corrosion rate (0.069 mm/year) and H_2 evolution rate (0.062 ± 0.036 ml/cm^2/day) within biosafety limits. After prolonged immersion in SBF, dipole interactions between opposite sides of PCL micropores lead to the mineralization of 3d flower-shaped HA by Vander Wall forces, as shown in Fig. 16(a). The XRD analysis (Fig. 16(b)) of mineralized HA in micropores of PCL/HA/TiO_2 hybrid coating shows that as the peaks corresponding to Mg–P compounds suppressed with an increase in immersion time, its tendency to substitute Ca from HA molecules and formation of Mg-PO_4^{3-} compounds is significantly reduced. In response, a chemically stable HA growth with a 3D micro-flower morphology and Ca/P ratio of 1.60 was observed, which provided dense shielding on a large surface area and hindered aggressive ions from interfering with the Mg substrate. Hence, PCL/HA/TiO_2 hybrid coatings provided effective corrosion resistance in physiological immersion for up to 28 days. It is worth noting that TiO_2-HA-PCL hybrid coated samples respond to bacteria and *L929* cells differently in this study. The viability of *S. aureus* and *E. coli* bacteria was suppressed by 57.15% and 62.35%, respectively. While for L*929* cell-line, cellular viability is enhanced by 50.47% compared to control, respectively. The individual role of coating ingredients like bactericidal yet biosafe response by TiO_2, enhanced biocompatibility provided by HA and PCL, was responsible for such a significant response. Hence, diverse property of each layer was combined into a single coating system to obtain significant corrosion resistance, cell viability, and anti-bacterial response necessary to meet the requirement of an orthopedic implant.

Chen et al. [147] developed a double-layered MAO/PLGA coating on Mg–4Zn-0.6Zr-0.4 Sr alloy by dip-coating technique. Apart from effective corrosion resistance, the author reported that stress corrosion cracking (*SCC*) susceptibility of coated Mg alloy was significantly reduced with prolonged immersion in physiological media. Li et al. [335] prepared a multilayered HA/$CaTiO_3$/TiO_2/PLA coating on AZ31 Mg alloy, which exceptionally suppressed the corrosion current density to 8.91 × 10^{-10} A/cm^2. Wei et al. [361] fabricated a multilayered plasma electrolytic oxidation/poly(l-lactic acid)/Heparinized polydopamine (PEO/PLLA/PDAM/Hep) coating on AZ31 Mg alloy by a dip-coating method. Along with improved hemocompatibility, the coating shows selective response by promoting human umbilical vein

Table 5
Summary of in-vitro corrosion performance and bio-functionalities of various organic/inorganic multilayered coatings on Mg and its alloys.

								E_{corr} (V_{SCE})			I_{corr}(A/cm^2)			Corrosion rate (mm/year)	Additional Bio functionality	Ref.
Class	substrate	L1	L2	Methods	Thickness	Adhesion	conditions	substrate	L1	L1+L2	substrate	L1	L1+L2			
A	Mg–Zn–Ca	MAO	Chitosan	Dip	10 μm	–	SBF, 37 °C	−1.77	−1.64	−1.49	1.43×10^{-4}	6.36×10^{-5}	5.90×10^{-7}	–	–	[330]
	AZ91	CaP	PLA	Spin	35.9 μm	–	–	–	–	–	–	–	–	–	–	[331]
	Mg–Li–Ca–Y	MAO	PLA	Dip	–	–	Hank's, 37.5 °C	−1.58	−1.55	−1.51	1.04×10^{-5}	6.31×10^{-6}	1.70×10^{-6}	–	–	[332]
	AM50	Ti–O	PLA	Dip	–	6.12 MPa	SBF, 37.5 °C	−1.40	−1.28	−0.83	–	–	–	–	Enhanced osteoblast for *MC3T3* cell-line	[333]
	AZ31	$Mg(OH)_2$	PCL	Electrospin	–	4B	SBF, 37 °C	–	–	–	–	–	–	–	Cell viability, adhesion and proliferation improved for *L6* cells.	[334]
	AZ31	HA/ $CaTiO_3$/ TiO_2	PLA	Dip	–	–	Hank's,37 °C	−1.60	−1.39	−0.43	3.48×10^{-5}	5.98×10^{-6}	8.91×10^{-10}	–	–	[335]
	Mg-1.2Ca	NiCrAlY/ YSZ	PCL	Dip	150–160 μm	14.5 MPa	3.5% NaCl	−1.63	−1.25	−0.91	2.85×10^{-4}	1.24×10^{-4}	1.40×10^{-7}	0.003	–	[336]
	Mg–4Zn-0.6Zr-0.4Sr	MAO	PLGA	Dip	70 μm	–	m-SBF, 37 °C	−1.66	−1.57	−1.54	1.95×10^{-1}	1.87×10^{-3}	1.39×10^{-4}	–	SCC susceptibility indices reduced for UTS and Elongation to failure	[147]
	AZ31D	MgO/ ZnONRs	*DS/Lys*	Spin assisted LbL	–	–	SBF, 37 °C	−1.66 *	−1.50 *	−1.49 *	5.89×10^{-4}	3.48×10^{-6}	8.38×10^{-8}	–	Anti-bacterial activity was enhanced against *S. aureus* and *E.coli* assays	[337]
B	Pure Mg	PCL	HA	Spraying	5–6 μm	–	Hank's	−1.64	−1.51	−1.46	2.93×10^{-5}	8.23×10^{-6}	1.13×10^{-6}	–	No microcrack appearance upto 10% tensile straining. Improved filopodia and osteoblast for *MC3T3-E1* cell line.	[338]
	Pure Mg	PDA	TiO_2	Dip	4.15 μm	–	PBS, 37 °C	−1.58	−1.54	−1.28	4.37×10^{-5}	1.38×10^{-5}	2.04×10^{-6}	–	–	[339]
	AZ31	PDA	HA	Dip	16–20 μm	–	SBF, 37 °C	−1.48 *	−1.36 *	−1.27 *	4.67×10^{-5}	2.38×10^{-5}	1.82×10^{-6}	–	Promoted cell growth observed for *L929* cell line	[340]
	Mg-Nd-Zn-Zr	PLA	*DCPD*	Dip	10–15 μm	5B	m-SBF, 37 °C	−1.92	–	−1.69	4.33×10^{-6}	–	0.95×10^{-6}	–	Improved ALP activity for *MC3T3-E1* cell line. Controlled Drug release profile observed for Paclitaxel (PTX).	[341]

(*continued on next page*)

Table 5 (*continued*)

Class	substrate	L1	L2	Methods	Thickness	Adhesion	conditions	E_{corr} (V_{SCE}) substrate	E_{corr} (V_{SCE}) L1	E_{corr} (V_{SCE}) L1+L2	I_{corr}(A/cm^2) substrate	I_{corr}(A/cm^2) L1	I_{corr}(A/cm^2) L1+L2	Corrosion rate (mm/year)	Additional Bio functionality	Ref.
	Pure Mg	PA	TiO_2	LPD and Dip	3.27 μm	–	PBS, 37 °C	−1.67	−1.67	−1.34	7.21×10^{-6}	2.66×10^{-6}	3.01×10^{-5}	0.006	Enhanced hydrophilicity, anticoagulant ability, endothelial cell adhesion for *MC3T3-E1* cell line.	[342]
	AZ60	PDA/ *DCPD*	Col	Dip	26 μm	–	SBF, 37 °C	−1.47	−1.39	−1.31	2.70×10^{-5}	4.31×10^{-6}	1.70×10^{-7}	–	Organized F-actin staining with obvious filopodia observed for *MC3T3-E1* cell line.	[121]
C	AZ31	PLGA	PCL,*Lev*	Dip	11–15 μm	–	Hank's, 37 °C	–	–	–	–	–	–	–	Targeted drug release kinetics observed for levofloxacin. Controlled antibiotic release improved the antimicrobial susceptibility against *S. aureus* and *S. epidermidis*.	[343]
	Pure Mg	SA	PLA	Dip	10.4 μm	–	PBS, 37 °C	−1.51	−1.44	−1.38	2.74×10^{-4}	6.23×10^{-6}	1.92×10^{-6}	–	–	[344]
			PCL		10.1 μm					−1.37			3.30×10^{-5}			
	AZ31	PCL	*PDLLA- SRL*	Spraying	1.5 μm		E-MEM + 10% fetal bovine serum	–	–	–	–	–	–	–	Long-time reservoir and slowest drug release rate for sirolimus (SRL).	[345]
	Mg–1Sr	PCL	PPy	Spin	40 μm	–	–	–	–	–	–	–	–	–	Thermally assisted Photo-controllable self-healing.	[346]
	AZ31	PSS	GS	Dip	9.6 μm	–	SBF, 37 °C	−1.73	–	−1.47	1.21×10^{-4}		1.52×10^{-7}	–	Controlled gentamicin release and Significant anti-bacterial activity againt *S. aureus*.	[347]
	AZ31	PCL	*PTMC*	Dip and Spin	–	–	PBS, 37 °C	–	–	–	–	–	–	–	Stent poses significant therapeutic effect for rabbit esophageal benign structure ever after 48 compression cycles.	[348]
D	AZ91D	MAO	SiO_2–ZrO_2	Dip	5.6 μm	–	3.5% NaCl	−1.42	−1.32	−0.40	3.39×10^{-5}	3.92×10^{-7}	1.57×10^{-9}	–	–	[349]
	Mg–Li	PEO	Ti–O	Dip	41 μm	–	3.5% NaCl	−1.68	−1.46	−1.38				–	–	[350]

(*continued on next page*)

Table 5 (*continued*)

Class	substrate	L1	L2	Methods	Thickness	Adhesion	conditions	E_{corr} (V_{SCE}) substrate	E_{corr} (V_{SCE}) L1	E_{corr} (V_{SCE}) L1+L2	I_{corr}(A/cm^2) substrate	I_{corr}(A/cm^2) L1	I_{corr}(A/cm^2) L1+L2	Corrosion rate (mm/year)	Additional Bio functionality	Ref.
											3.32×10^{-4}	5.56×10^{-6}	5.64×10^{-7}			
	Mg–Ca	PEO	ZrO_2	Spraying	60 μm	–	SBF	−1.60	−1.14	−0.91	2.80×10^{-4}	2.10×10^{-7}	6.20×10^{-8}	–	Enhanced anti-bacterial activity against *E. coli.*	[351]
	AZ31B	Silane	GO	Dip	1100 nm	4B	3.5% NaCl	−1.53	−1.41	−1.32	2.18×10^{-4}	4.37×10^{-5}	1.38×10^{-8}	–	–	[352]
	AZ31	SiO_2	CeO_2	Dip	–	–	HBBS	−1.46	–	−1.44	8.07×10^{-6}	–	2.69×10^{-6}	–	Self-Healing after 72 h of immersion is observed.	[353]
				Spray	630 nm					−1.36			7.58×10^{-7}			
	AZ31	MgO	$Mg(OH)_2$	Immersion/ Dip	3 μm	–	HBBS, 37 °C	−1.45	−1.64	−1.36	5.97×10^{-5}	3.72×10^{-7}	5.69×10^{-8}	–	–	[354]
E	AM50	L1+L2 PCL + nHAP		Dip	35.3 μm	–	SBF, 37 °C	−1.34*	−0.70*	−1.20*	1.03×10^{-4}	1.72×10^{-6}	3.60×10^{-6} –		Enhanced adsorption of extra cellular matrix (*ECM*) proteins. Increase in cell proliferation, growth and osteoblast for *MC3T3* cell line.	[355]
	–	HA + PCL		Sol-gel	–	–	SBF	–	–	–	–	–	– –		Improved young's modulus, UTS and max. load-bearing capacity against PCL alone.	[356]
	Pure Mg	Cu-BGNs + PCL		Spin	9.36 μm	–	*DMEM,* 37 °C	−1.33*	−1.14*	−1.01*	–	–	– –		Increased Anti-bacterial activity against *S. Carnosus* and *E. coli* Enhanced indirect and direct cyto-compatibility for *MG-63* cell line.	[357]
	AZ31	Saline + *PPy*		Dip	60 μm	1.4 N	3.5% NaCl	−1.51	−1.45	−1.38	4.96×10^{-5}	1.95×10^{-6}	9.08×10^{-8} 0.002		Superhydrophobic (162°) and low energy coating surface.	[358]
	AZ31	HAP + PAA/*GS*		Dip assisted LbL	21.82 μm	2.7 N	SBF	−1.78	−1.55	−1.43	3.52×10^{-5}	9.44×10^{-6}	8.58×10^{-7} –		High loading dosage of gentamicin sulfate (GS) with controlled release kinetics (15 days). Enhanced anti-	[359]

(*continued on next page*)

Table 5 (*continued*)

Class	substrate	L1	L2	Methods	Thickness	Adhesion	conditions	E_{corr} (V_{SCE}) substrate	E_{corr} (V_{SCE}) L1	E_{corr} (V_{SCE}) L1+L2	I_{corr}(A/cm^2) substrate	I_{corr}(A/cm^2) L1	I_{corr}(A/cm^2) L1+L2	Corrosion rate (mm/year)	Additional Bio functionality	Ref.
															bacterial activity against *S. aureus*. Improved osteoblasts towards *MC3T3* cell line.	
F	AZ81	Inner L MAO/PLLA	Outer L PLGA/ *PTX* + PLGA	Dip/Drop	–	–	Hank's, 37 °C	–	–	–	–	–	–	–	Linearly sustained slow PTX drug release. Enhanced blood compatibility with improved thromboxane A2 platelets.	[360]
	AZ31	PEO/PLLA	*PDAM*/ Hep	Dip	–	–	SBF, 37 °C	−1.62	−1.12	−1.45	6.95×10^{-5}	3.47×10^{-10}	1.02×10^{-7}	–	Improved hemocompatibility, selective response to promote *HUVEC* and inhibit *HUASMC* proliferation.	[361]
	Mg–1Ca	MAO/CS	*CS/Ce*	Spin	10 μm	–	*DMEM*, 37 °C	–	–	–	–	–	–	–	Encapsulated Inhibitor (Ce) induces self-sealing. Enhanced cytocompatibility towards *MC3T3* cell line.	[312]
	Mg–1Ca	Silk Fibroin/K_3PO_4	Silk Fibroin	Spin	–	0.82 mN	Hank's, 37 °C	–	–	–	–	–	–	–	Self -healing based on pH stimuli response ability at scratched site. Enhanced in-vitro cell viability, Adhesion and osteo-differentiation for CCK-8 assay.	[322]
	Mg–1Ca	Silk/PA	Silk	Spin	5 μm		Hank's, 37 °C	−1.48	−1.44	−1.43	1.53×10^{-6}	1.50×10^{-8}	3.85×10^{-8}	0.002	pH triggered Self-healing ability with enhanced cytocompatibility towards MC3T3 cell line.	[362]
	AZ31	HMS	*GSH* + *Cys*/ *CD*	Immersion	130 nm	–	3.5% NaCl	−1.52	–	−1.57	1.41×10^{-4}	–	5.13×10^{-5}	–	Triple trigger drug release model. Along with pH response, the drug delivery is responsive towards stalk of coating structure and release of Mg^{2+} ions.	[363]
	AZ31	PDA/HA	*BMP2*	Immersion	1.1 μm		SBF	−1.62	–	−1.50		–		–		[364]

(*continued on next page*)

Table 5 (*continued*)

Class	substrate	L1	L2	Methods	Thickness	Adhesion	conditions	E_{corr} (V_{SCE})			I_{corr}(A/cm^2)			Corrosion rate (mm/year)	Additional Bio functionality	Ref.
								substrate	L1	L1+L2	substrate	L1	L1+L2			
						5.6 MPa					1.72 × 10^{-4}		1.26 × 10^{-4}		New bone with direct contact around implant in medullar cavity is formed. Larger osteoid tissue formation is observed.	
	Mg–Zn–Y-Nd	HF	PDA/HA/PEI NPs	Immersion	–	–	HBBS	−1.49	−1.40	−1.47	2.49 × 10^{-5}	2.3 × 10^{-8}	1.7 × 10^{-6}		Improved anti-inflammatory response, blood compatibility, Inhibited endothelial cell apoptosis	[365]

endothelial cell (*HUVEC)* and inhibiting human umbilical artery smooth muscle cells (*HUASMC*) proliferation due to diverse ingredients in a single coating system. Based on the reported studies, it can be observed that the multilayered hybrid coating system is most suitable for obtaining diverse bio-functionalities to meet the clinical requirement of Mg-alloy based bone implants.

3.4. Self-healing coatings-

The surface scratches on implants seem unavoidable during surgery, and the partial damages provide pathways for the intake of the aggressive solution and lead to severe local corrosion and even premature coating failures [374]. Upon damage, self-healing coatings can repair defects by eliciting automatic repair mechanisms and restoring coating functions. Typically, self-healing coating consists of a 'guest' known as a healing agent, incorporated in the host (i.e., coating). When stimulated conditions damage the host in corrosive media, the guest is leaked to form a passive layer at the defect site, inhibiting the corrosion propagation [362]. Presently, self-healing coatings on Mg alloys are majorly achieved by encapsulation coating and layer-by-layer assembled coating techniques. This section provides an overview of the latest developments in self-healing coatings on Mg alloys.

3.4.1. Encapsulation coatings

In self-healing coatings on magnesium alloys, cerium ions, benzotriazole, and 8-hydroxyquinoline were widely reported as healing agents, which are acceptable for industrial applications but toxic for biomedical applications. In comparison with other corrosion inhibitor ions (i.e. MnO_4^-, La^{3+}, Pr^{3+}, VO_3^-), PO_4^{3-} demonstrate the best suitability for biomedical self-healing coatings [375]. The PO_4^{3-} have a strong tendency to chelate Ca^{2+} from physiological media and Mg^{2+} produced from corrosion into highly insoluble magnesium phosphates ($K_{sp} \sim 1.04 \times 10^{-24}$) and calcium phosphates ($K_{sp} \sim 3.7 \times 10^{-58}$) precipitates at the scratched site to repair the defects. Xiong et al. [322] prepared a self-healing coating comprising; Silk as host and K_3PO_4 as inhibition agent on Mg–1Ca alloy. After mechanical scratching, the PO_4^{3-} released from K_3PO_4 chelated the Mg^{2+} leached from the Mg substrate and formed an insoluble $Mg_3(PO_4)_2$ layer on scratched region. After 160 min, the cathodic and anodic current density at scratched region verged to zero planes, verifying the self-healing capacity. Furthermore, the rapid release of PO_4^{3-} in alkaline environment (pH 10) in comparison to neutral environment (pH 7.4) was deemed as pH stimuli response of coating. Li et al. [376] developed a three-layered coating structure, consisting of an inner layer of MgO, a middle of PLA containing curcumin loaded F-encapsulated mesoporous silica nanocontainers (cFMSNs) and an outer layer of dicalcium phosphate dehydrate on WE43 Mg alloy. After artificial scratching, the release of curcumin from ruptured nanocontainers exhibited self-healing capability during in-vitro and in-vivo testing conditions. Additionally, the curcumin release favored the osteo-differentiation, immunomodulatory efficiency and osseointegration response. However, the toxic potential of abruptly chelated phosphate compounds has not yet been fully explored [377]. To address the current issue, Dong. et al. [378] developed a pH-sensitive dicalcium phosphate dihydrate (DCPD) coating on Pure Mg. The DCPD itself plays the role of both 'host' and 'guest', indicating its self-healing without additional corrosion inhibitors. Owing to local alkalinity, DCPD crystals tend to dissolve and release calcium and phosphate ions near the scratches. At the scratched region, a rise in pH facilitates the formation of $Mg(OH)_2$ and Mg containing Ca–P compounds. The DCPD coating exhibits an efficient self-healing ability. Within 4 h of immersion in Hanks' solution, the scratches were sealed. No doubt, these recent works have greatly promoted the development of Mg alloys for biomedical applications. However, research on self-healing coatings is still at an early stage, so it would be worthwhile to provide theoretical and experimental support for future clinical applications.

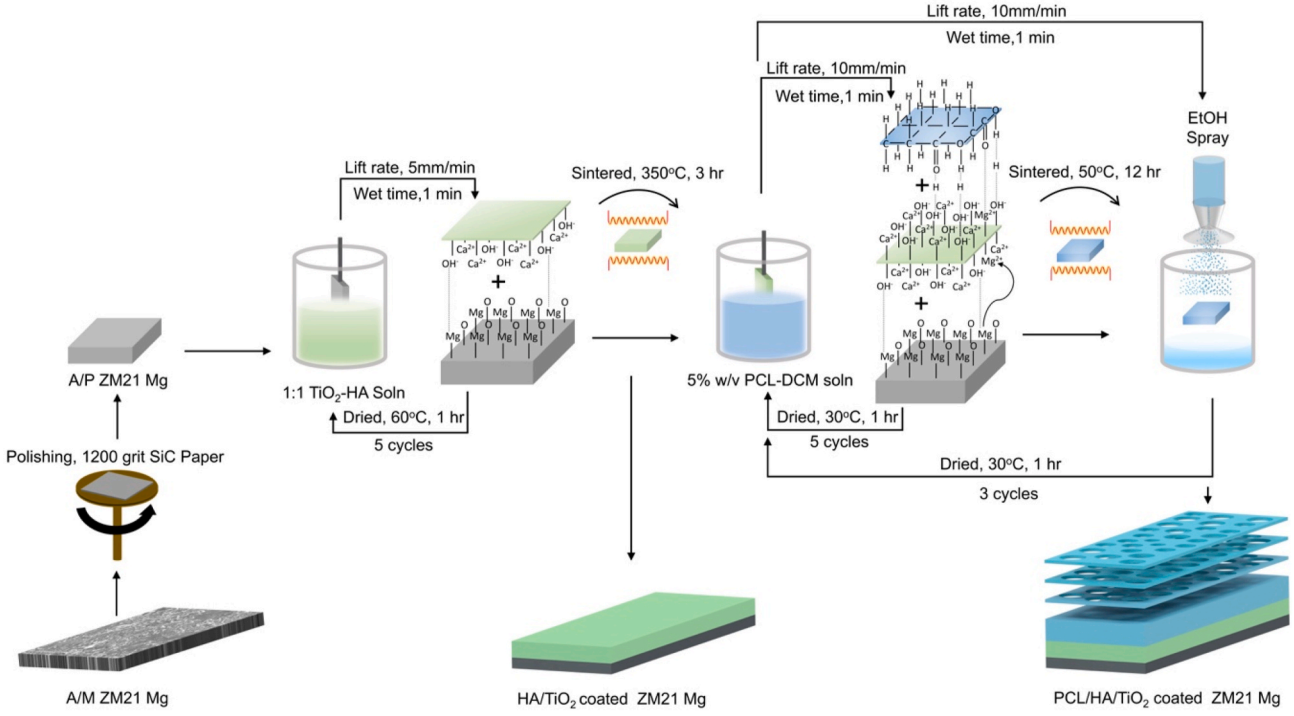

Fig. 15. A schematic process flow diagram for fabrication of multilayered PCL/HA/TiO_2 hybrid coating on ZM21 Mg alloy [372].

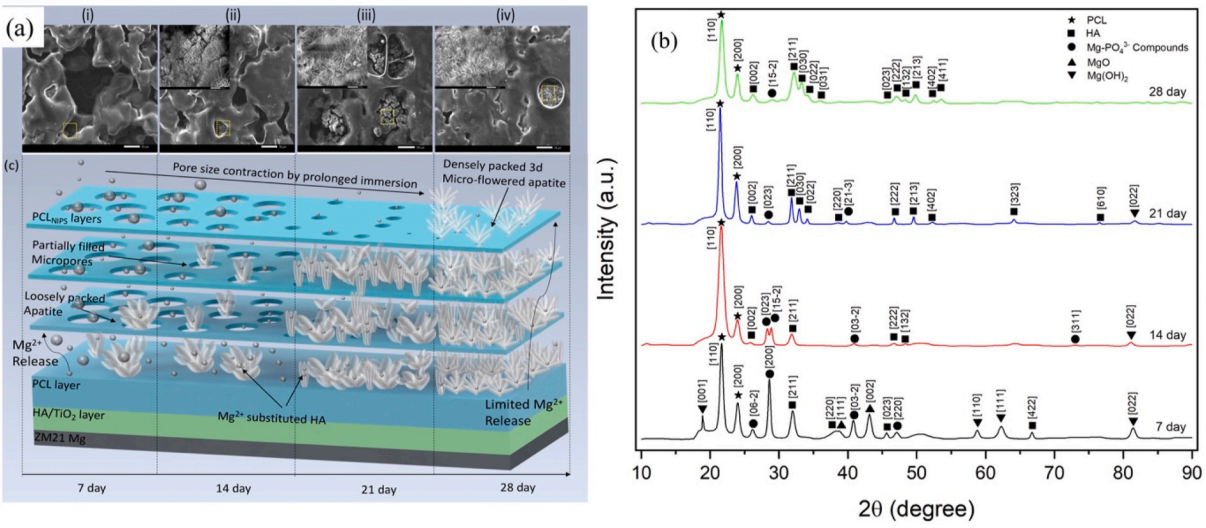

Fig. 16. (a) SEM analysis of apatite mineralized in PCL micropores after (i) 7, (ii) 14, (iii) 21 and (iv) 28 days of SBF immersion, and (b) XRD analysis of apatite mineralized on PCL/HA/TiO_2 hybrid coating after 7, 14, 21, and 28 days of SBF immersion [372].

3.4.2. Layer-by-layer (LbL) self-assembled coatings

These coatings involve a multilayered coating architecture in which the individual layers are self-assembled through electrostatic interaction, hydrogen bonding, covalent bonding, and charge-transfer interactions [51]. Various methods of depositing LbL coatings on Mg alloys are reported, including dip, spin, spray, and multistep methods [379]. The composition and thickness of the LbL coating can be easily modified by tailoring the composition, thickness, and number of deposited layers. Due to the involvement of multiple layers, it is possible to integrate a wide variety of corrosion inhibitors, drugs, proteins, and polyelectrolytes into the LbL coatings, providing diverse bio-functionalities in a single coating system. At present, the most commonly used LbL coating formulations are polymer multilayers incorporated with healing agents [380]. These coatings have been reported to self-heal when exposed to multiple stimuli conditions, including mechanical scratching, pH changes, and ion exchanges. Zhao et al. [294] prepared a multilayered polymethyltrimethoxysilane (PMTMS)/Silver nanoparticles (AgNPs)/Polyethyleneimine (PEI) LbL assembled coating on AZ31 Mg alloy by dip-coating method. Crosscut artificial scratches (50 mm thick) were used to evaluate the self-healing response. After immersion in Hank's balanced salt solution (HBSS), polysiloxane shows water-swelling behavior, which results in self-healing within 72 h. Additionally, during immersion, the release of Ag^{2+} from coating resulted in significant bactericidal activity towards *S. aureus*. A noble two-step spin-spray deposition process was utilized by Zhao et al. [353] for layer-by-layer deposition of polyacrylic acid (PAA)

modified CeO_2 nanoparticles and 3-aminopropyl trimethoxysilane (3-APTMS) modified SiO_2 nanoparticles on AZ31 magnesium alloy. It has been demonstrated that SiO_2 acted as physical barrier against corrosive media, and CeO_2 provides efficient self-healing by formation of Ce-rich passive layer at damage site. Recently, different but interesting work was reported by Ouyang et al. [221]. They coupled layers of an F^- incorporated layered double hydroxide (LDH) with bioactive-glass (Bg) by spin-coating method on AZ31 Mg alloy. The pH rise is a primary indicator of Mg corrosion. By increasing the pH value of SBF from 7.4 to 9.0, the fluoride-releasing equilibrium concentration was positively shifted, facilitating more leaching of F^- from LDH layers. The increase in alkalinity and F^- concentration together promotes rapid mineralization of highly stable and biocompatible fluorapatite ($Ca_{10}(PO_4)_6F_2$) at the spatial defects. Such a green and facile self-repairing response indicate great potential of LbL coating for clinical applications. Nevertheless, there are several concerns regarding LbL coatings. The preparation requires considerably more time, and the multilayers show weak adhesion to Mg alloys. In the future, work should focus on evaluating the LbL coatings in the context of diverse bio-functions, as well as automating the fabrication process for time savings.

4. Coatings challenges and outlook

The coatings for Mg-based implants are expected to facilitate biodegradation at a tailored rate by offering a limited barrier function based upon the bone reunion period [381]. However, coatings do not behave expectedly. Most coatings with single-constituent fail to meet the diverse bio-functionalities simultaneously. For instance, ceramic coatings lack adequate corrosion resistance, angiogenic, anti-bacterial, and osteogenic response. Despite effective corrosion resistance and biocompatibility, polymeric coatings suffered from poor adhesion and wear resistance issues. The highly anodic behaviour of Mg alloys stemmed the greatest challenge for coating's stability in a complex physiological environment. Due to electronegative potential difference, the conductive metallic/ceramic coatings affect Mg alloys by galvanic cell occurrence between the coating and Mg substrate. Such a galvanic setup resulted in the rapid dissolution of coating layers. Additionally, the localized potential difference between secondary phase particles and the Mg matrix results in variable electrostatic attraction, which mechanically destabilizes the whole coating structure and ultimately breaks down the coating [382]. Some studies have suggested pretreatment strategies like alkalization, which promote a uniform physiochemical surface composed of $MgO/Mg(OH)_2$ to coating layers [383–385]. However, unwanted hydrophilicity provided by these oxides/hydroxides further accelerate aggressive ions' attack [386]. In contrast, various biocompatible ceramic and polymers of insulating nature are reported to overcome issues related with conductive coatings. However, ceramic coatings are prone to inevitable spatial defects like micro-pores and cracks formed due to the evaporation of organic residue [387]. The corrosive media easily penetrate these micro-pores/cracks and start

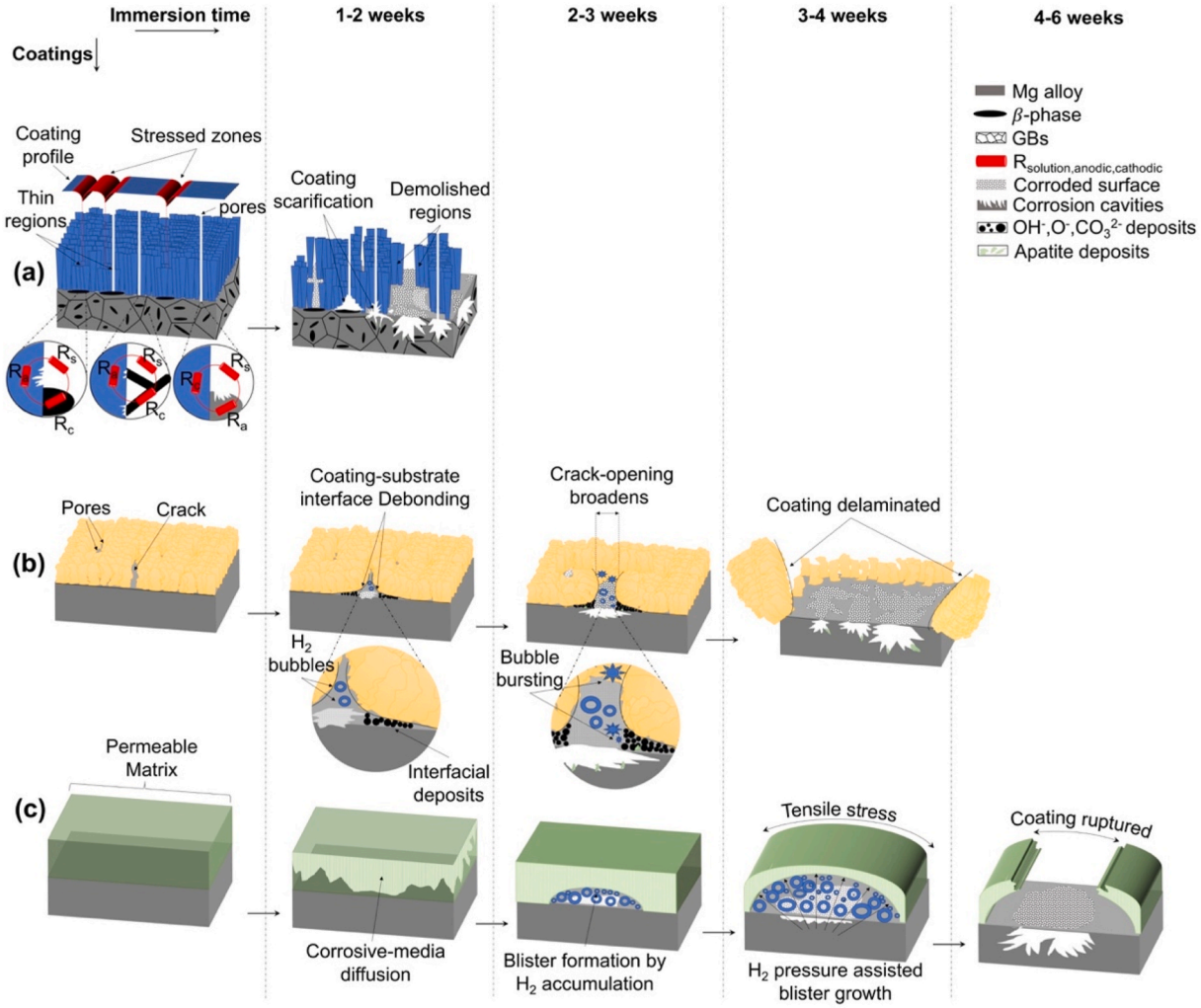

Fig. 17. Schematic illustration of immersion-time-based events responsible for failure of **(a)** Metallic/Conductive coatings, **(b)** ceramic coatings, and **(c)** polymer coatings on Mg alloys in physiological media.

active corrosion at the substrate/coating interface. The byproduct of such corrosion results in H_2 evolution and deposition of various oxide-hydroxide-carbonate species, which cause debonding of the coating layer from the substrate. With prolonged immersion, continuous byproduct formation critically weakens the adhesion strength, which ultimately leads to a failure by delamination [388]. However, polymeric coatings are relatively free from spatial defects compared to ceramic coatings. However, polymers are prone to hydrolysis in physiological media, which rapidly increases permeability and facilitates the absorption of aggressive ions [389]. Once corrosion starts at the coating/substrate interface, H_2 evolution cause formation of blisters. These blisters grow continuously with ongoing corrosion and finally burst, leaving a large exposed area [390]. The time-bound sequence of events responsible for failure of conductive, ceramic, and polymeric coatings with prolonged immersion are summarized in Fig. 17. Such coating failures lead to aseptic loosening, which occurs by erosion of fragmented particles from coating/substrate. Thus, enhanced degradation rate and loosening together trigger premature implant failure. Various advantages and disadvantages associated with different coatings on Mg alloys are summarized in Table 6.

Therefore, a singular organic or inorganic coating cannot address the required clinical functionalities and is prone to easy damage in complex physiological environments; therefore, additional barrages are required on Mg alloys to perform therapeutic tasks efficiently. Accordingly, the multilayered coatings provide additional barriers against aggressive ions, which translates into increased corrosion resistance. In a multilayer coating architecture, the intervening layers contribute to excellent adhesion. In addition, the use of multiple layers in a designated fashion permits the loading of inhibitors and drugs in order to provide smart characteristics like self-healing and sustained drug delivery. A broad range of bio-functionalities can now be obtained via multilayer coatings, and this is rapidly becoming a research hotspot.

5. Conclusions

Various in-situ and ex-situ coating techniques have been developed to improve corrosion resistance and induce diverse bio-functionalities for Mg and its alloys. However, no coating system is reached for clinical translation. The in-situ chemical conversion coating techniques resulted in significant adhesion strength, but their application mainly focuses on depositing inorganic layers on Mg alloys. Despite high insolubility and bioactivity, the corrosion resistance and adhesion strength offered by inorganic Ca–P coatings are compromised due to the presence of spatial defects and random orientation of Ca–P crystals, respectively. In parallel, R.E elements are introduced to overcome such issues, but their long-term biocompatibility in physiological conditions is still debatable. To date, in-situ techniques can produce coatings of weak organic acids like tannic acid, gallic acid, phytic acid, vanillic acid, stearic acid on Mg alloys. These acids endow unique bio-functionalities like an anti-inflammatory response, rapid wound healing, superhydrophobicity, rapid mineralization of apatite but suffer from substandard corrosion resistance. However, a Layered double hydroxides coating shows good corrosion resistance, adhesion strength, and structural functionalities like self-sealing and self-healing by intercalation of suitable inorganic anions, but processing parameters like high temperature and pressure conditions limit the intercalation of organic groups.

On the other hand, ex-situ coating techniques like sol-gel provide a wide range of applicability to deposit organic and inorganic layers. In particular, deposited natural polymers coatings like phytic acid (PA), chitosan (CS), and collagen (Col) provide significant anti-bacterial and osteoinduction response; PLGA and PLA are recognized for enhanced cellular viability and target drug delivery features; PCL is extensively reported for excellent corrosion resistance on Mg alloys. Nevertheless, the structural stability of ex-situ deposited layers is not promising due to poor adhesion strength.

It can be concluded that the majority of previous investigations are merely focused on one or two properties, such as corrosion performance and structural stability. In contrast, a broad range of coating properties, including clinical functionalities such as osteogenesis, angiogenesis, hemocompatibility, and anti-inflammatory response, have not been reported simultaneously. The reported work indicated that the coatings performed well in corrosion resistance and adhesion strength but lacked bio-functionalities and vice versa. Multilayered inorganic/organic

Table 6
Advantages and disadvantages associated with various coatings on Mg alloys.

Coatings	Advantages	Disadvantages
Phosphate conversion	Improved osteointegration, osteoconduction response, Biocompatible High adhesion strength	Inevitable spatial defects due to evaporation of organic residues, Structural destabilization and enhanced solubility of Ca–P due to Mg substitution.
Rare earth conversion	chemically stable and insoluble during long-term physiological immersion, Superior anti-bacterial response, Significant antitumor activity	Prolonged exposure to human body can decline the locomotor frequency, induce down-expressions and other behavioural deficits
Fluoride conversion	Promotes Ca–P mineralization, Highly insoluble, significant corrosion resistance, blood compatibility, cytocompatibility	Acceptable to micro-pores due to H_2 generation, internal stresses generation and cracking
Organic conversion	Biodegradable, remarkable chelation ability to mineralize Ca^{2+}, PO_4^{3-} and Mg^{2+} into stable compounds, Excellent self-healing and superhydrophobic characteristics.	Substandard corrosion resistance, Poor adhesion strength with Mg alloys.
MAO	Superior bonding strength, wear resistance, and cell-anchoring response.	Poor corrosion resistance, biocompatibility.
Ion Implantation	Selective surface modification, low temperature conditions, and reproducibility.	Residual stress generation, increased surface roughness, and uneven thickness of coating layer.
Layered Double hydroxides	High corrosion resistance, Self-repairing, biocompatible, anti-bacterial, and anti-inflammatory response	Unfavorable processing parameters including high temperature, and pressure conditions, and poor ion-exchangeability of bioactive molecules.
Physical vapor deposition	Highly uniform and crystalline coating structure, significant bone cell attachment, improved elastic strain to failure and plastic deformation resistance.	Difficult to control deposition temperature, complex equipment requirements and high cost.
Atomic layer deposition	excellent corrosion resistance, conformal and facile thickness control, and pin-hole free structure, high surface finish	Difficult to control deposition temperature, poor adhesion strength and lower growth rate.
Cathodic Electrodeposition	Versatility, short deposition time, room temperature conditions, and slight limitation on substrate shape	Poor adhesion strength, accumulated H_2 bubbles on the cathode (i.e., substrate) severely affects the coating deposition.
Layer-by-layer	Sustained and target drug-delivery, Self-healing, corrosion resistance	Time consuming, weak adhesion strength
Sol-gel	Superior corrosion resistance, mild temperature, and pressure conditions, facile multilayer arrangement incorporating organic and inorganic components.	Poor adhesion strength and thickness control, prone to spatial defects.

coating imparted diverse characteristics such as enhanced corrosion resistance, adhesion strength, and improved bio-functionalities with self-healing characteristics. Therefore, multilayered hybrid coatings with specific organic and inorganic ingredients should be devised on biodegradable Mg-based implants to fulfill the diverse clinical requirements.

6. Future developments and research directions

Recent research efforts are focused on producing novel bio-functional coatings that emulate the vital function of synchronized degradation and bone reunion rate. The latest coating studies demonstrate significant advancements in terms of corrosion resistance and other bioactive factors, resulting in improved cytocompatibility, hemocompatibility, anti-inflammatory and anti-microbial performance. Nevertheless, some issues are pending with the current studies which should be addressed comprehensively in the future. The administration of drugs through coatings is reported to be much more effective than conventional delivery systems. The coatings should be capable to hold variety of drugs to achieve specific therapeutic response at implanted site. Further, smart release mechanisms should be integrated into the coating system to ensure a controlled release of the drug upon arrival at the intended target site. The multilayered hybrid and composite organic/inorganic coatings can offer enough potential for futuristic applications. In such coating structures, biodegradable polymeric layers are served as outer coating layers for drug storage, the intermediate ceramic layers provide necessary adhesion electrostatic/chemical bonding between the outer polymeric layer and Mg substrate, which otherwise is a major concern for polymeric coatings on Mg substrate.

The handling of coated implants is always a difficult and delicate task, especially with Mg implants where a coating defect can have severe repercussions. For this reason, coatings should be equipped with self-reporting features. Self-reporting corrosion protection coatings can autonomously indicate coating damage and corrosion before implant fixation surgery. Till now, the development of self-reporting coatings on Mg alloy for biomedical applications has received minimal attention. A comprehensive knowledge framework should be developed for bio-safe fluorescent indicators. The coatings should be integrated with such indicators so that, in the event of mechanical damage, these indicators will provide visual confirmation of the defect. As per self-healing functionality is concerned, current reports are associated with stimuli-feedback response against mechanical damage or pH rise only. Only few studies reported the self-healing response of coatings against rise in concentration of Mg^{2+}, which is also a primary indicator of Mg corrosion. Preliminary work indicated that multi-responsive nanocontainers could be developed with self-healing responses triggered by three events; mechanical scratching, pH rise, and rise in magnesium concentration. In order to make self-healing coatings more intelligent, such containers should be incorporated. As moral obligation towards animal ethics to reduce and replace the animal testing, an advanced three-dimensional (3D) in-vitro model will be developed using data obtained from comparison of in-vivo and in-vitro performance of coatings. To cater the multifunctionalities, coating preparation processes are becoming more complex. Thus, facile coating preparation technologies need to be explored equally.

Apart from discussed future developments and research directions, few critical areas need to be addressed to better understand coating behavior on Mg alloys for clinical translation.

- *Surface chemistry* of the Mg substrate plays a significant role in deciding the coating's adhesion strength. Current research studies are focused on achieving chemically active homogeneous surfaces to promote additional bonding with Mg substrate. More attention should be paid to obtaining uniform microstructured surfaces with similar grain size and homogenously distributed β-phase particles. It can be achieved by thermo-mechanical surface modification techniques like FSP, SMAT, LSM, and LSP as pre-treatment techniques. Uniform electrostatic interaction offered by such surfaces has excellent potential to enhance the structural stability and adhesion strength of coatings.
- *Long-term corrosion behavior* of coated implants under physiological conditions must be investigated to get an accurate characterization of coating behaviour in terms of corrosion resistance, loss of adhesion strength and other bio-functional responses. various complex physiological environments. Generally, in vitro corrosion tests of coated Mg alloys are performed by simulating only the inorganic part of human blood plasma, either in a static or semi-dynamic environment. The coating's performance should be investigated in a dynamic physiological environment containing amino acids, plasma proteins, and a suitable buffering system.
- *Anodic or cathodic coatings?* It is still debatable to prefer anodic or cathodic coatings for Mg alloys for longer protection. As coatings defects are inevitable, once corrosive media penetrate conventional cathodic coatings, aggressive ions preferentially attack the highly anodic Mg substrate. An anodic coating layer with negative corrosion potential (i.e., Na, K, Ca, and Li) can delay Mg degradation by self-scarifying characteristics. A combined investigation of anodic coatings coupled with conventional inorganic-organic multilayered hybrid coatings on Mg alloys can be a breakthrough in the field of coatings.

Ethics approval and consent to participate

Not applicable in present case.

Declaration of competing interest

It is to declare that there is no conflict of Interest among the author and Co-authors for the manuscript entitled "**Progress in bioactive surface coatings on biodegradable Mg alloys: a critical review towards clinical translation**".

References

[1] J. Kang, E. Dong, D. Li, S. Dong, C. Zhang, L. Wang, Anisotropy characteristics of microstructures for bone substitutes and porous implants with application of additive manufacturing in orthopaedic, Mater. Des. 191 (2020) 108608, https://doi.org/10.1016/j.matdes.2020.108608.

[2] P. Sekar, N. S, V. Desai, Recent progress in in vivo studies and clinical applications of magnesium based biodegradable implants – a review, J. Magnes. Alloy. 9 (2021) 1147–1163, https://doi.org/10.1016/j.jma.2020.11.001.

[3] M.S. Song, R.C. Zeng, Y.F. Ding, R.W. Li, M. Easton, I. Cole, N. Birbilis, X.B. Chen, Recent advances in biodegradation controls over Mg alloys for bone fracture management: a review, J. Mater. Sci. Technol. 35 (2019) 535–544, https://doi.org/10.1016/j.jmst.2018.10.008.

[4] S. Cheng, D. Zhang, M. Li, X. Liu, Y. Zhang, S. Qian, F. Peng, Osteogenesis, angiogenesis and immune response of Mg-Al layered double hydroxide coating on pure Mg, Bioact. Mater. 6 (2021) 91–105, https://doi.org/10.1016/j.bioactmat.2020.07.014.

[5] S. Huang, B. Wang, X. Zhang, F. Lu, Z. Wang, S. Tian, D. Li, J. Yang, F. Cao, L. Cheng, Z. Gao, Y. Li, K. Qin, D. Zhao, High-purity weight-bearing magnesium screw: translational application in the healing of femoral neck fracture, Biomaterials 238 (2020) 119829, https://doi.org/10.1016/j.biomaterials.2020.119829.

[6] V. Tsakiris, C. Tardei, F.M. Clicinschi, Biodegradable Mg alloys for orthopedic implants – a review, J. Magnes. Alloy. 9 (2021) 1884–1905, https://doi.org/10.1016/j.jma.2021.06.024.

[7] H. Helmholz, O. Will, T. Penate-Medina, J. Humbert, T. Damm, B. Luthringer-Feyerabend, R. Willumeit-Römer, C.C. Glüer, O. Penate-Medina, Tissue responses after implantation of biodegradable Mg alloys evaluated by multimodality 3D micro-bioimaging in vivo, J. Biomed. Mater. Res. 109 (2021) 1521–1529, https://doi.org/10.1002/jbm.a.37148.

[8] M. Chen, M. Wang, B. Li, D.D. Winston, W. Cheng, Y. Han, B. Lei, Visual and antibacterial magnesium implants with low biocorrosion and bioactive surface for in vivo tracking and treating MRSA infection, Chem. Eng. J. 417 (2021) 129198, https://doi.org/10.1016/j.cej.2021.129198.

[9] A. Jana, M. Das, V.K. Balla, In vitro and in vivo degradation assessment and preventive measures of biodegradable Mg alloys for biomedical applications, J. Biomed. Mater. Res. 110 (2022) 462–487, https://doi.org/10.1002/jbm.a.37297.

[10] M.N. Sarian, N. Iqbal, P. Sotoudehbagha, M. Razavi, Q.U. Ahmed, C. Sukotjo, H. Hermawan, Potential bioactive coating system for high-performance absorbable magnesium bone implants, Bioact. Mater. 12 (2022) 42–63, https://doi.org/10.1016/j.bioactmat.2021.10.034.
[11] Y.F. Zheng, X.N. Gu, F. Witte, Biodegradable metals, Mater. Sci. Eng. R Rep. 77 (2014) 1–34, https://doi.org/10.1016/j.mser.2014.01.001.
[12] E. Gálvez-Sirvent, A. Ibarzábal-Gil2, E.C. Rodríguez-Merchán, Treatment options for aseptic tibial diaphyseal nonunion: a review of selected studies, EFORT Open Rev 5 (2020) 835–844, https://doi.org/10.1302/2058-5241.5.190077.
[13] Y. Zhang, Y. Huang, F. Feyerabend, C. Blawert, W. Gan, E. Maawad, S. You, S. Gavras, N. Scharnagl, J. Bode, C. Vogt, D. Zander, R. Willumeit-Römer, K. U. Kainer, N. Hort, Influence of the amount of intermetallics on the degradation of Mg-Nd alloys under physiological conditions, Acta Biomater. 121 (2021) 695–712, https://doi.org/10.1016/j.actbio.2020.11.050.
[14] D.E. Erişen, Y. Zhang, B. Zhang, K. Yang, S. Chen, X. Wang, Biosafety and biodegradation studies of AZ31B magnesium alloy carotid artery stent in vitro and in vivo, J. Biomed. Mater. Res. B Appl. Biomater. 110 (2022) 239–248, https://doi.org/10.1002/jbm.b.34907.
[15] T. Li, W. Xu, C. Liu, J. He, Q. Wang, D. Zhang, K. Sui, Z. Zhang, H. Sun, K. Yang, L. Tan, H. Shao, Anticancer effect of biodegradable magnesium on hepatobiliary carcinoma: an in vitro and in vivo study, ACS Biomater. Sci. Eng. 7 (2021) 2774–2782, https://doi.org/10.1021/acsbiomaterials.1c00288.
[16] C. Chen, J. Chen, W. Wu, Y. Shi, L. Jin, L. Petrini, L. Shen, G. Yuan, W. Ding, J. Ge, E.R. Edelman, F. Migliavacca, In vivo and in vitro evaluation of a biodegradable magnesium vascular stent designed by shape optimization strategy, Biomaterials 221 (2019) 119414, https://doi.org/10.1016/j.biomaterials.2019.119414.
[17] S. Höhn, S. Virtanen, A.R. Boccaccini, Protein adsorption on magnesium and its alloys: a review, Appl. Surf. Sci. 464 (2019) 212–219, https://doi.org/10.1016/j.apsusc.2018.08.173.
[18] M. Talha, Y. Ma, P. Kumar, Y. Lin, A. Singh, Role of protein adsorption in the bio corrosion of metallic implants – a review, Colloids Surf. B Biointerfaces 176 (2019) 494–506, https://doi.org/10.1016/j.colsurfb.2019.01.038.
[19] A.P. Md Saad, N. Jasmawati, M.N. Harun, M.R. Abdul Kadir, H. Nur, H. Hermawan, A. Syahrom, Dynamic degradation of porous magnesium under a simulated environment of human cancellous bone, Corrosion Sci. 112 (2016) 495–506, https://doi.org/10.1016/j.corsci.2016.08.017.
[20] N. Kawamura, Y. Nakao, R. Ishikawa, D. Tsuchida, M. Iijima, Degradation and biocompatibility of AZ31 magnesium alloy implants in vitro and in vivo: a micro-computed tomography study in rats, Materials 13 (2020), https://doi.org/10.3390/ma13020473.
[21] D. Bian, J. Deng, N. Li, X. Chu, Y. Liu, W. Li, H. Cai, P. Xiu, Y. Zhang, Z. Guan, Y. Zheng, Y. Kou, B. Jiang, R. Chen, In vitro and in vivo studies on biomedical magnesium low-alloying with elements gadolinium and zinc for orthopedic implant applications, ACS Appl. Mater. Interfaces 10 (2018) 4394–4408, https://doi.org/10.1021/acsami.7b15498.
[22] Y. Wang, X. Li, M. Chen, Y. Zhao, C. You, Y. Li, G. Chen, In vitro and in vivo degradation behavior and biocompatibility evaluation of microarc oxidation-fluoridated hydroxyapatite-coated Mg-Zn-Zr-Sr alloy for bone application, ACS Biomater. Sci. Eng. 5 (2019) 2858–2876, https://doi.org/10.1021/acsbiomaterials.9b00564.
[23] J. Gonzalez, R.Q. Hou, E.P.S. Nidadavolu, R. Willumeit-Römer, F. Feyerabend, Magnesium degradation under physiological conditions – best practice, Bioact. Mater. 3 (2018) 174–185, https://doi.org/10.1016/j.bioactmat.2018.01.003.
[24] K. Kumar, R.S. Gill, U. Batra, Challenges and opportunities for biodegradable magnesium alloy implants, Mater. Technol. 33 (2018) 153–172, https://doi.org/10.1080/10667857.2017.1377973.
[25] H. Li, Q. Peng, X. Li, K. Li, Z. Han, D. Fang, Microstructures, mechanical and cytocompatibility of degradable Mg-Zn based orthopedic biomaterials, Mater. Des. 58 (2014) 43–51, https://doi.org/10.1016/j.matdes.2014.01.031.
[26] Y. Yang, C. He, E. Dianyu, W. Yang, F. Qi, D. Xie, L. Shen, S. Peng, C. Shuai, Mg bone implant: features, developments and perspectives, Mater. Des. 185 (2020) 108259, https://doi.org/10.1016/j.matdes.2019.108259.
[27] U. Riaz, I. Shabib, W. Haider, The current trends of Mg alloys in biomedical applications—a review, J. Biomed. Mater. Res. B Appl. Biomater. 107 (2019) 1970–1996, https://doi.org/10.1002/jbm.b.34290.
[28] C. Wang, Y. Shuai, Y. Yang, D. Zeng, X. Liang, S. Peng, C. Shuai, Amorphous magnesium alloy with high corrosion resistance fabricated by laser powder bed fusion, J. Alloys Compd. 897 (2022) 163247, https://doi.org/10.1016/j.jallcom.2021.163247.
[29] W. Ge, K. Chen, H. Tang, X. Arken, X. Zhang, X. Gu, C. Zhu, Degradability and in vivo biocompatibility of micro-alloyed Mg-Ca-La alloys as orthopedic implants, Mater. Lett. 310 (2022) 131510, https://doi.org/10.1016/j.matlet.2021.131510.
[30] J.-H. Dong, L.-L. Tan, Y.-B. Ren, K. Yang, Effect of microstructure on corrosion behavior of Mg–Sr alloy in Hank's solution, Acta Metall. Sin. 32 (2019) 305–320.
[31] A. Atrens, Z. Shi, S.U. Mehreen, S. Johnston, G.-L. Song, X. Chen, F. Pan, Review of Mg alloy corrosion rates, J. Magnes. Alloy. 8 (2020) 989–998, https://doi.org/10.1016/j.jma.2020.08.002.
[32] K. Munir, J. Lin, C. Wen, P.F.A. Wright, Y. Li, Mechanical, corrosion, and biocompatibility properties of Mg-Zr-Sr-Sc alloys for biodegradable implant applications, Acta Biomater. 102 (2020) 493–507, https://doi.org/10.1016/j.actbio.2019.12.001.
[33] K. Kumar, A. Das, S.B. Prasad, in: B.P. Sharma, G.S. Rao, S. Gupta, P. Gupta, A. Prasad (Eds.), Biodegradable Metal Matrix Composites for Orthopedic Implant Applications: A Review BT - Advances in Engineering Materials, Springer Singapore, Singapore, 2021, pp. 557–565.
[34] H. Hu, X. Wang, Y. Huang, B. He, B. Jia, K. Sun, D. Hao, Y. Guo, Electrochemical techniques for monitoring the biodegradability of nanocomposite Mg-alloy/HA for repairing bone fracture, J. Mater. Res. Technol. 18 (2022) 1669–1681, https://doi.org/10.1016/j.jmrt.2022.03.040.
[35] V.K. Bommala, M.G. Krishna, C.T. Rao, Magnesium matrix composites for biomedical applications: a review, J. Magnes. Alloy. 7 (2019) 72–79, https://doi.org/10.1016/j.jma.2018.11.001.
[36] X. Li, X. Liu, S. Wu, K.W.K. Yeung, Y. Zheng, P.K. Chu, Design of magnesium alloys with controllable degradation for biomedical implants: from bulk to surface, Acta Biomater. 45 (2016) 2–30, https://doi.org/10.1016/j.actbio.2016.09.005.
[37] S. Agarwal, J. Curtin, B. Duffy, S. Jaiswal, Biodegradable magnesium alloys for orthopaedic applications: a review on corrosion, biocompatibility and surface modifications, Mater. Sci. Eng. C 68 (2016) 948–963, https://doi.org/10.1016/j.msec.2016.06.020.
[38] N. Ahuja, U. Batra, K. Kumar, Experimental investigation and optimization of wire electrical discharge machining for surface characteristics and corrosion rate of biodegradable Mg alloy, J. Mater. Eng. Perform. 29 (2020) 4117–4129, https://doi.org/10.1007/s11665-020-04905-8.
[39] G. Sharma, K. Kumar, P.S. Satsangi, N. Sharma, Surface modification of biodegradable Mg-4Zn alloy using PMEDM: an experimental investigation, optimization and corrosion analysis, Irbm (2021), https://doi.org/10.1016/j.irbm.2021.02.003. In press.
[40] T. Tokunaga, M. Ohno, K. Matsuura, Coatings on Mg alloys and their mechanical properties: a review, J. Mater. Sci. Technol. 34 (2018) 1119–1126, https://doi.org/10.1016/j.jmst.2017.12.004.
[41] W. Yao, L. Wu, J. Wang, B. Jiang, D. Zhang, M. Serdechnova, T. Shulha, C. Blawert, M.L. Zheludkevich, F. Pan, Micro-arc oxidation of magnesium alloys: a review, J. Mater. Sci. Technol. 118 (2022) 158–180, https://doi.org/10.1016/j.jmst.2021.11.053.
[42] M. Venkataiah, T. Anup Kumar, K. Venkata Rao, S. Anand Kumar, I. Siva, B. Ratna Sunil, Effect of grain refinement on corrosion rate, mechanical and machining behavior of friction stir processed ZE41 Mg alloy, Trans. Indian Inst. Met. 72 (2019) 123–132, https://doi.org/10.1007/s12666-018-1467-9.
[43] Z.Z. Yin, W.C. Qi, R.C. Zeng, X.B. Chen, C.D. Gu, S.K. Guan, Y.F. Zheng, Advances in coatings on biodegradable magnesium alloys, J. Magnes. Alloy. 8 (2020) 42–65, https://doi.org/10.1016/j.jma.2019.09.008.
[44] B. Manne, H. Thiruvayapati, S. Bontha, R. Motagondanahalli Rangarasaiah, M. Das, V.K. Balla, Surface design of Mg-Zn alloy temporary orthopaedic implants: tailoring wettability and biodegradability using laser surface melting, Surf. Coating. Technol. 347 (2018) 337–349, https://doi.org/10.1016/j.surfcoat.2018.05.017.
[45] T.C. Wu, Y.H. Ho, S.S. Joshi, R.S. Rajamure, N.B. Dahotre, Microstructure and corrosion behavior of laser surface-treated AZ31B Mg bio-implant material, Laser Med. Sci. 32 (2017) 797–803, https://doi.org/10.1007/s10103-017-2174-1.
[46] Q. Liu, Q. xian Ma, G. qiang Chen, X. Cao, S. Zhang, J. luan Pan, G. Zhang, Q. yu Shi, Enhanced corrosion resistance of AZ91 magnesium alloy through refinement and homogenization of surface microstructure by friction stir processing, Corrosion Sci. 138 (2018) 284–296, https://doi.org/10.1016/j.corsci.2018.04.028.
[47] R.S. Gill, K. Kumar, U. Batra, Apatite formation and weight loss study in EDMed perforated AZ31 Mg-alloy, J. Magnes. Alloy. 5 (2017) 362–367, https://doi.org/10.1016/j.jma.2017.08.008.
[48] R. Zhang, X. Zhou, H. Gao, S. Mankoci, Y. Liu, X. Sang, H. Qin, X. Hou, Z. Ren, G. L. Doll, A. Martini, Y. Dong, N. Sahai, C. Ye, The effects of laser shock peening on the mechanical properties and biomedical behavior of AZ31B magnesium alloy, Surf. Coating. Technol. 339 (2018) 48–56, https://doi.org/10.1016/j.surfcoat.2018.02.009.
[49] Z. Li, S. Shizhao, M. Chen, B.D. Fahlman, Debao Liu, H. Bi, In vitro and in vivo corrosion, mechanical properties and biocompatibility evaluation of MgF2-coated Mg-Zn-Zr alloy as cancellous screws, Mater. Sci. Eng. C 75 (2017) 1268–1280, https://doi.org/10.1016/j.msec.2017.02.168.
[50] H.R. Bakhsheshi-Rad, E. Hamzah, M. Kasiri-Asgarani, S. Jabbarzare, N. Iqbal, M. R. Abdul Kadir, Deposition of nanostructured fluorine-doped hydroxyapatite-polycaprolactone duplex coating to enhance the mechanical properties and corrosion resistance of Mg alloy for biomedical applications, Mater. Sci. Eng. C 60 (2016) 526–537, https://doi.org/10.1016/j.msec.2015.11.057.
[51] D. Zhang, F. Peng, X. Liu, Protection of magnesium alloys: from physical barrier coating to smart self-healing coating, J. Alloys Compd. 853 (2021) 157010, https://doi.org/10.1016/j.jallcom.2020.157010.
[52] D. Lee, K. Park, J. Seo, Recent advances in anti-inflammatory strategies for implantable biosensors and medical implants, Biochip J 14 (2020) 48–62, https://doi.org/10.1007/s13206-020-4105-7.
[53] M.K. Ahmed, S.F. Mansour, R. Al-Wafi, A.A. Menazea, Composition and design of nanofibrous scaffolds of Mg/Se- hydroxyapatite/graphene oxide @ ε-polycaprolactone for wound healing applications, J. Mater. Res. Technol. 9 (2020) 7472–7485, https://doi.org/10.1016/j.jmrt.2020.04.094.
[54] M. Echeverry-Rendon, J.P. Allain, S.M. Robledo, F. Echeverria, M.C. Harmsen, Coatings for biodegradable magnesium-based supports for therapy of vascular disease: a general view, Mater. Sci. Eng. C 102 (2019) 150–163, https://doi.org/10.1016/j.msec.2019.04.032.
[55] L. Tian, N. Tang, T. Ngai, C. Wu, Y. Ruan, L. Huang, L. Qin, Hybrid fracture fixation systems developed for orthopaedic applications: a general review, J. Orthop. Transl. 16 (2019) 1–13, https://doi.org/10.1016/j.jot.2018.06.006.
[56] X. Shen, Y. Zhang, P. Ma, L. Sutrisno, Z. Luo, Y. Hu, Y. Yu, B. Tao, C. Li, K. Cai, Fabrication of magnesium/zinc-metal organic framework on titanium implants to

inhibit bacterial infection and promote bone regeneration, Biomaterials 212 (2019) 1–16, https://doi.org/10.1016/j.biomaterials.2019.05.008.
[57] S. Pommiers-Belin, J. Frayret, A. Uhart, J. Ledeuil, J.C. Dupin, A. Castetbon, M. Potin-Gautier, Determination of the chemical mechanism of chromate conversion coating on magnesium alloys EV31A, Appl. Surf. Sci. 298 (2014) 199–207, https://doi.org/10.1016/j.apsusc.2014.01.162.
[58] L. Lei, J. Shi, X. Wang, D. Liu, H. Xu, Microstructure and electrochemical behavior of cerium conversion coating modified with silane agent on magnesium substrates, Appl. Surf. Sci. 376 (2016) 161–171, https://doi.org/10.1016/j.apsusc.2016.03.150.
[59] Z. Mahidashti, T. Shahrabi, B. Ramezanzadeh, The role of post-treatment of an ecofriendly cerium nanostructure Conversion coating by green corrosion inhibitor on the adhesion and corrosion protection properties of the epoxy coating, Prog. Org. Coating 114 (2018) 19–32, https://doi.org/10.1016/j.porgcoat.2017.09.015.
[60] N. Van Phuong, M. Gupta, S. Moon, Enhanced corrosion performance of magnesium phosphate conversion coating on AZ31 magnesium alloy, Trans. Nonferrous Met. Soc. China 27 (2017) 1087–1095, https://doi.org/10.1016/S1003-6326(17)60127-4.
[61] X. jun Cui, C. hai Liu, R. song Yang, Q. shan Fu, X. zhou Lin, M. Gong, Duplex-layered manganese phosphate conversion coating on AZ31 Mg alloy and its initial formation mechanism, Corrosion Sci. 76 (2013) 474–485, https://doi.org/10.1016/j.corsci.2013.07.024.
[62] W. Zai, Y. Su, H.C. Man, J. Lian, G. Li, Effect of pH value and preparation temperature on the formation of magnesium phosphate conversion coatings on AZ31 magnesium alloy, Appl. Surf. Sci. 492 (2019) 314–327, https://doi.org/10.1016/j.apsusc.2019.05.309.
[63] H. Du, X. Ren, D. Pan, Y. An, Y. Wei, X. Liu, L. Hou, B. Liu, M. Liu, Z. Guo, Effect of phosphating solution pH value on the formation of phosphate conversion coatings for corrosion behaviors on AZ91D, Adv. Compos. Hybrid Mater. 4 (2021) 401–414, https://doi.org/10.1007/s42114-021-00222-3.
[64] X.B. Chen, D.R. Nisbet, R.W. Li, P.N. Smith, T.B. Abbott, M.A. Easton, D.-H. Zhang, N. Birbilis, Controlling initial biodegradation of magnesium by a biocompatible strontium phosphate conversion coating, Acta Biomater. 10 (2014) 1463–1474, https://doi.org/10.1016/j.actbio.2013.11.016.
[65] G. Duan, L. Yang, S. Liao, C. Zhang, X. Lu, Y. Yang, B. Zhang, Y. Wei, T. Zhang, B. Yu, X. Zhang, F. Wang, Designing for the chemical conversion coating with high corrosion resistance and low electrical contact resistance on AZ91D magnesium alloy, Corrosion Sci. 135 (2018) 197–206, https://doi.org/10.1016/j.corsci.2018.02.051.
[66] Z. Chunyan, L. Shangju, Y. Baoxing, L. Xiaopeng, C. Xiao-Bo, Z. Tao, W. Fuhui, Ratio of total acidity to pH value of coating bath: a new strategy towards phosphate conversion coatings with optimized corrosion resistance for magnesium alloys, Corrosion Sci. 150 (2019) 279–295, https://doi.org/10.1016/j.corsci.2019.01.046.
[67] H. Hornberger, S. Virtanen, A.R. Boccaccini, Biomedical coatings on magnesium alloys - a review, Acta Biomater. 8 (2012) 2442–2455, https://doi.org/10.1016/j.actbio.2012.04.012.
[68] E. Wierzbicka, B. Vaghefinazari, S.V. Lamaka, M.L. Zheludkevich, M. Mohedano, L. Moreno, P. Visser, A. Rodriguez, J. Velasco, R. Arrabal, E. Matykina, Flash-PEO as an alternative to chromate conversion coatings for corrosion protection of Mg alloy, Corrosion Sci. 180 (2021) 109189, https://doi.org/10.1016/j.corsci.2020.109189.
[69] S. Fintová, J. Drábiková, F. Pastorek, J. Tkacz, I. Kuběna, L. Trško, B. Hadzima, J. Minda, P. Doležal, J. Wasserbauer, P. Ptáček, Improvement of electrochemical corrosion characteristics of AZ61 magnesium alloy with unconventional fluoride conversion coatings, Surf. Coating. Technol. 357 (2019) 638–650, https://doi.org/10.1016/j.surfcoat.2018.10.038.
[70] I. Cacciotti, Cationic and anionic substitutions in hydroxyapatite, in: Handb. Bioceram. Biocomposites, Springer International Publishing, Cham, 2016, pp. 145–211, https://doi.org/10.1007/978-3-319-12460-5_7.
[71] M. Catauro, F. Bollino, R. Giovanardi, P. Veronesi, Modification of Ti6Al4V implant surfaces by biocompatible TiO2/PCL hybrid layers prepared via sol-gel dip coating: structural characterization, mechanical and corrosion behavior, Mater. Sci. Eng. C 74 (2017) 501–507, https://doi.org/10.1016/j.msec.2016.12.046.
[72] H.R. Bakhsheshi-Rad, E. Hamzah, M.R. Abdul-Kadir, S.N. Saud, M. Kasiri-Asgarani, R. Ebrahimi-Kahrizsangi, The mechanical properties and corrosion behavior of double-layered nano hydroxyapatite-polymer coating on Mg-Ca alloy, J. Mater. Eng. Perform. 24 (2015) 4010–4021, https://doi.org/10.1007/s11665-015-1661-4.
[73] M. Rahman, Y. Li, C. Wen, Realization and characterization of double-layer Ca-P coating on WE43 Mg alloy for biomedical applications, Surf. Coating. Technol. 398 (2020) 126091, https://doi.org/10.1016/j.surfcoat.2020.126091.
[74] K. Lin, C. Wu, J. Chang, Advances in synthesis of calcium phosphate crystals with controlled size and shape, Acta Biomater. 10 (2014) 4071–4102, https://doi.org/10.1016/j.actbio.2014.06.017.
[75] M. Rahman, Y. Li, C. Wen, HA coating on Mg alloys for biomedical applications: a review, J. Magnes. Alloy. 8 (2020) 929–943, https://doi.org/10.1016/j.jma.2020.05.003.
[76] J. Gao, Y. Su, Y.X. Qin, Calcium phosphate coatings enhance biocompatibility and degradation resistance of magnesium alloy: correlating in vitro and in vivo studies, Bioact. Mater. 6 (2021) 1223–1229, https://doi.org/10.1016/j.bioactmat.2020.10.024.
[77] S. Liao, B. Yu, B. Zhang, P. Zhou, T. Zhang, F. Wang, Chemically depleting the noble impurities from AZ91-T4 magnesium alloy: a new and efficient pretreatment method to improve the corrosion resistance of phosphate conversion coatings, Corrosion Sci. 191 (2021) 109725, https://doi.org/10.1016/j.corsci.2021.109725.
[78] J. Chen, X. Lan, C. Wang, Q. Zhang, The formation mechanism and corrosion resistance of a composite phosphate conversion film on AM60 alloy, Materials 11 (2018) 402, https://doi.org/10.3390/ma11030402.
[79] J. Jayaraj, K.R. Rajesh, S. Amruth Raj, A. Srinivasan, S. Ananthakumar, N.G. K. Dhaipule, S.K. Kalpathy, U.T.S. Pillai, U.K. Mudali, Investigation on the corrosion behavior of lanthanum phosphate coatings on AZ31 Mg alloy obtained through chemical conversion technique, J. Alloys Compd. 784 (2019) 1162–1174, https://doi.org/10.1016/j.jallcom.2019.01.121.
[80] S.Y. Jian, Y.C. Tzeng, M. Der Ger, K.L. Chang, G.N. Shi, W.H. Huang, C.Y. Chen, C. C. Wu, The study of corrosion behavior of manganese-based conversion coating on LZ91 magnesium alloy: effect of addition of pyrophosphate and cerium, Mater. Des. 192 (2020) 108707, https://doi.org/10.1016/j.matdes.2020.108707.
[81] C. Ke, M.S. Song, R.C. Zeng, Y. Qiu, Y. Zhang, R.F. Zhang, R.L. Liu, I. Cole, N. Birbilis, X.B. Chen, Interfacial study of the formation mechanism of corrosion resistant strontium phosphate coatings upon Mg-3Al-4.3Ca-0.1Mn, Corrosion Sci. 151 (2019) 143–153, https://doi.org/10.1016/j.corsci.2019.02.024.
[82] W. Zai, X. Zhang, Y. Su, H.C. Man, G. Li, J. Lian, Comparison of corrosion resistance and biocompatibility of magnesium phosphate (MgP), zinc phosphate (ZnP) and calcium phosphate (CaP) conversion coatings on Mg alloy, Surf. Coating. Technol. 397 (2020) 125919, https://doi.org/10.1016/j.surfcoat.2020.125919.
[83] R. Maurya, A.R. Siddiqui, K. Balani, In vitro degradation and biomineralization ability of hydroxyapatite coated Mg-9Li-7Al-1Sn and Mg-9Li-5Al-3Sn-1Zn alloys, Surf. Coating. Technol. 325 (2017) 65–74, https://doi.org/10.1016/j.surfcoat.2017.06.027.
[84] L. Han, Z. Zhang, J. Dai, X. Li, J. Bai, Z. Huang, C. Guo, F. Xue, C. Chu, The influence of alternating cyclic dynamic loads with different low frequencies on the bio-corrosion behaviors of AZ31B magnesium alloy in vitro, Bioact. Mater. 7 (2022) 263–274, https://doi.org/10.1016/j.bioactmat.2021.05.049.
[85] G. Hu, L. Zeng, H. Du, X. Fu, X. Jin, M. Deng, Y. Zhao, X. Liu, The formation mechanism and bio-corrosion properties of Ag/HA composite conversion coating on the extruded Mg-2Zn-1Mn-0.5Ca alloy for bone implant application, Surf. Coating. Technol. 325 (2017) 127–135, https://doi.org/10.1016/j.surfcoat.2017.06.023.
[86] E.C. Moreno, T.M. Gregory, W.E. Brown, Preparation and solubility of hydroxyapatite, J. Res. Natl. Bur. Stand. Sect. A Phys. Chem. 72A (1968) 773, https://doi.org/10.6028/jres.072a.052.
[87] A. Farzadi, F. Bakhshi, M. Solati-Hashjin, M. Asadi-Eydivand, N.A.A. Osman, Magnesium incorporated hydroxyapatite: synthesis and structural properties characterization, Ceram. Int. 40 (2014) 6021–6029, https://doi.org/10.1016/j.ceramint.2013.11.051.
[88] A.L. Rudd, C.B. Breslin, F. Mansfeld, The corrosion protection afforded by rare earth conversion coatings applied to magnesium, Corrosion Sci. 42 (2000) 275–288, https://doi.org/10.1016/S0010-938X(99)00076-1.
[89] X. Wu, Z. Liu, X. Liu, H. Xie, F. Liu, C. Lu, J. Li, Designing for the cerium-based conversion coating with excellent corrosion resistance on Mg–4Y–2Al magnesium alloy, Mater. Corros. 72 (2021) 925–935, https://doi.org/10.1002/maco.202012166.
[90] Y. Huang, X. Zhai, T. Ma, M. Zhang, H. Pan, W. Weijia Lu, X. Zhao, T. Sun, Y. Li, J. Shen, C. Yan, Y. Du, Rare earth-based materials for bone regeneration: breakthroughs and advantages, Coord. Chem. Rev. 450 (2022) 214236, https://doi.org/10.1016/j.ccr.2021.214236.
[91] B. Han, D. Gu, Y. Yang, L. Fang, G. Peng, C. Yang, Preparation of yttrium-based rare earth conversion coating and its effect on corrosion resistance of AZ91D magnesium alloy, Int. J. Electrochem. Sci. 12 (2017) 374–385, https://doi.org/10.20964/2017.01.53.
[92] K. Saranya, M. Kalaiyarasan, N. Rajendran, Selenium conversion coating on AZ31 Mg alloy: a solution for improved corrosion rate and enhanced bio-adaptability, Surf. Coating. Technol. 378 (2019) 124902, https://doi.org/10.1016/j.surfcoat.2019.124902.
[93] S. Kannan, R. Nallaiyan, Anticancer activity of samarium-coated magnesium implants for immunocompromised patients, ACS Appl. Bio Mater. 3 (2020) 4408–4416, https://doi.org/10.1021/acsabm.0c00400.
[94] S.Y. Jian, C.Y. Yang, J.K. Chang, Robust corrosion resistance and self-healing characteristics of a novel Ce/Mn conversion coatings on EV31 magnesium alloys, Appl. Surf. Sci. 510 (2020) 145385, https://doi.org/10.1016/j.apsusc.2020.145385.
[95] S. Shafighi, M. Reza, M. Shafiee, M. Ghashang, M. Reza, M. Shafiee, M. Ghashang, MgO-CeO 2 nanocomposite : efficient catalyst for the preparation of 2-amino-thiophenes and, J. Sulfur Chem. (2018) 402–413. https://doi.org/10.1080/17415993.2018.1436710.
[96] J. Machhi, P. Yeapuri, M. Markovic, M. Patel, W. Yan, Y. Lu, J.D. Cohen, M. Hasan, M.M. Abdelmoaty, Y. Zhou, Europium-doped cerium oxide nanoparticles for microglial amyloid beta clearance and homeostasis, ACS Chem. Neurosci. 13 (8) (2022) 1232–1244, https://doi.org/10.1021/acschemneuro.1c00847.
[97] S. Ren, Y. Zhou, K. Zheng, X. Xu, J. Yang, X. Wang, L. Miao, H. Wei, Y. Xu, Cerium oxide nanoparticles loaded nanofibrous membranes promote bone regeneration for periodontal tissue engineering, Bioact. Mater. 7 (2022) 242–253.
[98] M. Fu, F. Xu, Y. Juntao, W. Chunlei, G. Fan, G. Song, B. Chai, Mixed valence state cerium metal organic framework with prominent oxidase-mimicking activity for ascorbic acid detection: mechanism and performance, Colloids Surfaces A Physicochem. Eng. Asp. (2022) 128610.

[99] G. Pulido-Reyes, I. Rodea-Palomares, S. Das, T.S. Sakthivel, F. Leganes, R. Rosal, S. Seal, F. Fernández-Piñas, Untangling the biological effects of cerium oxide nanoparticles: the role of surface valence states, Sci. Rep. 5 (2015) 15613, https://doi.org/10.1038/srep15613.
[100] T. Xu, M. Zhang, J. Hu, Z. Li, T. Wu, J. Bao, S. Wu, L. Lei, D. He, Behavioral deficits and neural damage of Caenorhabditis elegans induced by three rare earth elements, Chemosphere 181 (2017) 55–62, https://doi.org/10.1016/j.chemosphere.2017.04.068.
[101] K. Saranya, M. Kalaiyarasan, S. Chatterjee, N. Rajendran, Dynamic electrochemical impedance study of fluoride conversion coating on AZ31 magnesium alloy to improve bio-adaptability for orthopedic application, Mater. Corros. 70 (2019) 698–710, https://doi.org/10.1002/maco.201810360.
[102] S. Fintová, J. Drábiková, B. Hadzima, L. Trško, M. Březina, P. Doležal, J. Wasserbauer, Degradation of unconventional fluoride conversion coating on AZ61 magnesium alloy in SBF solution, Surf. Coating. Technol. 380 (2019) 125012, https://doi.org/10.1016/j.surfcoat.2019.125012.
[103] J. Drábiková, S. Fintová, P. Ptáček, I. Kuběna, M. Březina, J. Wasserbauer, P. Doležal, F. Pastorek, Structure and growth kinetic of unconventional fluoride conversion coating prepared on wrought AZ61 magnesium alloy, Surf. Coating. Technol. 399 (2020) 126101, https://doi.org/10.1016/j.surfcoat.2020.126101.
[104] S. Li, L. Yi, X. Zhu, T. Liu, Ultrasonic treatment induced fluoride conversion coating without pores for high corrosion resistance of Mg alloy, Coatings 10 (2020), https://doi.org/10.3390/coatings10100996.
[105] J.D. Barajas, J.C. Joya, K.S. Durán, C.A. Hernández-Barrios, A.E. Coy, F. Viejo, Relationship between microstructure and formation-biodegradation mechanism of fluoride conversion coatings synthesised on the AZ31 magnesium alloy, Surf. Coating. Technol. 374 (2019) 424–436, https://doi.org/10.1016/j.surfcoat.2019.06.010.
[106] V.S. Saji, T.S.N. Sankara Narayanan, X. Chen, Conversion Coatings for Magnesium and its Alloys, Springer International Publishing, Cham, 2022, https://doi.org/10.1007/978-3-030-89976-9.
[107] J. Dziková, S. Fintová, D. Kajánek, Z. Florková, J. Wasserbauer, P. Doležal, Characterization and corrosion properties of fluoride conversion coating prepared on AZ31 magnesium alloy, Coatings 11 (2021), https://doi.org/10.3390/coatings11060675.
[108] M.S. P, R. K, S.N. Tsn, Controlling the rate of degradation of Mg using magnesium fluoride and magnesium fluoride-magnesium phosphate duplex coatings, J. Magnes. Alloy. 10 (2022) 295–312, https://doi.org/10.1016/j.jma.2021.06.005.
[109] C. Zhang, S. Zhang, D. Sun, J. Lin, F. Meng, H. Liu, Superhydrophobic fluoride conversion coating on bioresorbable magnesium alloy – fabrication, characterization, degradation and cytocompatibility with BMSCs, J. Magnes. Alloy. 9 (2021) 1246–1260, https://doi.org/10.1016/j.jma.2020.05.017.
[110] G.P. Abatti, A.T. Nunes Pires, A. Spinelli, N. Scharnagl, T.F. da Conceição, Conversion coating on magnesium alloy sheet (AZ31) by vanillic acid treatment: preparation, characterization and corrosion behavior, J. Alloys Compd. 738 (2018) 224–232, https://doi.org/10.1016/j.jallcom.2017.12.115.
[111] V.K. Korrapati, N. Scharnagl, D. Letzig, M.L. Zheludkevich, Bilayer coatings for temporary and long–term corrosion protection of magnesium–AZ31 alloy, Prog. Org. Coating 163 (2022) 106608, https://doi.org/10.1016/j.porgcoat.2021.106608.
[112] V.S. Saji, Organic conversion coatings for magnesium and its alloys, J. Ind. Eng. Chem. 75 (2019) 20–37, https://doi.org/10.1016/j.jiec.2019.03.018.
[113] M.L. Zheludkevich, J. Tedim, C.S.R. Freire, S.C.M. Fernandes, S. Kallip, A. Lisenkov, A. Gandini, M.G.S. Ferreira, Self-healing protective coatings with "green" chitosan based pre-layer reservoir of corrosion inhibitor, J. Mater. Chem. 21 (2011) 4805–4812, https://doi.org/10.1039/c1jm10304k.
[114] J.H. Chu, G.X. Sun, L.B. Tong, Z.H. Jiang, Facile one-step hydrothermal fabrication of Allium giganteum-like superhydrophobic coating on Mg alloy with self-cleaning and anti-corrosion properties, Colloids Surfaces A Physicochem. Eng. Asp. 617 (2021) 126370, https://doi.org/10.1016/j.colsurfa.2021.126370.
[115] C. shih Hsu, M.H. Nazari, Q. Li, X. Shi, Enhancing degradation and corrosion resistance of AZ31 magnesium alloy through hydrophobic coating, Mater. Chem. Phys. 225 (2019) 426–432, https://doi.org/10.1016/j.matchemphys.2018.12.106.
[116] M. Zhang, S. Cai, F. Zhang, G. Xu, F. Wang, N. Yu, X. Wu, Preparation and corrosion resistance of magnesium phytic acid/hydroxyapatite composite coatings on biodegradable AZ31 magnesium alloy, J. Mater. Sci. Mater. Med. 28 (2017) 1–8, https://doi.org/10.1007/s10856-017-5876-9.
[117] J. Ou, X. Chen, Corrosion resistance of phytic acid/Ce (III) nanocomposite coating with superhydrophobicity on magnesium, J. Alloys Compd. 787 (2019) 145–151, https://doi.org/10.1016/j.jallcom.2019.02.003.
[118] S. Li, L. Yi, T. Liu, H. Deng, B. Ji, K. Zhang, L. Zhou, Formation of a protective layer against corrosion on Mg alloy via alkali pretreatment followed by vanillic acid treatment, Mater. Corros. 71 (2020) 1330–1338, https://doi.org/10.1002/maco.201911488.
[119] M. Zhang, R. Chen, X. Liu, Q. Liu, J. Liu, J. Yu, P. Liu, L. Gao, J. Wang, Anticorrosion study of phytic acid ligand binding with exceptional self-sealing functionality, J. Alloys Compd. 818 (2020) 152875, https://doi.org/10.1016/j.jallcom.2019.152875.
[120] F. Wang, S. Cai, S. Shen, N. Yu, F. Zhang, R. Ling, Y. Li, G. Xu, Preparation of phytic acid/silane hybrid coating on magnesium alloy and its corrosion resistance in simulated body fluid, J. Mater. Eng. Perform. 26 (2017) 4282–4290, https://doi.org/10.1007/s11665-017-2897-y.
[121] Y. Guo, S. Jia, L. Qiao, Y. Su, R. Gu, G. Li, J. Lian, Enhanced corrosion resistance and biocompatibility of polydopamine/dicalcium phosphate dihydrate/collagen composite coating on magnesium alloy for orthopedic applications, J. Alloys Compd. 817 (2020) 152782, https://doi.org/10.1016/j.jallcom.2019.152782.
[122] B. Zhu, S. Wang, L. Wang, Y. Yang, J. Liang, B. Cao, Preparation of hydroxyapatite/tannic acid coating to enhance the corrosion resistance and cytocompatibility of AZ31 magnesium alloys, Coatings 7 (2017), https://doi.org/10.3390/coatings7070105.
[123] P. Wang, J. Liu, X. Luo, P. Xiong, S. Gao, J. Yan, Y. Li, Y. Cheng, T. Xi, A tannic acid-modified fluoride pre-treated Mg-Zn-Y-Nd alloy with antioxidant and platelet-repellent functionalities for vascular stent application, J. Mater. Chem. B. 7 (2019) 7314–7325, https://doi.org/10.1039/c9tb01587f.
[124] B. Kaczmarek, M. Wekwejt, K. Nadolna, A. Owczarek, O. Mazur, A. Pałubicka, The mechanical properties and bactericidal degradation effectiveness of tannic acid-based thin films for wound care, J. Mech. Behav. Biomed. Mater. 110 (2020) 103916, https://doi.org/10.1016/j.jmbbm.2020.103916.
[125] A. Francis, Y. Yang, A.R. Boccaccini, A new strategy for developing chitosan conversion coating on magnesium substrates for orthopedic implants, Appl. Surf. Sci. 466 (2019) 854–862, https://doi.org/10.1016/j.apsusc.2018.10.002.
[126] S. Chen, S. Zhao, M. Chen, X. Zhang, J. Zhang, X. Li, H. Zhang, X. Shen, J. Wang, N. Huang, The anticorrosion mechanism of phenolic conversion coating applied on magnesium implants, Appl. Surf. Sci. 463 (2019) 953–967, https://doi.org/10.1016/j.apsusc.2018.08.261.
[127] H. Zhang, L. Xie, X. Shen, T. Shang, R. Luo, X. Li, T. You, J. Wang, N. Huang, Y. Wang, Catechol/polyethyleneimine conversion coating with enhanced corrosion protection of magnesium alloys: potential applications for vascular implants, J. Mater. Chem. B. 6 (2018) 6936–6949, https://doi.org/10.1039/c8tb01574k.
[128] H. Zhang, X. Shen, J. Wang, N. Huang, R. Luo, B. Zhang, Y. Wang, Multistep instead of one-step: a versatile and multifunctional coating platform for biocompatible corrosion protection, ACS Biomater. Sci. Eng. 5 (2019) 6541–6556, https://doi.org/10.1021/acsbiomaterials.9b01459.
[129] X. Xun, Y. Wan, Q. Zhang, D. Gan, J. Hu, H. Luo, Low adhesion superhydrophobic AZ31B magnesium alloy surface with corrosion resistant and anti-bioadhesion properties, Appl. Surf. Sci. 505 (2020) 144566, https://doi.org/10.1016/j.apsusc.2019.144566.
[130] L. Liu, Q. Yang, L. Huang, X. Liu, Y. Liang, Z. Cui, X. Yang, S. Zhu, Z. Li, Y. Zheng, K.W.K. Yeung, S. Wu, The effects of a phytic acid/calcium ion conversion coating on the corrosion behavior and osteoinductivity of a magnesium-strontium alloy, Appl. Surf. Sci. 484 (2019) 511–523, https://doi.org/10.1016/j.apsusc.2019.04.107.
[131] L.H. Lin, H.P. Lee, M.L. Yeh, Characterization of a sandwich plga-gallic acid-plga coating on mg alloy zk60 for bioresorbable coronary artery stents, Materials 13 (2020) 1–16, https://doi.org/10.3390/ma13235538.
[132] L.-Y. Cui, G.-B. Wei, R.-C. Zeng, S.-Q. Li, Y.-H. Zou, E.-H. Han, Corrosion resistance of a novel SnO2-doped dicalcium phosphate coating on AZ31 magnesium alloy, Bioact. Mater. 3 (2018) 245–249, https://doi.org/10.1016/j.bioactmat.2017.11.001.
[133] S. Jiang, Y. Cao, S. Li, Y. Pang, Z. Sun, Dual function of poly(acrylic acid) on controlling amorphous mediated hydroxyapatite crystallization, J. Cryst. Growth 557 (2021) 125991, https://doi.org/10.1016/j.jcrysgro.2020.125991.
[134] A. Shanaghi, B. Mehrjou, P.K. Chu, Enhanced corrosion resistance and reduced cytotoxicity of the AZ91 Mg alloy by plasma nitriding and a hierarchical structure composed of ciprofloxacin-loaded polymeric multilayers and calcium phosphate coating, J. Biomed. Mater. Res. 109 (2021) 2657–2672, https://doi.org/10.1002/jbm.a.37258.
[135] K. Yang, B. Hu, S.-N. An, W.-T. Chen, L.-Y. Cui, S.-Q. Li, Corrosion resistance of polyelectrolyte/SiO2 nanoparticles multilayers on magnesium alloy: effect of heat treatment, J. Mater. Eng. Perform. 30 (2021) 9283–9289, https://doi.org/10.1007/s11665-021-06130-3.
[136] S. Liu, G. Li, Y. Qi, Z. Peng, Y. Ye, J. Liang, Corrosion and tribocorrosion resistance of MAO-based composite coating on AZ31 magnesium alloy, J. Magnes. Alloy (2021), https://doi.org/10.1016/j.jma.2021.04.004. In press.
[137] B.L. Jiang, Y.F. Ge, Micro-arc oxidation (MAO) to improve the corrosion resistance of magnesium (Mg) alloys. https://doi.org/10.1533/9780857098962.2.163, 2013.
[138] L. Zhang, J. Zhang, C. fu Chen, Y. Gu, Advances in microarc oxidation coated AZ31 Mg alloys for biomedical applications, Corrosion Sci. 91 (2015) 7–28, https://doi.org/10.1016/j.corsci.2014.11.001.
[139] N. Attarzadeh, A. Kazemi, M. Molaei, A. Fattah-alhosseini, Multipurpose surface modification of PEO coatings using tricalcium phosphate addition to improve the bedding for apatite compounds, J. Alloys Compd. 877 (2021) 160275, https://doi.org/10.1016/j.jallcom.2021.160275.
[140] W. Yu, R. Sun, Z. Guo, Z. Wang, Y. He, G. Lu, P. Chen, K. Chen, Novel fluoridated hydroxyapatite/MAO composite coating on AZ31B magnesium alloy for biomedical application, Appl. Surf. Sci. 464 (2019) 708–715, https://doi.org/10.1016/j.apsusc.2018.09.148.
[141] J. Han, B. Luthringer, S. Tang, J. Hu, C. Blawert, M.L. Zheludkevich, Evolution and performance of a MgO/HA/DCPD gradient coating on pure magnesium, J. Alloys Compd. 883 (2021) 160793, https://doi.org/10.1016/j.jallcom.2021.160793.
[142] M. Tang, Y. Shao, Z. Feng, W. Wang, G. Li, Z. Yan, R. Zhang, Self-sealing Microarc Oxidation Coating Mainly Containing ZrO2 and Nano Mg2Zr5O12 on AZ91D Mg Alloy, Int. J. Electrochem. Sci. 15 (2020) 12447–12461.
[143] C. Wen, X. Zhan, X. Huang, F. Xu, L. Luo, C. Xia, Characterization and corrosion properties of hydroxyapatite/graphene oxide bio-composite coating on magnesium alloy by one-step micro-arc oxidation method, Surf. Coating. Technol. 317 (2017) 125–133, https://doi.org/10.1016/j.surfcoat.2017.03.034.

[144] Y. Gu, X. Zheng, Q. Liu, H. Ma, L. Zhang, D. Yang, Investigating corrosion performance and corrosive wear behavior of sol–gel/MAO-coated Mg alloy, Tribol. Lett. 66 (2018), https://doi.org/10.1007/s11249-018-1052-8, 0.
[145] M. Daavari, M. Atapour, M. Mohedano, R. Arrabal, E. Matykina, A. Taherizadeh, Biotribology and Biocorrosion of MWCNTs-Reinforced PEO Coating on AZ31B Mg Alloy, Elsevier B.V., 2021, https://doi.org/10.1016/j.surfin.2020.100850.
[146] Z. Lin, T. Wang, X. Yu, X. Sun, H. Yang, Functionalization treatment of micro-arc oxidation coatings on magnesium alloys: a review, J. Alloys Compd. 879 (2021) 160453, https://doi.org/10.1016/j.jallcom.2021.160453.
[147] L. Chen, Y. Sheng, H. Zhou, Z. Li, X. Wang, W. Li, Influence of a MAO + PLGA coating on biocorrosion and stress corrosion cracking behavior of a magnesium alloy in a physiological environment, Corrosion Sci. 148 (2019) 134–143, https://doi.org/10.1016/j.corsci.2018.12.005.
[148] F. Soleymani, R. Emadi, S. Sadeghzade, F. Tavangarian, Applying baghdadite/PCL/chitosan nanocomposite coating on AZ91 magnesium alloy to improve corrosion behavior, bioactivity, and biodegradability, Coatings 9 (2019), https://doi.org/10.3390/coatings9120789.
[149] X.J. Cui, C.M. Ning, G.A. Zhang, L.L. Shang, L.P. Zhong, Y.J. Zhang, Properties of polydimethylsiloxane hydrophobic modified duplex microarc oxidation/diamond-like carbon coatings on AZ31B Mg alloy, J. Magnes. Alloy. 9 (2021) 1285–1296, https://doi.org/10.1016/j.jma.2020.04.009.
[150] S. Effendy, T. Zhou, H. Eichman, M. Petr, M.Z. Bazant, Blistering failure of elastic coatings with applications to corrosion resistance, Soft Matter 17 (2021) 9480–9498, https://doi.org/10.1039/d1sm00986a.
[151] A. Saberi, H.R. Bakhsheshi-Rad, S. Abazari, A.F. Ismail, S. Sharif, S. Ramakrishna, M. Daroonparvar, F. Berto, A comprehensive review on surface modifications of biodegradable magnesium-based implant alloy: polymer coatings opportunities and challenges, Coatings 11 (2021) 747, https://doi.org/10.3390/coatings11070747.
[152] M. Bobby Kannan, R. Walter, H. Khakbaz, R. Zeng, C. Blawert, A triple-layered hybrid coating with self-organized microporous polymer film on magnesium for biodegradable implant applications, Med. Devices Sensors 3 (2020) 1–10, https://doi.org/10.1002/mds3.10070.
[153] M.S. Butt, A. Maqbool, M. Saleem, M.A. Umer, F. Javaid, R.A. Malik, M. A. Hussain, Z. Rehman, Revealing the effects of microarc oxidation on the mechanical and degradation properties of Mg-based biodegradable composites, ACS Omega 5 (2020) 13694–13702, https://doi.org/10.1021/acsomega.0c00836.
[154] J. Guo, X. Liu, K. Du, Q. Guo, Y. Wang, Y. Liu, L. Feng, An anti-stripping and self-healing micro-arc oxidation/acrylamide gel composite coating on magnesium alloy AZ31, Mater. Lett. 260 (2020) 126912, https://doi.org/10.1016/j.matlet.2019.126912.
[155] Z. Zheng, M.C. Zhao, L. Tan, Y.C. Zhao, B. Xie, D. Yin, K. Yang, A. Atrens, Corrosion behavior of a self-sealing coating containing CeO2 particles on pure Mg produced by micro-arc oxidation, Surf. Coating. Technol. 386 (2020) 125456, https://doi.org/10.1016/j.surfcoat.2020.125456.
[156] Z.Q. Zhang, L. Wang, M.Q. Zeng, R.C. Zeng, M.B. Kannan, C.G. Lin, Y.F. Zheng, Biodegradation behavior of micro-arc oxidation coating on magnesium alloy-from a protein perspective, Bioact. Mater. 5 (2020) 398–409, https://doi.org/10.1016/j.bioactmat.2020.03.005.
[157] X. Ly, S. Yang, T. Nguyen, Effect of equal channel angular pressing as the pretreatment on microstructure and corrosion behavior of micro-arc oxidation (MAO) composite coating on biodegradable Mg-Zn-Ca alloy, Surf. Coating. Technol. 395 (2020) 125923, https://doi.org/10.1016/j.surfcoat.2020.125923.
[158] Y. Xiong, Q. Hu, R. Song, X. Hu, LSP/MAO composite bio-coating on AZ80 magnesium alloy for biomedical application, Mater. Sci. Eng. C 75 (2017) 1299–1304, https://doi.org/10.1016/j.msec.2017.03.003.
[159] M. Wu, Y. Guo, G. Xu, Y. Cui, Effects of deposition thickness on electrochemical behaviors of AZ31B magnesium alloy with composite coatings prepared by micro-arc oxidation and electrophoretic deposition, Int. J. Electrochem. Sci. 15 (2020) 1378–1390, https://doi.org/10.20964/2020.02.08.
[160] Y. Xiong, C. Lu, C. Wang, R. Song, The n-MAO/EPD bio-ceramic composite coating fabricated on ZK60 magnesium alloy using combined micro-arc oxidation with electrophoretic deposition, Appl. Surf. Sci. 322 (2014) 230–235.
[161] Y. Xiong, C. Lu, C. Wang, R. Song, Degradation behavior of n-MAO/EPD bio-ceramic composite coatings on magnesium alloy in simulated body fluid, J. Alloys Compd. 625 (2015) 258–265.
[162] R. Manoj Kumar, K.K. Kuntal, S. Singh, P. Gupta, B. Bhushan, P. Gopinath, D. Lahiri, Electrophoretic deposition of hydroxyapatite coating on Mg-3Zn alloy for orthopaedic application, Surf. Coating. Technol. 287 (2016) 82–92, https://doi.org/10.1016/j.surfcoat.2015.12.086.
[163] V.S. Saji, Electrophoretic (EPD) coatings for magnesium alloys, J. Ind. Eng. Chem. 103 (2021) 358–372.
[164] M. Razavi, M. Fathi, O. Savabi, D. Vashaee, L. Tayebi, Biodegradable magnesium alloy coated by fluoridated hydroxyapatite using MAO/EPD technique, Surf. Eng. 30 (2014) 545–551.
[165] M. Razavi, M. Fathi, O. Savabi, D. Vashaee, L. Tayebi, In vivo assessments of bioabsorbable AZ91 magnesium implants coated with nanostructured fluoridated hydroxyapatite by MAO/EPD technique for biomedical applications, Mater. Sci. Eng. C 48 (2015) 21–27.
[166] H.R. Bakhsheshi-Rad, E. Hamzah, A.F. Ismail, M. Aziz, M. Daroonparvar, E. Saebnoori, A. Chami, In vitro degradation behavior, antibacterial activity and cytotoxicity of TiO2-MAO/ZnHA composite coating on Mg alloy for orthopedic implants, Surf. Coating. Technol. 334 (2018) 450–460, https://doi.org/10.1016/j.surfcoat.2017.11.027.
[167] M.S. Uddin, C. Hall, P. Murphy, Surface treatments for controlling corrosion rate of biodegradable Mg and Mg-based alloy implants, Sci. Technol. Adv. Mater. 16 (2015), https://doi.org/10.1088/1468-6996/16/5/053501.
[168] X. Lu, X. Feng, Y. Zuo, P. Zhang, C. Zheng, Improvement of protection performance of Mg-rich epoxy coating on AZ91D magnesium alloy by DC anodic oxidation, Prog. Org. Coating 104 (2017) 188–198.
[169] S. Moon, Y. Nam, Anodic oxidation of Mg–Sn alloys in alkaline solutions, Corrosion Sci. 65 (2012) 494–501.
[170] G. Zhang, L. Wu, A. Tang, X.-B. Chen, Y. Ma, Y. Long, P. Peng, X. Ding, H. Pan, F. Pan, Growth behavior of MgAl-layered double hydroxide films by conversion of anodic films on magnesium alloy AZ31 and their corrosion protection, Appl. Surf. Sci. 456 (2018) 419–429.
[171] L. Wu, D. Yang, G. Zhang, Z. Zhang, S. Zhang, A. Tang, F. Pan, Fabrication and characterization of Mg-M layered double hydroxide films on anodized magnesium alloy AZ31, Appl. Surf. Sci. 431 (2018) 177–186.
[172] A. Zaffora, F. Di Franco, D. Virtù, F. Carfì Pavia, G. Ghersi, S. Virtanen, M. Santamaria, Tuning of the Mg alloy AZ31 anodizing process for biodegradable implants, ACS Appl. Mater. Interfaces 13 (2021) 12866–12876, https://doi.org/10.1021/acsami.0c22933.
[173] Z. Geng, X. Li, Y. Zhang, E. Lin, S.-Z. Kure-Chu, X. Li, X. Xiao, Corrosion resistance and degradation behavior of anodized Mg-Gd alloys: a comparative study, Surf. Coating. Technol. 412 (2021) 127042, https://doi.org/10.1016/j.surfcoat.2021.127042.
[174] V. Jothi, A.Y. Adesina, A.M. Kumar, M.M. Rahman, J.S.N. Ram, Enhancing the biodegradability and surface protective performance of AZ31 Mg alloy using polypyrrole/gelatin composite coatings with anodized Mg surface, Surf. Coating. Technol. 381 (2020) 125139, https://doi.org/10.1016/j.surfcoat.2019.125139.
[175] A. Bahatibieke, H. Qin, T. Cui, Y. Liu, Z. Wang, In vivo and in simulated body fluid degradation behavior and biocompatibility evaluation of anodic oxidation-silane-chitosan-coated Mg-4.0Zn-0.8Sr alloy for bone application, Mater. Sci. Eng. C 120 (2021) 111771, https://doi.org/10.1016/j.msec.2020.111771.
[176] T. Lei, C. Ouyang, W. Tang, L.-F. Li, L.-S. Zhou, Enhanced corrosion protection of MgO coatings on magnesium alloy deposited by an anodic electrodeposition process, Corrosion Sci. 52 (2010) 3504–3508, https://doi.org/10.1016/j.corsci.2010.06.028.
[177] M. Kaseem, K. Ramachandraiah, S. Hossain, B. Dikici, A review on LDH-smart functionalization of anodic films of Mg alloys, Nanomaterials 11 (2021) 536.
[178] S. Nezamdoust, D. Seifzadeh, Z. Rajabalizadeh, Application of novel sol–gel composites on magnesium alloy, J. Magnes. Alloy. 7 (2019) 419–432, https://doi.org/10.1016/j.jma.2019.03.004.
[179] K.H. Cheon, C. Park, M.H. Kang, I.G. Kang, M.K. Lee, H. Lee, H.E. Kim, H. Do Jung, T.S. Jang, Construction of tantalum/poly(ether imide) coatings on magnesium implants with both corrosion protection and osseointegration properties, Bioact. Mater. 6 (2021) 1189–1200, https://doi.org/10.1016/j.bioactmat.2020.10.007.
[180] X. Wei, P. Liu, S. Ma, Z. Li, X. Peng, R. Deng, Q. Zhao, Improvement on corrosion resistance and biocompability of ZK60 magnesium alloy by carboxyl ion implantation, Corrosion Sci. 173 (2020) 108729, https://doi.org/10.1016/j.corsci.2020.108729.
[181] T. Liang, L. Zeng, Y. Shi, H. Pan, P.K. Chu, K.W.K. Yeung, Y. Zhao, In vitro and in vivo antibacterial performance of Zr & O PIII magnesium alloys with high concentration of oxygen vacancies, Bioact. Mater. 6 (2021) 3049–3061, https://doi.org/10.1016/j.bioactmat.2021.02.025.
[182] S. Somasundaram, M. Ionescu, B.K. Mathan, Ion implantation of calcium and zinc in magnesium for biodegradable implant applications, Metals 8 (2018) 1–10, https://doi.org/10.3390/met8010030.
[183] H. Wu, G. Wu, P.K. Chu, Effects of cerium ion implantation on the corrosion behavior of magnesium in different biological media, Surf. Coating. Technol. 306 (2016) 6–10, https://doi.org/10.1016/j.surfcoat.2016.01.034.
[184] G. Wu, R. Xu, K. Feng, S. Wu, Z. Wu, G. Sun, G. Zheng, G. Li, P.K. Chu, Retardation of surface corrosion of biodegradable magnesium-based materials by aluminum ion implantation, Appl. Surf. Sci. 258 (2012) 7651–7657, https://doi.org/10.1016/j.apsusc.2012.04.112.
[185] Q. Dong, Y. Jia, Z. Ba, X. Tao, Z. Wang, F. Xue, J. Bai, Exploring the corrosion behavior of Mn-implanted biomedical Mg, J. Alloys Compd. 873 (2021), https://doi.org/10.1016/j.jallcom.2021.159739, 159739.
[186] Y. Liu, D. Bian, Y. Wu, N. Li, K. Qiu, Y. Zheng, Y. Han, Influence of biocompatible metal ions (Ag, Fe, Y) on the surface chemistry, corrosion behavior and cytocompatibility of Mg-1Ca alloy treated with MEVVA, Colloids Surf. B Biointerfaces 133 (2015) 99–107, https://doi.org/10.1016/j.colsurfb.2015.05.050.
[187] M.I. Jamesh, G. Wu, Y. Zhao, D.R. McKenzie, M.M.M. Bilek, P.K. Chu, Effects of zirconium and oxygen plasma ion implantation on the corrosion behavior of ZK60 Mg alloy in simulated body fluids, Corrosion Sci. 82 (2014) 7–26, https://doi.org/10.1016/j.corsci.2013.11.044.
[188] S. Vasanthavel, M. Kumar, S. Kannan, Structural, morphological and mechanical analysis of Mg2+ substituted calcium zirconium phosphate [CaZr4(PO4)6], J. Alloys Compd. 854 (2021) 157185, https://doi.org/10.1016/j.jallcom.2020.157185.
[189] M.I. Jamesh, G. Wu, Y. Zhao, W. Jin, D.R. McKenzie, M.M.M. Bilek, P.K. Chu, Effects of zirconium and nitrogen plasma immersion ion implantation on the electrochemical corrosion behavior of Mg-Y-RE alloy in simulated body fluid and cell culture medium, Corrosion Sci. 86 (2014) 239–251, https://doi.org/10.1016/j.corsci.2014.05.020.
[190] M. Cheng, Y. Qiao, Q. Wang, H. Qin, X. Zhang, X. Liu, Dual ions implantation of zirconium and nitrogen into magnesium alloys for enhanced corrosion resistance,

antimicrobial activity and biocompatibility, Colloids Surf. B Biointerfaces 148 (2016) 200–210, https://doi.org/10.1016/j.colsurfb.2016.08.056.
[191] Y. Zhao, G. Wu, Q. Lu, J. Wu, R. Xu, K.W.K. Yeung, P.K. Chu, Improved surface corrosion resistance of WE43 magnesium alloy by dual titanium and oxygen ion implantation, Thin Solid Films 529 (2013) 407–411, https://doi.org/10.1016/j.tsf.2012.05.046.
[192] Z. Ba, Q. Dong, J. Yin, J. Wang, B. Ma, X. Zhang, Z. Wang, Surface properties of Mg-Gd-Zn-Zr alloy modified by Sn ion implantation, Mater. Lett. 190 (2017) 90–94, https://doi.org/10.1016/j.matlet.2016.12.038.
[193] J. Liu, Y. Zheng, Y. Bi, Y. Li, Y. Zheng, Improved cytocompatibility of Mg-1Ca alloy modified by Zn ion implantation and deposition, Mater. Lett. 205 (2017) 87–89, https://doi.org/10.1016/j.matlet.2017.06.055.
[194] Z. Li, Z. Shang, X. Wei, Q. Zhao, Corrosion resistance and cytotoxicity of AZ31 magnesium alloy with N+ ion implantation, Mater. Technol. 34 (2019) 730–736, https://doi.org/10.1080/10667857.2019.1623529.
[195] Z. Ba, Y. Jia, Q. Dong, Z. Li, J. Kuang, Effects of Zr ion implantation on surface mechanical properties and corrosion resistance of pure magnesium, J. Mater. Eng. Perform. 28 (2019) 2543–2551, https://doi.org/10.1007/s11665-019-04055-6.
[196] B. Istrate, J. V Rau, C. Munteanu, I. V Antoniac, V. Saceleanu, Properties and in vitro assessment of ZrO2-based coatings obtained by atmospheric plasma jet spraying on biodegradable Mg-Ca and Mg-Ca-Zr alloys, Ceram. Int. 46 (2020) 15897–15906, https://doi.org/10.1016/j.ceramint.2020.03.138.
[197] L.C. Zhang, M. Xu, Y.D. Hu, F. Gao, T. Gong, T. Liu, X. Li, C.J. Pan, Biofunctionization of biodegradable magnesium alloy to improve the in vitro corrosion resistance and biocompatibility, Appl. Surf. Sci. 451 (2018) 20–31, https://doi.org/10.1016/j.apsusc.2018.04.235.
[198] H. Tang, T. Wu, F. Xu, W. Tao, X. Jian, Fabrication and characterization of Mg (OH)2 films on AZ31 magnesium alloy by alkali treatment, Int. J. Electrochem. Sci. 12 (2017) 1377–1388, https://doi.org/10.20964/2017.02.35.
[199] L.Y. Li, B. Liu, R.C. Zeng, S.Q. Li, F. Zhang, Y.H. Zou, H.G. Jiang, X.B. Chen, S. K. Guan, Q.Y. Liu, In vitro corrosion of magnesium alloy AZ31 — a synergetic influence of glucose and Tris, Front. Mater. Sci. 12 (2018) 184–197, https://doi.org/10.1007/s11706-018-0424-1.
[200] C. Zhang, B. Liu, B. Yu, X. Lu, Y. Wei, T. Zhang, J.M.C. Mol, F. Wang, Influence of surface pretreatment on phosphate conversion coating on AZ91 Mg alloy, Surf. Coating. Technol. 359 (2019) 414–425, https://doi.org/10.1016/j.surfcoat.2018.12.091.
[201] M. Uddin, C. Hall, V. Santos, R. Visalakshan, G. Qian, K. Vasilev, Synergistic effect of deep ball burnishing and HA coating on surface integrity, corrosion and immune response of biodegradable AZ31B Mg alloys, Mater. Sci. Eng. C 118 (2021) 111459, https://doi.org/10.1016/j.msec.2020.111459.
[202] M. You, M. Echeverry-Rendón, L. Zhang, J. Niu, J. Zhang, J. Pei, G. Yuan, Effects of composition and hierarchical structures of calcium phosphate coating on the corrosion resistance and osteoblast compatibility of Mg alloys, Mater. Sci. Eng. C 120 (2021) 111734, https://doi.org/10.1016/j.msec.2020.111734.
[203] C. Pan, Y. Hu, Y. Hou, T. Liu, Y. Lin, W. Ye, Y. Hou, T. Gong, Corrosion resistance and biocompatibility of magnesium alloy modified by alkali heating treatment followed by the immobilization of poly (ethylene glycol), fibronectin and heparin, Mater. Sci. Eng. C 70 (2017) 438–449, https://doi.org/10.1016/j.msec.2016.09.028.
[204] Z. Gu, J.J. Atherton, Z.P. Xu, Hierarchical layered double hydroxide nanocomposites: structure, synthesis and applications, Chem. Commun. 51 (2015) 3024–3036, https://doi.org/10.1039/c4cc07715f.
[205] M. Tabish, G. Yasin, M.J. Anjum, M.U. Malik, J. Zhao, Q. Yang, S. Manzoor, H. Murtaza, W.Q. Khan, Reviewing the current status of layered double hydroxide-based smart nanocontainers for corrosion inhibiting applications, J. Mater. Res. Technol. 10 (2021) 390–421, https://doi.org/10.1016/j.jmrt.2020.12.025.
[206] L. Guo, W. Wu, Y. Zhou, F. Zhang, R. Zeng, J. Zeng, Layered double hydroxide coatings on magnesium alloys: a review, J. Mater. Sci. Technol. 34 (2018) 1455–1466, https://doi.org/10.1016/j.jmst.2018.03.003.
[207] Y. Cao, D. Zheng, F. Zhang, J. Pan, C. Lin, Layered double hydroxide (LDH) for multi-functionalized corrosion protection of metals: a review, J. Mater. Sci. Technol. 102 (2022) 232–263, https://doi.org/10.1016/j.jmst.2021.05.078.
[208] K. Cao, Z. Yu, L. Zhu, D. Yin, L. Chen, Y. Jiang, J. Wang, Fabrication of superhydrophobic layered double hydroxide composites to enhance the corrosion-resistant performances of epoxy coatings on Mg alloy, Surf. Coating. Technol. 407 (2021) 126763, https://doi.org/10.1016/j.surfcoat.2020.126763.
[209] M. Kaseem, Y.G. Ko, A novel hybrid composite composed of albumin, WO3, and LDHs film for smart corrosion protection of Mg alloy, Compos. B Eng. 204 (2021) 108490, https://doi.org/10.1016/j.compositesb.2020.108490.
[210] J.K.E. Tan, P. Balan, N. Birbilis, Advances in LDH coatings on Mg alloys for biomedical applications: a corrosion perspective, Appl. Clay Sci. 202 (2021) 105948, https://doi.org/10.1016/j.clay.2020.105948.
[211] L.X. Li, Z.H. Xie, C. Fernandez, L. Wu, D. Cheng, X.H. Jiang, C.J. Zhong, Development of a thiophene derivative modified LDH coating for Mg alloy corrosion protection, Electrochim. Acta 330 (2020) 135186, https://doi.org/10.1016/j.electacta.2019.135186.
[212] V. Zahedi Asl, J. Zhao, M.J. Anjum, S. Wei, W. Wang, Z. Zhao, The effect of cerium cation on the microstructure and anti-corrosion performance of LDH conversion coatings on AZ31 magnesium alloy, J. Alloys Compd. 821 (2020) 153248, https://doi.org/10.1016/j.jallcom.2019.153248.
[213] Y. Tang, F. Wu, L. Fang, T. Guan, J. Hu, S.F. Zhang, A comparative study and optimization of corrosion resistance of ZnAl layered double hydroxides films intercalated with different anions on AZ31 Mg alloys, Surf. Coating. Technol. 358 (2019) 594–603, https://doi.org/10.1016/j.surfcoat.2018.11.070.
[214] H. Wu, L. Zhang, Y. Zhang, S. Long, X. Jie, Corrosion behavior of Mg–Al LDH film in-situ assembled with graphene on Mg alloy pre-sprayed Al layer, J. Alloys Compd. 834 (2020) 155107, https://doi.org/10.1016/j.jallcom.2020.155107.
[215] J. Chen, J. Feng, L. Yan, H. Li, C. Xiong, S. Ma, In situ growth process of Mg–Fe layered double hydroxide conversion film on MgCa alloy, J. Magnes. Alloy. 9 (2021) 1019–1027, https://doi.org/10.1016/j.jma.2020.05.019.
[216] Y. Zhao, Y. Chen, W. Wang, Z. Zhou, S. Shi, W. Li, M. Chen, Z. Li, One-step in situ synthesis of nano silver-hydrotalcite coating for enhanced antibacterial and degradation property of magnesium alloys, Mater. Lett. 265 (2020) 2–5, https://doi.org/10.1016/j.matlet.2020.127349.
[217] J. Chen, S. Liang, D. Fu, W. Fan, W. Lin, W. Ren, L. Zou, X. Cui, Design and in situ prepare a novel composite coating on Mg alloy for active anti-corrosion protection, J. Alloys Compd. 831 (2020) 154580, https://doi.org/10.1016/j.jallcom.2020.154580.
[218] W. Wu, X. Sun, C.L. Zhu, F. Zhang, R.C. Zeng, Y.H. Zou, S.Q. Li, Biocorrosion resistance and biocompatibility of Mg–Al layered double hydroxide/poly-L-glutamic acid hybrid coating on magnesium alloy AZ31, Prog. Org. Coating 147 (2020) 105746, https://doi.org/10.1016/j.porgcoat.2020.105746.
[219] X. Sun, Q.S. Yao, Y.C. Li, F. Zhang, R.C. Zeng, Y.H. Zou, S.Q. Li, Biocorrosion resistance and biocompatibility of Mg-Al layered double hydroxide/poly(L-lactic acid) hybrid coating on magnesium alloy AZ31, Front. Mater. Sci. 14 (2020) 426–441, https://doi.org/10.1007/s11706-020-0522-8.
[220] F. Peng, S. Cheng, R. Zhang, M. Li, J. Zhou, D. Wang, Y. Zhang, Zn-contained mussel-inspired film on Mg alloy for inhibiting bacterial infection and promoting bone regeneration, Regen. Biomater. 8 (2021) 1–15, https://doi.org/10.1093/rb/rbaa044.
[221] J. Ouyang, X. Hong, Y. Gao, Retardation and self-repair of erosion pits by a two-stage barrier on bioactive-glass/layered double hydroxide coating of biomedical magnesium alloys, Surf. Coating. Technol. 405 (2021) 126562, https://doi.org/10.1016/j.surfcoat.2020.126562.
[222] J. ling Chen, L. Fang, F. Wu, X. guang Zeng, J. Hu, S. fang Zhang, B. Jiang, H. jun Luo, Comparison of corrosion resistance of MgAl-LDH and ZnAl-LDH films intercalated with organic anions ASP on AZ31 Mg alloys, Trans. Nonferrous Met. Soc. China 30 (2020) 2424–2434, https://doi.org/10.1016/S1003-6326(20)65389-4.
[223] Y. Song, Y. Tang, L. Fang, F. Wu, X.G. Zeng, J. Hu, S.F. Zhang, B. Jiang, H.J. Luo, Enhancement of corrosion resistance of AZ31 Mg alloys by one-step in situ synthesis of ZnAl-LDH films intercalated with organic anions (ASP, La), J. Magnes. Alloy. 9 (2021) 658–667, https://doi.org/10.1016/j.jma.2020.03.013.
[224] M.J. Anjum, J. Zhao, V. Zahedi Asl, G. Yasin, W. Wang, S. Wei, Z. Zhao, W. Qamar Khan, In-situ intercalation of 8-hydroxyquinoline in Mg-Al LDH coating to improve the corrosion resistance of AZ31, Corrosion Sci. 157 (2019) 1–10, https://doi.org/10.1016/j.corsci.2019.05.022.
[225] Z.M. Qiu, F. Zhang, J.T. Chu, Y.C. Li, L. Song, Corrosion resistance and hydrophobicity of myristic acid modified Mg-Al LDH/Mg(OH)2 steam coating on magnesium alloy AZ31, Front. Mater. Sci. 14 (2020) 96–107, https://doi.org/10.1007/s11706-020-0492-x.
[226] E. Petrova, M. Serdechnova, T. Shulha, S.V. Lamaka, D.C.F. Wieland, P. Karlova, C. Blawert, M. Starykevich, M.L. Zheludkevich, Use of synergistic mixture of chelating agents for in situ LDH growth on the surface of PEO-treated AZ91, Sci. Rep. 10 (2020) 1–11, https://doi.org/10.1038/s41598-020-65396-0.
[227] J. Kuang, Z. Ba, Z. Li, Y. Jia, Z. Wang, Fabrication of a superhydrophobic Mg-Mn layered double hydroxides coating on pure magnesium and its corrosion resistance, Surf. Coating. Technol. 361 (2019) 75–82, https://doi.org/10.1016/j.surfcoat.2019.01.009.
[228] D. Zhang, S. Cheng, J. Tan, J. Xie, Y. Zhang, S. Chen, H. Du, S. Qian, Y. Qiao, F. Peng, X. Liu, Black Mn-containing layered double hydroxide coated magnesium alloy for osteosarcoma therapy, bacteria killing, and bone regeneration, Bioact. Mater. (2022), https://doi.org/10.1016/j.bioactmat.2022.01.032.
[229] M. Zarka, B. Dikici, M. Niinomi, K.V. Ezirmik, M. Nakai, H. Yilmazer, A systematic study of β-type Ti-based PVD coatings on magnesium for biomedical application, Vacuum 183 (2021) 109850, https://doi.org/10.1016/j.vacuum.2020.109850.
[230] H. Shakeri, M.A. Mofid, Physical vapor deposition assisted diffusion bonding of Al alloy to Mg alloy using silver interlayer, Met. Mater. Int. 27 (2021) 4132–4141, https://doi.org/10.1007/s12540-020-00731-8.
[231] X. Yan, W. Cao, H. Li, Biomedical alloys and physical surface modifications: a mini-review, Materials 15 (2022), https://doi.org/10.3390/ma15010066.
[232] K.R. Sinju, A.K. Debnath, N.S. Ramgir, in: A.K. Tyagi, R.S. Ningthoujam (Eds.), Techniques for Thin Films of Advanced Materials, Springer Singapore, Singapore, 2022, pp. 81–117, https://doi.org/10.1007/978-981-16-1803-1_3.
[233] M. Qadir, Y. Li, C. Wen, Ion-substituted calcium phosphate coatings by physical vapor deposition magnetron sputtering for biomedical applications: a review, Acta Biomater. 89 (2019) 14–32, https://doi.org/10.1016/j.actbio.2019.03.006.
[234] V.S. Yadav, A. Kumar, A. Das, D. Pamu, L.M. Pandey, M.R. Sankar, Degradation kinetics and surface properties of bioceramic hydroxyapatite coated AZ31 magnesium alloys for biomedical applications, Mater. Lett. 270 (2020) 127732, https://doi.org/10.1016/j.matlet.2020.127732.
[235] M. Dinu, A.A. Ivanova, M.A. Surmeneva, M. Braic, A.I. Tyurin, V. Braic, R. A. Surmenev, A. Vladescu, Tribological behaviour of RF-magnetron sputter deposited hydroxyapatite coatings in physiological solution, Ceram. Int. 43 (2017) 6858–6867, https://doi.org/10.1016/j.ceramint.2017.02.106.
[236] M.A. Surmeneva, A.I. Tyurin, T.M. Mukhametkaliyev, T.S. Pirozhkova, I. A. Shuvarin, M.S. Syrtanov, R.A. Surmenev, Enhancement of the mechanical properties of AZ31 magnesium alloy via nanostructured hydroxyapatite thin films fabricated via radio-frequency magnetron sputtering, J. Mech. Behav. Biomed. Mater. 46 (2015) 127–136, https://doi.org/10.1016/j.jmbbm.2015.02.025.

[237] D. Zhang, Z. Qi, B. Wei, Z. Wang, Microstructure and corrosion behavior of hafnium coatings on AZ91D magnesium alloys by magnetron sputtering, RSC Adv. 6 (2016) 100676–100682, https://doi.org/10.1039/c6ra23718e.
[238] W. Jin, G. Wang, Z. Lin, H. Feng, W. Li, X. Peng, A.M. Qasim, P.K. Chu, Corrosion resistance and cytocompatibility of tantalum-surface-functionalized biomedical ZK60 Mg alloy, Corrosion Sci. 114 (2017) 45–56, https://doi.org/10.1016/j.corsci.2016.10.021.
[239] İ. Çelik, Structure and surface properties of Al2O3–TiO2 ceramic coated AZ31 magnesium alloy, Ceram. Int. 42 (2016) 13659–13663, https://doi.org/10.1016/j.ceramint.2016.05.162.
[240] M.S. Kabir, P. Munroe, V. Gonçales, Z. Zhou, Z. Xie, Structure and properties of hydrophobic CeO2−x coatings synthesized by reactive magnetron sputtering for biomedical applications, Surf. Coating. Technol. 349 (2018) 667–676, https://doi.org/10.1016/j.surfcoat.2018.06.031.
[241] G. Wu, A. Shanaghi, Y. Zhao, X. Zhang, R. Xu, Z. Wu, G. Li, P.K. Chu, The effect of interlayer on corrosion resistance of ceramic coating/Mg alloy substrate in simulated physiological environment, Surf. Coating. Technol. 206 (2012) 4892–4898, https://doi.org/10.1016/j.surfcoat.2012.05.088.
[242] H.R. Bakhsheshi-Rad, E. Hamzah, M. Daroonparvar, M.A.M. Yajid, M. Medraj, Fabrication and corrosion behavior of Si/HA nano-composite coatings on biodegradable Mg-Zn-Mn-Ca alloy, Surf. Coating. Technol. 258 (2014) 1090–1099, https://doi.org/10.1016/j.surfcoat.2014.07.025.
[243] H.C.M. Knoops, S.E. Potts, A.A. Bol, W.M.M. Kessels, Atomic Layer Deposition, second ed., Elsevier B.V., 2015 https://doi.org/10.1016/B978-0-444-63304-0.00027-5.
[244] A. Kania, M.M. Szindler, M. Szindler, Structure and corrosion behavior of TiO2 thin films deposited by ALD on a biomedical magnesium alloy, Coatings 11 (2021) 1–14, https://doi.org/10.3390/coatings11010070.
[245] Z. Xu, Z. Ao, M. Yang, S. Wang, Recent progress in single-atom alloys: synthesis, properties, and applications in environmental catalysis, J. Hazard Mater. 424 (2022) 127427, https://doi.org/10.1016/j.jhazmat.2021.127427.
[246] M. Peron, A. Bin Afif, A. Dadlani, F. Berto, J. Torgersen, Comparing physiologically relevant corrosion performances of Mg AZ31 alloy protected by ALD and sputter coated TiO2, Surf. Coating. Technol. 395 (2020) 125922, https://doi.org/10.1016/j.surfcoat.2020.125922.
[247] Y. Li, H. Li, Q. Xiong, X. Wu, J. Zhou, J. Wu, X. Wu, W. Qin, Multipurpose surface functionalization on AZ31 magnesium alloys by atomic layer deposition: tailoring the corrosion resistance and electrical performance, Nanoscale 9 (2017) 8591–8599, https://doi.org/10.1039/c7nr00127d.
[248] P.C. Wang, Y.T. Shih, M.C. Lin, H.C. Lin, M.J. Chen, K.M. Lin, A study of atomic layer deposited LiAlxOy films on Mg-Li alloys, Thin Solid Films 518 (2010) 7501–7504, https://doi.org/10.1016/j.tsf.2010.05.033.
[249] Q. Yang, W. Yuan, X. Liu, Y. Zheng, Z. Cui, X. Yang, H. Pan, S. Wu, Atomic layer deposited ZrO2 nanofilm on Mg-Sr alloy for enhanced corrosion resistance and biocompatibility, Acta Biomater. 58 (2017) 515–526, https://doi.org/10.1016/j.actbio.2017.06.015.
[250] M. Peron, F. Berto, J. Torgersen, Stress corrosion cracking behavior of zirconia ALD–coated AZ31 alloy in simulated body fluid, Mater. Des. Process. Commun. 2 (2020) 1–7, https://doi.org/10.1002/mdp2.126.
[251] W. Weng, W. Wu, X. Yu, M. Sun, Z. Lin, M. Ibrahim, H. Yang, Effect of GelMA hydrogel coatings on corrosion resistance and biocompatibility of MAO-coated Mg alloys, Materials 13 (2020), https://doi.org/10.3390/ma13173834.
[252] X. Liu, Q. Yang, Z. Li, W. Yuan, Y. Zheng, Z. Cui, X. Yang, K.W.K. Yeung, S. Wu, A combined coating strategy based on atomic layer deposition for enhancement of corrosion resistance of AZ31 magnesium alloy, Appl. Surf. Sci. 434 (2018) 1101–1111, https://doi.org/10.1016/j.apsusc.2017.11.032.
[253] C.Y. Li, C. Yu, R.C. Zeng, B.C. Zhang, L.Y. Cui, J. Wan, Y. Xia, In vitro corrosion resistance of a Ta2O5 nanofilm on MAO coated magnesium alloy AZ31 by atomic layer deposition, Bioact. Mater. 5 (2020) 34–43, https://doi.org/10.1016/j.bioactmat.2019.12.001.
[254] T.T. Li, L. Ling, M.C. Lin, H.K. Peng, H.T. Ren, C.W. Lou, J.H. Lin, Recent advances in multifunctional hydroxyapatite coating by electrochemical deposition, J. Mater. Sci. 55 (2020) 6352–6374, https://doi.org/10.1007/s10853-020-04467-z.
[255] S. Pang, Y. He, P. He, X. Luo, Z. Guo, H. Li, Fabrication of two distinct hydroxyapatite coatings and their effects on MC3T3-E1 cell behavior, Colloids Surf. B Biointerfaces 171 (2018) 40–48, https://doi.org/10.1016/j.colsurfb.2018.06.046.
[256] L. Fathyunes, J. Khalil-Allafi, The effect of graphene oxide on surface features, biological performance and bio-stability of calcium phosphate coating applied by pulse electrochemical deposition, Appl. Surf. Sci. 437 (2018) 122–135, https://doi.org/10.1016/j.apsusc.2017.12.133.
[257] M. Razavi, M. Fathi, O. Savabi, L. Tayebi, D. Vashaee, Improvement of in vitro behavior of an Mg alloy using a nanostructured composite bioceramic coating, J. Mater. Sci. Mater. Med. 29 (2018) 1–11, https://doi.org/10.1007/s10856-018-6170-1.
[258] M.M. Rahman, R. Balu, A. Abraham, N.K. Dutta, N.R. Choudhury, Engineering a bioactive hybrid coating for in vitro corrosion control of magnesium and its alloy, ACS Appl. Bio Mater. 4 (2021) 5542–5555, https://doi.org/10.1021/acsabm.1c00366.
[259] P. Amrollahi, J.S. Krasinski, R. Vaidyanathan, L. Tayebi, D. Vashaee, Electrophoretic deposition (Epd): fundamentals and applications from nano-to microscale structures, Handb. Nanoelectrochemistry Electrochem. Synth. Methods, Prop. Charact. Tech. (2016) 561–592, https://doi.org/10.1007/978-3-319-15266-0_17.
[260] L. Besra, M. Liu, A review on fundamentals and applications of electrophoretic deposition (EPD), Prog. Mater. Sci. 52 (2007) 1–61, https://doi.org/10.1016/j.pmatsci.2006.07.001.
[261] Y.W. Song, D.Y. Shan, E.H. Han, Electrodeposition of hydroxyapatite coating on AZ91D magnesium alloy for biomaterial application, Mater. Lett. 62 (2008) 3276–3279, https://doi.org/10.1016/j.matlet.2008.02.048.
[262] T.T. Li, L. Ling, M.C. Lin, Q. Jiang, Q. Lin, C.W. Lou, J.H. Lin, Effects of ultrasonic treatment and current density on the properties of hydroxyapatite coating via electrodeposition and its in vitro biomineralization behavior, Mater. Sci. Eng. C 105 (2019) 110062, https://doi.org/10.1016/j.msec.2019.110062.
[263] M.B. Kannan, Electrochemical deposition of calcium phosphates on magnesium and its alloys for improved biodegradation performance: a review, Surf. Coating. Technol. 301 (2016) 36–41, https://doi.org/10.1016/j.surfcoat.2015.12.044.
[264] S. Mohajernia, S. Hejazi, A. Eslami, M. Saremi, Modified nanostructured hydroxyapatite coating to control the degradation of magnesium alloy AZ31 in simulated body fluid, Surf. Coating. Technol. 263 (2015) 54–60, https://doi.org/10.1016/j.surfcoat.2014.12.059.
[265] M. Wei, A.J. Ruys, M.V. Swain, S.H. Kim, B.K. Milthorpe, C.C. Sorrell, Interfacial bond strength of electrophoretically deposited hydroxyapatite coatings on metals, J. Mater. Sci. Mater. Med. 10 (1999) 401–409, https://doi.org/10.1023/A:1008923029945.
[266] W. Li, S. Guan, J. Chen, J. Hu, S. Chen, L. Wang, S. Zhu, Preparation and in vitro degradation of the composite coating with high adhesion strength on biodegradable Mg-Zn-Ca alloy, Mater. Char. 62 (2011) 1158–1165, https://doi.org/10.1016/j.matchar.2011.07.005.
[267] S. Chen, S. Guan, W. Li, H. Wang, J. Chen, Y. Wang, H. Wang, In vivo degradation and bone response of a composite coating on Mg-Zn-Ca alloy prepared by microarc oxidation and electrochemical deposition, J. Biomed. Mater. Res. B Appl. Biomater. 100 B (2012) 533–543, https://doi.org/10.1002/jbm.b.31982.
[268] L. Yu, T.M. Silva Santisteban, Q. Liu, C. Hu, J. Bi, M. Wei, Effect of three-dimensional porosity gradients of biomimetic coatings on their bonding strength and cell behavior, J. Biomed. Mater. Res. 109 (2021) 615–626, https://doi.org/10.1002/jbm.a.37046.
[269] Y. Liu, D. Luo, T. Wang, Hierarchical structures of bone and bioinspired bone tissue engineering, Small 12 (2016) 4611–4632, https://doi.org/10.1002/smll.201600626.
[270] A. Sugawara-Narutaki, J. Nakamura, C. Ohtsuki, Polymer-induced Liquid Precursors (PILPs) and Bone Regeneration, Elsevier Ltd., 2021, https://doi.org/10.1016/b978-0-08-102999-2.00017-x.
[271] A. Abdal-Hay, H. Foaud, B.A. Alshammari, K.A. Khalil, Biosynthesis of bonelike apatite 2d nanoplate structures using fenugreek seed extract, Nanomaterials 10 (2020), https://doi.org/10.3390/nano10050919.
[272] S.S. Jee, T.T. Thula, L.B. Gower, Development of bone-like composites via the polymer-induced liquid-precursor (PILP) process. Part 1: influence of polymer molecular weight, Acta Biomater. 6 (2010) 3676–3686, https://doi.org/10.1016/j.actbio.2010.03.036.
[273] S. Yao, X. Lin, Y. Xu, Y. Chen, P. Qiu, C. Shao, B. Jin, Z. Mu, N.A.J.M. Sommerdijk, R. Tang, Osteoporotic bone recovery by a highly bone-inductive calcium phosphate polymer-induced liquid-precursor, Adv. Sci. 6 (2019), https://doi.org/10.1002/advs.201900683.
[274] Y. Liu, H. Li, J. Xu, J. TerBush, W. Li, M. Setty, S. Guan, T.D. Nguyen, L. Qin, Y. Zheng, Biodegradable metal-derived magnesium and sodium enhances bone regeneration by angiogenesis aided osteogenesis and regulated biological apatite formation, Chem. Eng. J. 410 (2021) 127616, https://doi.org/10.1016/j.cej.2020.127616.
[275] M. Šupová, The significance and utilisation of biomimetic and bioinspired strategies in the field of biomedical material engineering: the case of calcium phosphat - protein template constructs, Materials 13 (2020), https://doi.org/10.3390/ma13020327.
[276] H.Y. Wan, R.L.Y. Shin, J.C.H. Chen, M. Assunção, D. Wang, S.K. Nilsson, R. S. Tuan, A. Blocki, Dextran sulfate-amplified extracellular matrix deposition promotes osteogenic differentiation of mesenchymal stem cells, Acta Biomater. 140 (2021) 163–177, https://doi.org/10.1016/j.actbio.2021.11.049.
[277] J. Yao, W. Fang, J. Guo, D. Jiao, S. Chen, S. Ifuku, H. Wang, A. Walther, Highly mineralized biomimetic polysaccharide nanofiber materials using enzymatic mineralization, Biomacromolecules 21 (2020) 2176–2186, https://doi.org/10.1021/acs.biomac.0c00160.
[278] E. Colaço, D. Brouri, C. Méthivier, L. Valentin, F. Oudet, K. El Kirat, C. Guibert, J. Landoulsi, Calcium phosphate mineralization through homogenous enzymatic catalysis: investigation of the early stages, J. Colloid Interface Sci. 565 (2020) 43–54, https://doi.org/10.1016/j.jcis.2019.12.097.
[279] N. Koju, P. Sikder, Y. Ren, H. Zhou, S.B. Bhaduri, Biomimetic coating technology for orthopedic implants, Curr. Opin. Chem. Eng. 15 (2017) 49–55, https://doi.org/10.1016/j.coche.2016.11.005.
[280] J. Sun, S. Cai, J. Wei, K. Shen, R. Ling, J. Sun, J. Liu, G. Xu, Long-term corrosion resistance and fast mineralization behavior of micro-nano hydroxyapatite coated magnesium alloy in vitro, Ceram. Int. 46 (2020) 824–832, https://doi.org/10.1016/j.ceramint.2019.09.038.
[281] W. Zhou, Z. Hu, T. Wang, G. Yang, W. Xi, Y. Gan, W. Lu, J. Hu, Enhanced corrosion resistance and bioactivity of Mg alloy modified by Zn-doped nanowhisker hydroxyapatite coatings, Colloids Surf. B Biointerfaces 186 (2020) 110710, https://doi.org/10.1016/j.colsurfb.2019.110710.
[282] N. Yu, S. Cai, F. Wang, F. Zhang, R. Ling, Y. Li, Y. Jiang, G. Xu, Microwave assisted deposition of strontium doped hydroxyapatite coating on AZ31 magnesium alloy with enhanced mineralization ability and corrosion resistance,

Ceram. Int. 43 (2017) 2495–2503, https://doi.org/10.1016/j.ceramint.2016.11.050.
[283] M. Rahimi, R. Mehdinavaz Aghdam, M.H. Sohi, A.H. Rezayan, M. Ettelaei, Improving biocompatibility and corrosion resistance of anodized AZ31 Mg alloy by electrospun chitosan/mineralized bone allograft (MBA) nanocoatings, Surf. Coating. Technol. 405 (2021) 126627, https://doi.org/10.1016/j.surfcoat.2020.126627.
[284] Q. Li, X. Bao, J. Sun, S. Cai, Y. Xie, Y. Liu, J. Liu, G. Xu, Fabrication of superhydrophobic composite coating of hydroxyapatite/stearic acid on magnesium alloy and its corrosion resistance, antibacterial adhesion, J. Mater. Sci. 56 (2021) 5233–5249, https://doi.org/10.1007/s10853-020-05592-5.
[285] S. Yang, R. Sun, K. Chen, Self-healing performance and corrosion resistance of phytic acid/cerium composite coating on microarc-oxidized magnesium alloy, Chem. Eng. J. 428 (2022) 131198, https://doi.org/10.1016/j.cej.2021.131198.
[286] Y. Wang, X. Zhou, M. Yin, J. Pu, N. Yuan, J. Ding, Superhydrophobic and self-healing Mg-Al layered double hydroxide/silane composite coatings on the Mg alloy surface with a long-term anti-corrosion lifetime, Langmuir 37 (2021) 8129–8138, https://doi.org/10.1021/acs.langmuir.1c00678.
[287] R.B. Figueira, I.R. Fontinha, C.J.R. Silva, E.V. Pereira, Hybrid sol-gel coatings: smart and green materials for corrosion mitigation, Coatings 6 (2016) 12, https://doi.org/10.3390/coatings6010012.
[288] D. Wang, G.P. Bierwagen, Sol-gel coatings on metals for corrosion protection, Prog. Org. Coating 64 (2009) 327–338, https://doi.org/10.1016/j.porgcoat.2008.08.010.
[289] B. Fotovvati, N. Namdari, A. Dehghanghadikolaei, On coating techniques for surface protection: a review, J. Manuf. Mater. Process. 3 (2019), https://doi.org/10.3390/jmmp3010028.
[290] V. Hernández-Montes, C.P. Betancur-Henao, J.F. Santa-Marín, Recubrimientos de dioxido de titanio sobre aleaciones de magnesio para biomateriales: una revisión, Dyna 84 (2017) 261–270, https://doi.org/10.15446/dyna.v84n200.59664.
[291] S. Amiri, A. Rahimi, Hybrid nanocomposite coating by sol–gel method: a review, Iran. Polym. J. 25 (2016) 559–577, https://doi.org/10.1007/s13726-016-0440-x.
[292] Y. Song, Y. Li, W. Song, K. Yee, K.Y. Lee, V.L. Tagarielli, Measurements of the mechanical response of unidirectional 3D-printed PLA, Mater. Des. 123 (2017) 154–164, https://doi.org/10.1016/j.matdes.2017.03.051.
[293] A. Alabbasi, S. Liyanaarachchi, M.B. Kannan, Polylactic acid coating on a biodegradable magnesium alloy: an in vitro degradation study by electrochemical impedance spectroscopy, Thin Solid Films 520 (2012) 6841–6844, https://doi.org/10.1016/j.tsf.2012.07.090.
[294] Y. Zhao, L. Shi, X. Ji, J. Li, Z. Han, S. Li, R. Zeng, F. Zhang, Z. Wang, Corrosion resistance and antibacterial properties of polysiloxane modified layer-by-layer assembled self-healing coating on magnesium alloy, J. Colloid Interface Sci. 526 (2018) 43–50, https://doi.org/10.1016/j.jcis.2018.04.071.
[295] M. Dusselier, P. Van Wouwe, A. Dewaele, P.A. Jacobs, B.F. Sels, Shape-selective zeolite catalysis for bioplastics production, Science 349 (2015) 78–80, https://doi.org/10.1126/science.aaa7169.
[296] Y. Hua, Y. Su, H. Zhang, N. Liu, Z. Wang, X. Gao, J. Gao, A. Zheng, Poly(lactic-co-glycolic acid) microsphere production based on quality by design: a review, Drug Deliv. 28 (2021) 1342–1355, https://doi.org/10.1080/10717544.2021.1943056.
[297] L.Y. Li, L.Y. Cui, R.C. Zeng, S.Q. Li, X.B. Chen, Y. Zheng, M.B. Kannan, Advances in functionalized polymer coatings on biodegradable magnesium alloys – a review, Acta Biomater. 79 (2018) 23–36, https://doi.org/10.1016/j.actbio.2018.08.030.
[298] K. Zhang, X. Tang, J. Zhang, W. Lu, X. Lin, Y. Zhang, B. Tian, H. Yang, H. He, PEG-PLGA copolymers: their structure and structure-influenced drug delivery applications, J. Contr. Release 183 (2014) 77–86, https://doi.org/10.1016/j.jconrel.2014.03.026.
[299] Y. Zhu, W. Liu, T. Ngai, Polymer coatings on magnesium-based implants for orthopedic applications, J. Polym. Sci. 60 (2022) 32–51, https://doi.org/10.1002/pol.20210578.
[300] J.H. Lee, S.M. Baek, G. Lee, S.J. Kim, H.S. Kim, S.K. Hahn, Biocompatible magnesium implant double-coated with dexamethasone-loaded black phosphorus and poly(lactide- co-glycolide), ACS Appl. Bio Mater. 3 (2020) 8879–8889, https://doi.org/10.1021/acsabm.0c01179.
[301] D. Mishra, K. Glover, S. Gade, R. Sonawane, T.R. Raj Singh, Safety, biodegradability, and biocompatibility considerations of long-acting drug delivery systems, in: E. Larrañeta, T. Raghu Raj Singh, R.F. Donnelly (Eds.), Long-Acting Drug Delivery Systems: Pharmaceutical, Clinical, and Regulatory Aspects, Woodhead Publishing, 2022, pp. 289–317.
[302] C. Chen, J. Tan, W. Wu, L. Petrini, L. Zhang, Y. Shi, E. Cattarinuzzi, J. Pei, H. Huang, W. Ding, G. Yuan, F. Migliavacca, Modeling and experimental studies of coating delamination of biodegradable magnesium alloy cardiovascular stents, ACS Biomater. Sci. Eng. 4 (2018) 3864–3873, https://doi.org/10.1021/acsbiomaterials.8b00700.
[303] W. Jiang, Q. Tian, T. Vuong, M. Shashaty, C. Gopez, T. Sanders, H. Liu, Comparison study on four biodegradable polymer coatings for controlling magnesium degradation and human endothelial cell adhesion and spreading, ACS Biomater. Sci. Eng. 3 (2017) 936–950, https://doi.org/10.1021/acsbiomaterials.7b00215.
[304] A. Kulkarni, J. Reiche, J. Hartmann, K. Kratz, A. Lendlein, Selective enzymatic degradation of poly(ε-caprolactone) containing multiblock copolymers, Eur. J. Pharm. Biopharm. 68 (2008) 46–56, https://doi.org/10.1016/j.ejpb.2007.05.021.
[305] J.W. Kim, K.H. Shin, Y.H. Koh, M.J. Hah, J. Moon, H.E. Kim, Production of poly (ε-caprolactone)/hydroxyapatite composite scaffolds with a tailored macro/micro-porous structure, high mechanical properties, and excellent bioactivity, Materials 10 (2017), https://doi.org/10.3390/ma10101123.
[306] C. Shuai, L. Yu, P. Feng, Y. Zhong, Z. Zhao, Z. Chen, W. Yang, Organic montmorillonite produced an interlayer locking effect in a polymer scaffold to enhance interfacial bonding, Mater. Chem. Front. 4 (2020) 2398–2408, https://doi.org/10.1039/d0qm00254b.
[307] Y. Zhao, Z. Li, S. Song, K. Yang, H. Liu, Z. Yang, J. Wang, B. Yang, Q. Lin, Skin-inspired antibacterial conductive hydrogels for epidermal sensors and diabetic foot wound dressings, Adv. Funct. Mater. 29 (2019) 1901474, https://doi.org/10.1002/adfm.201901474.
[308] P. Xian, Y. Chen, S. Gao, J. Qian, W. Zhang, A. Udduttula, N. Huang, G. Wan, Polydopamine (PDA) mediated nanogranular-structured titanium dioxide (TiO2) coating on polyetheretherketone (PEEK) for oral and maxillofacial implants application, Surf. Coating. Technol. 401 (2020) 126282, https://doi.org/10.1016/j.surfcoat.2020.126282.
[309] Y. Yu, S.J. Zhu, H.T. Dong, X.Q. Zhang, J.A. Li, S.K. Guan, A novel MgF2/PDA/S-HA coating on the bio-degradable ZE21B alloy for better multi-functions on cardiovascular application, J. Magnes. Alloy (2021), https://doi.org/10.1016/j.jma.2021.06.015. In press.
[310] H. Li, D. Yin, W. Li, Q. Tang, L. Zou, Q. Peng, Polydopamine-based nanomaterials and their potentials in advanced drug delivery and therapy, Colloids Surf. B Biointerfaces 199 (2021) 111502, https://doi.org/10.1016/j.colsurfb.2020.111502.
[311] D.L. Roman, V. Ostafe, A. Isvoran, Deeper inside the specificity of lysozyme when degrading chitosan. A structural bioinformatics study, J. Mol. Graph. Model. 100 (2020) 107676, https://doi.org/10.1016/j.jmgm.2020.107676.
[312] Z. Jia, P. Xiong, Y. Shi, W. Zhou, Y. Cheng, Y. Zheng, T. Xi, S. Wei, Inhibitor encapsulated, self-healable and cytocompatible chitosan multilayer coating on biodegradable Mg alloy: a pH-responsive design, J. Mater. Chem. B. 4 (2016) 2498–2511, https://doi.org/10.1039/c6tb00117c.
[313] A. Saadati, B.N. Khiarak, A.A. Zahraei, A. Nourbakhsh, H. Mohammadzadeh, Electrochemical characterization of electrophoretically deposited hydroxyapatite/chitosan/graphene oxide composite coating on Mg substrate, Surface. Interfac. 25 (2021) 101290, https://doi.org/10.1016/j.surfin.2021.101290.
[314] E. Avcu, F.E. Baştan, H.Z. Abdullah, M.A.U. Rehman, Y.Y. Avcu, A.R. Boccaccini, Electrophoretic deposition of chitosan-based composite coatings for biomedical applications: a review, Prog. Mater. Sci. 103 (2019) 69–108, https://doi.org/10.1016/j.pmatsci.2019.01.001.
[315] B. Hu, Y. Guo, H. Li, X. Liu, Y. Fu, F. Ding, Recent advances in chitosan-based layer-by-layer biomaterials and their biomedical applications, Carbohydr. Polym. 271 (2021) 118427, https://doi.org/10.1016/j.carbpol.2021.118427.
[316] C. Ma, H. Wang, Y. Chi, Y. Wang, L. Jiang, N. Xu, Q. Wu, Q. Feng, X. Sun, Preparation of oriented collagen fiber scaffolds and its application in bone tissue engineering, Appl. Mater. Today 22 (2021) 100902, https://doi.org/10.1016/j.apmt.2020.100902.
[317] F. Wang, D. Xia, S. Wang, R. Gu, F. Yang, X. Zhao, X. Liu, Y. Zhu, H. Liu, Y. Xu, Y. Liu, Y. Zhou, Photocrosslinkable Col/PCL/Mg composite membrane providing spatiotemporal maintenance and positive osteogenetic effects during guided bone regeneration, Bioact. Mater. 13 (2021) 53–63, https://doi.org/10.1016/j.bioactmat.2021.10.019.
[318] S. Bose, S. Li, E. Mele, V.V. Silberschmidt, Dry vs. wet: properties and performance of collagen films. Part I. Mechanical behaviour and strain-rate effect, J. Mech. Behav. Biomed. Mater. 111 (2020) 103983, https://doi.org/10.1016/j.jmbbm.2020.103983.
[319] N. Zhao, D. Zhu, Collagen self-assembly on orthopedic magnesium biomaterials surface and subsequent bone cell attachment, PLoS One 9 (2014), e110420, https://doi.org/10.1371/journal.pone.0110420.
[320] Z.L. Wang, Y.H. Yan, T. Wan, H. Yang, Poly(L-lactic acid)/hydroxyapatite/collagen composite coatings on AZ31 magnesium alloy for biomedical application, Proc. Inst. Mech. Eng. Part H J. Eng. Med. 227 (2013) 1094–1103, https://doi.org/10.1177/0954411913493845.
[321] R. Wang, S. Guo, Phytic acid and its interactions: contributions to protein functionality, food processing, and safety, Compr. Rev. Food Sci. Food Saf. 20 (2021) 2081–2105, https://doi.org/10.1111/1541-4337.12714.
[322] P. Xiong, J.L. Yan, P. Wang, Z.J. Jia, W. Zhou, W. Yuan, Y. Li, Y. Liu, Y. Cheng, D. Chen, Y. Zheng, A pH-sensitive self-healing coating for biodegradable magnesium implants, Acta Biomater. 98 (2019) 160–173, https://doi.org/10.1016/j.actbio.2019.04.045.
[323] S. Puvvada, P. Latha Professor, A.K. Selvan, C. Saketh puvvada Post Graduate, P. Latha, Comparative assessment of chelating and antimicrobial efficacy of phytic acid alone and in combination with other irrigants, ~ 19, Int. J. Appl. Decis. Sci. 3 (2017) 19–22. www.oraljournal.com.
[324] S. Jiang, S. Cai, F. Zhang, P. Xu, R. Ling, Y. Li, Y. Jiang, G. Xu, Synthesis and characterization of magnesium phytic acid/apatite composite coating on AZ31 Mg alloy by microwave assisted treatment, Mater. Sci. Eng. C 91 (2018) 218–227, https://doi.org/10.1016/j.msec.2018.05.041.
[325] A. Ancion, S. Allepaerts, S. Robinet, C. Oury, L.A. Pierard, P. Lancellotti, Serum albumin level and long-term outcome in acute heart failure, Acta Cardiol. 74 (2019) 465–471, https://doi.org/10.1080/00015385.2018.1521557.
[326] J. Wang, L. Cui, Y. Ren, Y. Zou, J. Ma, C. Wang, Z. Zheng, K. Chen, R. Zeng, Y. Zheng, In vitro and in vivo biodegradation and biocompatibility of an MMT/BSA composite coating upon magnesium alloy AZ31, J. Mater. Sci. Technol. 47 (2020) 52–67, https://doi.org/10.1016/j.jmst.2020.02.006.
[327] W. Yan, Y.J. Lian, Z.Y. Zhang, M.Q. Zeng, Z.Q. Zhang, Z.Z. Yin, L.Y. Cui, R. C. Zeng, In vitro degradation of pure magnesium–the synergetic influences of

glucose and albumin, Bioact. Mater. 5 (2020) 318–333, https://doi.org/10.1016/j.bioactmat.2020.02.015.
[328] S.E. Harandi, P.C. Banerjee, C.D. Easton, R.K. Singh Raman, Influence of bovine serum albumin in Hanks' solution on the corrosion and stress corrosion cracking of a magnesium alloy, Mater. Sci. Eng. C 80 (2017) 335–345, https://doi.org/10.1016/j.msec.2017.06.002.
[329] F. El-Taib Heakal, A.M. Bakry, Serum albumin can influence magnesium alloy degradation in simulated blood plasma for cardiovascular stenting, Mater. Chem. Phys. 220 (2018) 35–49, https://doi.org/10.1016/j.matchemphys.2018.08.060.
[330] K. Bai, Y. Zhang, Z. Fu, C. Zhang, X. Cui, E. Meng, S. Guan, J. Hu, Fabrication of chitosan/magnesium phosphate composite coating and the in vitro degradation properties of coated magnesium alloy, Mater. Lett. 73 (2012) 59–61, https://doi.org/10.1016/j.matlet.2011.12.102.
[331] M.B. Kannan, S. Liyanaarachchi, Hybrid coating on a magnesium alloy for minimizing the localized degradation for load-bearing biodegradable mini-implant applications, Mater. Chem. Phys. 142 (2013) 350–354, https://doi.org/10.1016/j.matchemphys.2013.07.028.
[332] R.C. Zeng, W.C. Qi, Y.W. Song, Q.K. He, H.Z. Cui, E.H. Han, In vitro degradation of MAO/PLA coating on Mg-1.21Li-1.12Ca-1.0Y alloy, Front. Mater. Sci. 8 (2014) 343–353, https://doi.org/10.1007/s11706-014-0264-6.
[333] A. Abdal-Hay, M. Dewidar, J. Lim, J.K. Lim, Enhanced biocorrosion resistance of surface modified magnesium alloys using inorganic/organic composite layer for biomedical applications, Ceram. Int. 40 (2014) 2237–2247, https://doi.org/10.1016/j.ceramint.2013.07.142.
[334] T. Hanas, T.S. Sampath Kumar, G. Perumal, M. Doble, Tailoring degradation of AZ31 alloy by surface pre-treatment and electrospun PCL fibrous coating, Mater. Sci. Eng. C 65 (2016) 43–50, https://doi.org/10.1016/j.msec.2016.04.017.
[335] B. Li, K. Zhang, W. Yang, X. Yin, Y. Liu, Enhanced corrosion resistance of HA/CaTiO3/TiO2/PLA coated AZ31 alloy, Rev. Mex. Urol. 76 (2016) 465–473, https://doi.org/10.1016/j.jtice.2015.07.028.
[336] H.R. Bakhsheshi-Rad, E. Hamzah, A.F. Ismail, M. Daroonparvar, M.A.M. Yajid, M. Medraj, Preparation and characterization of NiCrAlY/nano-YSZ/PCL composite coatings obtained by combination of atmospheric plasma spraying and dip coating on Mg-Ca alloy, J. Alloys Compd. 658 (2016) 440–452, https://doi.org/10.1016/j.jallcom.2015.10.196.
[337] M. Du, M. Peng, B. Mai, F. Hu, X. Zhang, Y. Chen, C. Wang, A multifunctional hybrid inorganic-organic coating fabricated on magnesium alloy surface with antiplatelet adhesion and antibacterial activities, Surf. Coating. Technol. 384 (2020) 125336, https://doi.org/10.1016/j.surfcoat.2020.125336.
[338] J.H. Jo, Y. Li, S.M. Kim, H.E. Kim, Y.H. Koh, Hydroxyapatite/poly (Éε-caprolactone) double coating on magnesium for enhanced corrosion resistance and coating flexibility, J. Biomater. Appl. 28 (2013) 617–625, https://doi.org/10.1177/0885328212468921.
[339] Y. Chen, S. Zhao, M. Chen, W. Zhang, J. Mao, Y. Zhao, M.F. Maitz, N. Huang, G. Wan, Sandwiched polydopamine (PDA) layer for titanium dioxide (TiO2) coating on magnesium to enhance corrosion protection, Corrosion Sci. 96 (2015) 67–73, https://doi.org/10.1016/j.corsci.2015.03.020.
[340] B. Lin, M. Zhong, C. Zheng, L. Cao, D. Wang, L. Wang, J. Liang, B. Cao, Preparation and characterization of dopamine-induced biomimetic hydroxyapatite coatings on the AZ31 magnesium alloy, Surf. Coating. Technol. 281 (2015) 82–88, https://doi.org/10.1016/j.surfcoat.2015.09.033.
[341] L. Zhang, J. Pei, H. Wang, Y. Shi, J. Niu, F. Yuan, H. Huang, H. Zhang, G. Yuan, Facile preparation of poly(lactic acid)/brushite bilayer coating on biodegradable magnesium alloys with multiple functionalities for orthopedic application, ACS Appl. Mater. Interfaces 9 (2017) 9437–9448, https://doi.org/10.1021/acsami.7b00209.
[342] X. Tang, X. Zhang, Y. Chen, W. Zhang, J. Qian, H. Soliman, A. Qu, Q. Liu, S. Pu, N. Huang, G. Wan, Ultraviolet irradiation assisted liquid phase deposited titanium dioxide (TiO2)-incorporated into phytic acid coating on magnesium for slowing-down biodegradation and improving osteo-compatibility, Mater. Sci. Eng. C 108 (2020) 110487, https://doi.org/10.1016/j.msec.2019.110487.
[343] A. Zomorodian, I.A. Ribeiro, J.C.S. Fernandes, A.C. Matos, C. Santos, A. F. Bettencourt, M.F. Montemor, Biopolymeric coatings for delivery of antibiotic and controlled degradation of bioresorbable Mg AZ31 alloys, Int. J. Polym. Mater. Polym. Biomater. 66 (2017) 533–543, https://doi.org/10.1080/00914037.2016.1252347.
[344] W. Zhang, Y. Chen, M. Chen, S. Zhao, J. Mao, A. Qu, W. Li, Y. Zhao, N. Huang, G. Wan, Strengthened corrosion control of poly (lactic acid) (PLA) and poly (ε-caprolactone) (PCL) polymer-coated magnesium by imbedded hydrophobic stearic acid (SA) thin layer, Corrosion Sci. 112 (2016) 327–337, https://doi.org/10.1016/j.corsci.2016.07.027.
[345] W. Xu, K. Yagoshi, Y. Koga, M. Sasaki, T. Niidome, Optimized polymer coating for magnesium alloy-based bioresorbable scaffolds for long-lasting drug release and corrosion resistance, Colloids Surf. B Biointerfaces 163 (2018) 100–106, https://doi.org/10.1016/j.colsurfb.2017.12.032.
[346] L. Huang, J. Li, W. Yuan, X. Liu, Z. Li, Y. Zheng, Y. Liang, S. Zhu, Z. Cui, X. Yang, K.W.K. Yeung, S. Wu, Near-infrared light controlled fast self-healing protective coating on magnesium alloy, Corrosion Sci. 163 (2020) 108257, https://doi.org/10.1016/j.corsci.2019.108257.
[347] R.C. Zeng, L.J. Liu, K.J. Luo, L. Shen, F. Zhang, S.Q. Li, Y.H. Zou, In vitro corrosion and antibacterial properties of layer-by-layer assembled GS/PSS coating on AZ31 magnesium alloys, Trans. Nonferrous Met. Soc. China 25 (2015) 4028–4039, https://doi.org/10.1016/S1003-6326(15)64052-3.
[348] T. Yuan, J. Yu, J. Cao, F. Gao, Y. Zhu, Y. Cheng, W. Cui, Fabrication of a delaying biodegradable magnesium alloy-based esophageal stent via coating elastic polymer, Materials 9 (2016), https://doi.org/10.3390/ma9050384.
[349] W. Shang, B. Chen, X. Shi, Y. Chen, X. Xiao, Electrochemical corrosion behavior of composite MAO/sol-gel coatings on magnesium alloy AZ91D using combined micro-arc oxidation and sol-gel technique, J. Alloys Compd. 474 (2009) 541–545, https://doi.org/10.1016/j.jallcom.2008.06.135.
[350] Z. Li, X. Jing, Y. Yuan, M. Zhang, Composite coatings on a Mg-Li alloy prepared by combined plasma electrolytic oxidation and sol-gel techniques, Corrosion Sci. 63 (2012) 358–366, https://doi.org/10.1016/j.corsci.2012.06.018.
[351] M. Daroonparvar, M.A. Mat Yajid, R. Kumar Gupta, N. Mohd Yusof, H. R. Bakhsheshi-Rad, H. Ghandvar, E. Ghasemi, Antibacterial activities and corrosion behavior of novel PEO/nanostructured ZrO2 coating on Mg alloy, Trans. Nonferrous Met. Soc. China 28 (2018) 1571–1581, https://doi.org/10.1016/S1003-6326(18)64799-5.
[352] Y. Wang, Z. Gu, J. Liu, J. Jiang, N. Yuan, J. Pu, J. Ding, An organic/inorganic composite multi-layer coating to improve the corrosion resistance of AZ31B Mg alloy, Surf. Coating. Technol. 360 (2019) 276–284, https://doi.org/10.1016/j.surfcoat.2018.12.125.
[353] Y. Zhao, Z. Zhang, L. Shi, F. Zhang, S. Li, R. Zeng, Corrosion resistance of a self-healing multilayer film based on SiO2 and CeO2 nanoparticles layer-by-layer assembly on Mg alloys, Mater. Lett. 237 (2019) 14–18, https://doi.org/10.1016/j.matlet.2018.11.069.
[354] C.Y. Li, X.L. Fan, R.C. Zeng, L.Y. Cui, S.Q. Li, F. Zhang, Q.K. He, M.B. Kannan, H. W. George Jiang, D.C. Chen, S.K. Guan, Corrosion resistance of in-situ growth of nano-sized Mg(OH) 2 on micro-arc oxidized magnesium alloy AZ31—influence of EDTA, J. Mater. Sci. Technol. 35 (2019) 1088–1098, https://doi.org/10.1016/j.jmst.2019.01.006.
[355] A. Abdal-Hay, K.C. In, J.K. Lim, Biocorrosion and osteoconductivity of PCL/nHAp composite porous film-based coating of magnesium alloy, Solid State Sci. 18 (2013) 131–140, https://doi.org/10.1016/j.solidstatesciences.2012.11.017.
[356] A. Rezaei, M.R. Mohammadi, In vitro study of hydroxyapatite/polycaprolactone (HA/PCL) nanocomposite synthesized by an in situ sol-gel process, Mater. Sci. Eng. C 33 (2013) 390–396, https://doi.org/10.1016/j.msec.2012.09.004.
[357] A. Manuscript, Cu-releasing BG/PCL Coating on Mg with Antibacterial and Anticorrosive Properties for Bone Tissue Engineering, 2018, 0–18.
[358] Z.Q. Zhang, R.C. Zeng, C.G. Lin, L. Wang, X.B. Chen, D.C. Chen, Corrosion resistance of self-cleaning silane/polypropylene composite coatings on magnesium alloy AZ31, J. Mater. Sci. Technol. 41 (2020) 43–55, https://doi.org/10.1016/j.jmst.2019.08.056.
[359] X.J. Ji, L. Gao, J.C. Liu, J. Wang, Q. Cheng, J.P. Li, S.Q. Li, K.Q. Zhi, R.C. Zeng, Z. L. Wang, Corrosion resistance and antibacterial properties of hydroxyapatite coating induced by gentamicin-loaded polymeric multilayers on magnesium alloys, Colloids Surf. B Biointerfaces 179 (2019) 429–436, https://doi.org/10.1016/j.colsurfb.2019.04.029.
[360] P. Lu, H. Fan, Y. Liu, L. Cao, X. Wu, X. Xu, Controllable biodegradability, drug release behavior and hemocompatibility of PTX-eluting magnesium stents, Colloids Surf. B Biointerfaces 83 (2011) 23–28, https://doi.org/10.1016/j.colsurfb.2010.10.038.
[361] Z. Wei, P. Tian, X. Liu, B. Zhou, Hemocompatibility and selective cell fate of polydopamine-assisted heparinized PEO/PLLA composite coating on biodegradable AZ31 alloy, Colloids Surf. B Biointerfaces 121 (2014) 451–460, https://doi.org/10.1016/j.colsurfb.2014.06.036.
[362] P. Xiong, Z. Jia, W. Zhou, J. Yan, P. Wang, W. Yuan, Y. Li, Y. Cheng, Z. Guan, Y. Zheng, Osteogenic and pH stimuli-responsive self-healing coating on biomedical Mg-1Ca alloy, Acta Biomater. 92 (2019) 336–350, https://doi.org/10.1016/j.actbio.2019.05.027.
[363] S.S. Yang, Z. Chen, T.Q. Chen, C.Y. Fu, Hollow mesoporous silica nanoparticles decorated with cyclodextrin for inhibiting the corrosion of Mg alloys, ACS Appl. Nano Mater. 3 (2020) 4542–4552, https://doi.org/10.1021/acsanm.0c00616.
[364] Y. Jiang, B. Wang, Z. Jia, X. Lu, L. Fang, K. Wang, F. Ren, Polydopamine mediated assembly of hydroxyapatite nanoparticles and bone morphogenetic protein-2 on magnesium alloys for enhanced corrosion resistance and bone regeneration, J. Biomed. Mater. Res. 105 (2017) 2750–2761, https://doi.org/10.1002/jbm.a.36138.
[365] J. Li, S. Wang, Y. Sheng, C. Liu, Z. Xue, P. Tong, S. Guan, Designing HA/PEI nanoparticle composite coating on biodegradable Mg–Zn–Y-Nd alloy to direct cardiovascular cells fate, Smart Mater. Med. 2 (2021) 124–133, https://doi.org/10.1016/j.smaim.2021.03.003.
[366] I. Johnson, J. Lin, H. Liu, Surface modification and coatings for controlling the degradation and bioactivity of magnesium alloys for medical applications, in: Orthop. Biomater., Springer International Publishing, Cham, 2017, pp. 331–363, https://doi.org/10.1007/978-3-319-73664-8_13.
[367] H.R. Bakhsheshi-Rad, E. Hamzah, W.S. Ying, M. Razzaghi, S. Sharif, A.F. Ismail, F. Berto, Improved bacteriostatic and anticorrosion effects of polycaprolactone/chitosan coated magnesium via incorporation of zinc oxide, Materials 14 (2021), https://doi.org/10.3390/ma14081930.
[368] Q. Li, Y. Yan, H. Gao, Improving the corrosion resistance and osteogenic differentiation of ZK60 magnesium alloys by hydroxyapatite/graphene/graphene oxide composite coating, Ceram. Int. (2022), https://doi.org/10.1016/j.ceramint.2022.02.161.
[369] Y. Dong, T. Wang, Y. Xu, Y. Guo, G. Li, J. Lian, A polydopamine-based calcium phosphate/graphene oxide composite coating on magnesium alloy to improve corrosion resistance and biocompatibility for biomedical applications, Materialia 21 (2022) 101315, https://doi.org/10.1016/j.mtla.2022.101315.
[370] H. Fang, C. Wang, S. Zhou, G. Li, Y. Tian, T. Suga, Exploration of the enhanced performances for silk fibroin/sodium alginate composite coatings on biodegradable Mg−Zn−Ca alloy, J. Magnes. Alloy. 9 (2021) 1578–1594, https://doi.org/10.1016/j.jma.2020.08.017.

[371] M. Tian, S. Cai, L. Ling, Y. Zuo, Z. Wang, P. Liu, X. Bao, G. Xu, Superhydrophilic hydroxyapatite/hydroxypropyltrimethyl ammonium chloride chitosan composite coating for enhancing the antibacterial and corrosion resistance of magnesium alloy, Prog. Org. Coating 165 (2022) 106745, https://doi.org/10.1016/j.porgcoat.2022.106745.
[372] N. Singh, U. Batra, K. Kumar, A. Mahapatro, Evaluation of corrosion resistance, mechanical integrity loss and biocompatibility of PCL/HA/TiO2 hybrid coated biodegradable ZM21 Mg alloy, J. Magnes. Alloy (2021), https://doi.org/10.1016/j.jma.2021.10.004. In press.
[373] N. Singh, U. Batra, K. Kumar, A. Mahapatro, Investigating TiO2–HA–PCL hybrid coating as an efficient corrosion resistant barrier of ZM21 Mg alloy, J. Magnes. Alloy. 9 (2021) 627–646, https://doi.org/10.1016/j.jma.2020.08.003.
[374] P. Tong, Y. Sheng, R. Hou, M. Iqbal, L. Chen, J. Li, Recent progress on coatings of biomedical magnesium alloy, Smart Mater. Med. 3 (2022) 104–116, https://doi.org/10.1016/j.smaim.2021.12.007.
[375] N.A. Johari, J. Alias, A. Zanurin, N.S. Mohamed, N.A. Alang, M.Z.M. Zain, Recent progress of self-healing coatings for magnesium alloys protection, J. Coating Technol. Res. (2022), https://doi.org/10.1007/s11998-021-00599-2. In press.
[376] B. Li, R. Huang, J. Ye, L. Liu, L. Qin, J. Zhou, Y. Zheng, S. Wu, Y. Han, A self-healing coating containing curcumin for osteoimmunomodulation to ameliorate osseointegration, Chem. Eng. J. 403 (2021) 126323, https://doi.org/10.1016/j.cej.2020.126323.
[377] E. Kim, S. Yoo, H.-Y. Ro, H.-J. Han, Y.-W. Baek, I.-C. Eom, H.-M. Kim, P. Kim, K. Choi, Aquatic toxicity assessment of phosphate compounds, Environ. Health Toxicol. 28 (2013), https://doi.org/10.5620/eht.2013.28.e2013002 e2013002–e2013002.
[378] Q. Dong, X. Zhou, Y. Feng, K. Qian, H. Liu, M. Lu, C. Chu, F. Xue, J. Bai, Insights into self-healing behavior and mechanism of dicalcium phosphate dihydrate coating on biomedical Mg, Bioact. Mater. 6 (2021) 158–168, https://doi.org/10.1016/j.bioactmat.2020.07.019.
[379] L.-J. He, Y. Shao, S.-Q. Li, L.-Y. Cui, X.-J. Ji, Y.-B. Zhao, R.-C. Zeng, Advances in layer-by-layer self-assembled coatings upon biodegradable magnesium alloys, Sci. China Mater. 64 (2021) 2093–2106, https://doi.org/10.1007/s40843-020-1661-1.
[380] Y. Liu, Y. Zhang, Y.-L. Wang, Y.-Q. Tian, L.-S. Chen, Research progress on surface protective coatings of biomedical degradable magnesium alloys, J. Alloys Compd. 885 (2021) 161001, https://doi.org/10.1016/j.jallcom.2021.161001.
[381] M. Peron, J. Torgersen, F. Berto, Mg and its alloys for biomedical applications: exploring corrosion and its interplay with mechanical failure, Metals 7 (2017) 252, https://doi.org/10.3390/met7070252.
[382] S. Mersagh Dezfuli, M. Sabzi, Deposition of ceramic nanocomposite coatings by electroplating process: a review of layer-deposition mechanisms and effective parameters on the formation of the coating, Ceram. Int. 45 (2019) 21835–21842, https://doi.org/10.1016/j.ceramint.2019.07.190.
[383] M. Toorani, M. Aliofkhazraei, M. Mahdavian, R. Naderi, Superior corrosion protection and adhesion strength of epoxy coating applied on AZ31 magnesium alloy pre-treated by PEO/Silane with inorganic and organic corrosion inhibitors, Corrosion Sci. 178 (2021) 109065, https://doi.org/10.1016/j.corsci.2020.109065.
[384] R. Rojaee, M. Fathi, K. Raeissi, Controlling the degradation rate of AZ91 magnesium alloy via sol-gel derived nanostructured hydroxyapatite coating, Mater. Sci. Eng. C 33 (2013) 3817–3825, https://doi.org/10.1016/j.msec.2013.05.014.
[385] T.S.N. Sankara Narayanan, I.S. Park, M.H. Lee, Strategies to improve the corrosion resistance of microarc oxidation (MAO) coated magnesium alloys for degradable implants: prospects and challenges, Prog. Mater. Sci. 60 (2014) 1–71, https://doi.org/10.1016/j.pmatsci.2013.08.002.
[386] X. He, G. Zhang, Y. Pei, H. Zhang, Layered hydroxide/polydopamine/hyaluronic acid functionalized magnesium alloys for enhanced anticorrosion, biocompatibility and antithrombogenicity in vascular stents, J. Biomater. Appl. 34 (2020) 1131–1141, https://doi.org/10.1177/0885328219899233.
[387] Y. Guo, Y. Su, S. Jia, G. Sun, R. Gu, D. Zhu, G. Li, J. Lian, Hydroxyapatite/titania composite coatings on biodegradable magnesium alloy for enhanced corrosion resistance, cytocompatibility and antibacterial properties, J. Electrochem. Soc. 165 (2018) C962–C972, https://doi.org/10.1149/2.1171814jes.
[388] M. Toorani, M. Aliofkhazraei, Review of electrochemical properties of hybrid coating systems on Mg with plasma electrolytic oxidation process as pretreatment, Surface. Interfac. 14 (2019) 262–295, https://doi.org/10.1016/j.surfin.2019.01.004.
[389] A.I. Visan, G. Popescu-Pelin, G. Socol, Degradation behavior of polymers used as coating materials for drug delivery—a basic review, Polymers 13 (2021), https://doi.org/10.3390/polym13081272.
[390] R.N. Oosterbeek, C.K. Seal, J.M. Seitz, M.M. Hyland, Polymer-bioceramic composite coatings on magnesium for biomaterial applications, Surf. Coating. Technol. 236 (2013) 420–428, https://doi.org/10.1016/j.surfcoat.2013.10.029.